Exxon Valdez Oil Spill

State/Federal Natural Resource Damage Assessment Final Report

Mussel Tissue and Sediment Hydrocarbon Data Synthesis, 1989 - 1995

Subtidal Study Number 8
Final Report

Jeffrey W. Short
Bonita D. Nelson
Ron A. Heintz
Jacek M. Maselko
Marshal Kendziorek
Mark G. Carls
Sid Korn

National Oceanic and Atmospheric Administration
National Marine Fisheries Service
Auke Bay Laboratory
11305 Glacier Highway
Juneau, Alaska 99801-8626

November 1996

PART I

User Manual:

Exxon Valdez Oil Spill of 1989:
State/Federal Trustee Council Hydrocarbon Database 1989 - 1995

Auke Bay Fisheries Laboratory

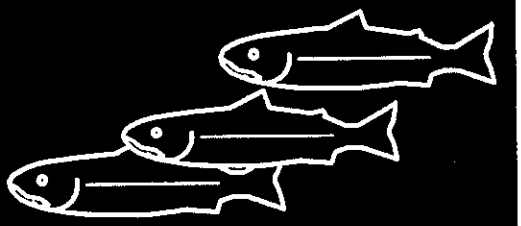

User Manual
Exxon Valdez Oil Spill of 1989:
State/Federal Trustee Council Hydrocarbon Database
1989 - 1995

Authors:
Jeffrey W. Short
Ron A. Heintz
Bonita D. Nelson
Jacek M. Maselko
Marshal F. Kendziorek
Mark G. Carls
Sid Korn

voice: (907) 789-6071
fax: (907) 789-6094
email: bnelson@abl.afsc.noaa.gov

Stanley D. Rice Program Director

National Marine Fisheries Service
11305 Glacier Highway
Juneau, Alaska USA 99801-8626

Mussel Tissue and Sediment Hydrocarbon Data Synthesis, 1989 - 1995

Subtidal Study Number 8
Final Report

Study History: Technical Services Study Number 1 (Hydrocarbon Analytical Support Services and Analysis of Distribution and Weathering of Spilled Oil) was funded in 1989, 1990, 1991, and 1992. Technical Services Study Number 1 was primarily a services project, coordinating sample analysis and controlling and dissemination of the data to principal investigators. Also funded in 1992 was Subtidal Study Number 8 (Mussel Tissue and Sediment Hydrocarbon Data Synthesis). This project was designed to evaluate the internal consistency of sediment and mussel tissue hydrocarbon data. In 1993 the Technical Services Study Number 1 project was continued as 93053 (Hydrocarbon Data Analysis, Interpretation, and Database Management for Restoration and NRDA Environmental Samples Associated with the *Exxon Valdez* Oil Spill). An additional task was assigned to the 93053 investigators of distinguishing samples containing oil from the *Exxon Valdez* oil spill from samples containing oil from other sources, although this task fell upon the Subtidal Study Number 8 (ST8) principal investigators. ST8 was slated to produce this final report while projects 94290, 95290, 96290, and 97290 (Hydrocarbon Data Analysis, Interpretation, and Database Maintenance) were funded to continue to service investigators needs for hydrocarbon samples analysis, data interpretation, database maintenance, and data dissemination. The hydrocarbon source identification procedure used to determine the presence of *Exxon Valdez* oil in samples has been published in the volume 31, number 7 issue of *Environmental Science & Technology*, 1997.

Abstract: This report comprises three parts: Part I is "*Exxon Valdez* oil spill of 1989: State/Federal trustee council hydrocarbon database 1989 - 1995" (EVTHD). The EVTHD is an electronic database with user documentation that provides a relatively user-friendly interface for the hydrocarbon and source identification results. The documentation describes how any subset of these data may be defined and then exported to an external spreadsheet. The rationale for the hydrocarbon source identifications presented in the EVTHD follows as part II. The descriptive documentation for identification of samples that were analyzed but excluded from the EVTHD because of suspected extraneous hydrocarbon contamination follows as part III.

Keywords: *Exxon Valdez*, fingerprinting, hydrocarbon database, oil spill, PAH, petroleum, weathering

Citation: Short, J. W., B. D. Nelson, R. A. Heintz, J. M. Maselko, M. Kendziorek, M. G. Carls, and S. Korn. 1996. Mussel tissue and sediment hydrocarbon data synthesis, 1989 - 1995. *Exxon Valdez* Oil Spill State/Federal Natural Resource Damage Assessment Final Report. (Subtidal Study Number 8), National Oceanic and Atmospheric Administration, National Marine Fisheries Service, Auke Bay Laboratory, Juneau, Alaska.

The specific objectives of this project are as follows: (1) Identify sediment and tissue samples that were during or after sample collection, and are therefore not indicative of environmental hydrocarbon contamination; (2) Identify sources of hydrocarbons detected in the remaining samples, especially oil spilled from the T/V *Exxon Valdez*; and (3) Present the hydrocarbon data and source identifications in a readily accessible format. These three objectives are respectively addressed in the following three documents/products that constitute the substance of this final report: (1) "Descriptive documentation for identification of biased sediment and mussel tissue samples in the *Exxon Valdez* oil spill of 1989: State/Federal trustee council hydrocarbon database 1989 - 1995"; (2) "Identification of *Exxon Valdez* oil in sediments and tissues from Prince William Sound and the Northwestern Gulf of Alaska based on PAH weathering"; and (3) "*Exxon Valdez* oil spill of 1989: State/Federal trustee council hydrocarbon database 1989 - 1995" (EVTHD). The EVTHD is an electronic database with user documentation that provides a relatively user-friendly interface for the hydrocarbon and source identification results. The documentation of the EVTHD follows as part I of this final report, and describes how any subset of these data may be defined and then exported to an external spreadsheet. The rationale for the hydrocarbon source identifications presented in the EVTHD follows as part II, and consists of a manuscript submitted to Environmental Science and Technology for separate publication. Finally the descriptive documentation for identification of biased samples follows as part III. Collectively, these three documents/products address all of the original objectives of this project, which are reproduced below from the initial workplan for project ST8.

Objectives:

A. Develop appropriate criteria for the final acceptance of hydrocarbon data prior to further analysis.

B. Calculate a hydrocarbon summary index that expresses quantitative amount and qualitative character of all hydrocarbons detected in sediment and mussel tissue samples.

C. Provide PI's with evaluated sediment and mussel tissue hydrocarbon summaries in the form of tables, charts, graphs and maps.

D. Prepare a comprehensive interpretation of sediment and mussel tissue hydrocarbon data identifying patterns of contamination across all the NRDA projects that generated these samples.

Executive Summary: This report contains the results of hydrocarbon analyses of environmental samples collected during the period 1989 through 1995 for the *Exxon Valdez* State/Federal natural resource damage assessment and restoration efforts. A total of 41,130 environmental samples were collected during this period, of which 9,419 were chemically analyzed for each of 63 hydrocarbons to provide a basis for evaluating the distribution of oil spilled from the T/V *Exxon Valdez* in the environment. This report describes the procedures used to evaluate likely sources of detected hydrocarbons in these samples, and the results of these evaluations. The results are presented in electronic format that affords relatively straightforward access to user-defined data subsets, supported by full documentation included herein.

The hydrocarbon data were evaluated in two stages. The first stage involved examination of the data for evidence that samples may have become contaminated by extraneous hydrocarbons introduced after sample collection, thereby compromising the relevance of these samples. A total of 371 sediment samples were identified as probably contaminated by hydrocarbons from such sources, and were excluded from further consideration. The criteria used to identify these samples was based on statistical examination of aggregations of extreme outliers in certain batches of samples analyzed together. Remaining samples were evaluated for the explicit presence of oil spilled from the T/V *Exxon Valdez* (EVO), and hydrocarbons present from natural sources in the area affected by the spill. Of the 7,767 samples of sediments, mussels, and other tissues considered, the patterns of hydrocarbon abundances in 1,133 were consistent with weathered EVO, and 110 were consistent with hydrocarbons from natural sources (all of which latter samples were sediments). Hydrocarbon concentrations in most of the remaining samples were too often below detection limits for source evaluation. Identification of EVO is based on the discovery that the polynuclear aromatic hydrocarbons in the spilled oil change according to consistent first-order loss-rate kinetics, regardless of environmental disposition, and that the absolute loss-rate depends on the surface:volume ratio of petroleum in the environment.

Introduction: This project evolved from the need to evaluate the enormous quantity of hydrocarbon analysis data that was produced for the NRDA and restoration efforts following the *Exxon Valdez* oil spill. During the period 1989 through 1995, 9,419 environmental samples of sediments and tissues were collected and analyzed for a suite of 63 different hydrocarbon analytes. The primary purpose of these analyses was to determine the extent of contamination caused by the spilled oil, especially in environmental compartments where contamination was suspected but was not obvious. The analytical methods employed (summarized in Short et al. 1996) are able to routinely detect as little as 10 parts per million of the spilled oil in sediments and tissues. Materials that comprise hydrocarbons from other sources are detected with comparable sensitivity, such as eroded coal particles in sediments, oil from natural oil seeps, diesel oil contamination introduced during or after sample collection, etc. The task at hand is to assess the contributions from these alternative sources to the hydrocarbons measured in the samples analyzed. This final report presents the results of these efforts for sediment and tissue samples collected form 1989 through 1995.

TABLE OF CONTENTS FOR EVTHD USERS MANUAL

Abstract 2
Database Overview 3
User Requirements 4
General Overview for Making Queries 5
Detailed Instructions for Making Queries 7
- Selecting Fields 7
- Building Conditional Statements with Query Builder 9
- Building Conditional Statements with SQL 10
- Modifying Query Results 11
- Exporting Query Results 12

Complex Query & Interpreting Model Results 13
Using Saved Setting & Specifying by Region 15
Literature Citations 18
Descriptions of Field Names (Table 1) 19
List of Hydrocarbon Names and Abbreviations (Table 2) 24
Descriptions of Projects Listed in EVTHD (Table 3) 27
Location Abbreviations, Site Names, Latitude and Longitude (Table 4) 29
List of Agencies that Contributed Samples to EVTHD (Table 5) 40
Collection Methods for Samples in EVTHD (Table 6) 41
Submatrix Types in EVTHD (Table 7) 42
List of Species Sampled and Reported in EVTHD (Table 8) 43

EVTHD Version 1.0 printed October, 1996.

Exxon Valdez Oil Spill of 1989: State/Federal Trustee Council Hydrocarbon Database 1989 - 1995 Users Guide

Abstract/Description:

The *Exxon Valdez* Oil Spill of 1989: State/Federal Trustee Council Hydrocarbon Database (EVTHD) is the collection and hydrocarbon analysis information for environmental samples obtained for the *Exxon Valdez* National Resource Damage Assessment and Restoration efforts. The data are organized into three matrix types: 4,334 tissues (representing 66 species), 3,804 sediment and 238 seawater samples collected from 350 locations in or near the spill area. The samples were derived from 38 projects administrated by investigators from 13 research organizations between 1989 and 1995. The analytical results include concentrations of 63 hydrocarbons, summary statistics for the evaluation of the hydrocarbon sources and laboratory quality control data. Features of the database include identification of replicate samples, presentation of results in dry or wet weight, correction for method detection limits (MDL) of the analytes, and easy identification of samples contaminated with *Exxon Valdez* crude oil. Individual copies of the database are available from the Auke Bay Laboratory, 11305 Glacier Hwy. Juneau, AK 99801 (attn: Bonita Nelson).

DATABASE OVERVIEW

The EVTHD was produced to facilitate access to results for hydrocarbon analysis for samples collected by State and Federal resource agencies from the area affected by the *Exxon Valdez* oil spill of March 24, 1989. Principle Investigators provided the sample collection information, and chemical analyses were performed and reported by two laboratories. These data were combined to produce this product which allows: (1) an interactive and relatively straightforward extraction of hydrocarbon data subsets, so that selected hydrocarbon data for samples collected at specific locations and dates can be easily exported into a spreadsheet; (2) ready identification of replicate samples for statistical analysis; (3) choice of wet weight or dry weight basis for data format; (4) ready application of built-in data censoring options such as sample- and analyte-specific method detection limits (MDL); and (5) access to results of hydrocarbon interpretation efforts so that samples that contain hydrocarbons from the spilled oil can be readily identified.

Samples included herein are limited to environmental samples, i.e. samples collected from the oil-spill impact area for the explicit purpose of determining the extent of oil contamination in the environment. Other kinds of samples such as samples generated by laboratory experiments, field blank samples, other quality control samples analyzed as part of the chemical analysis procedure, etc., are not included here. Also excluded are samples from unknown locations or of unknown collection dates. These standards are applied very loosely, so that any indication of field collection location (whether latitude & longitude, or geographic place name) or sampling date (i.e. year) are accepted. Results for all samples not included here are maintained in a data-archive database at the Auke Bay Laboratory, and are available on request.

A primary objective of the EVTHD is to be useful and accessible to people of widely varying technical backgrounds, ranging from college students to professional environmental chemists. For example, a user with basic knowledge of database query techniques will be able to identify the locations from which the most grossly contaminated mussels were collected in 1989. A more sophisticated user will be able to compare coefficients of variation among hydrocarbon analytes based on replicated sediment samples. However, the price of such flexibility is an abundance of choices that have consequences which may not be apparent to the general public. As a result, some of the options, filters and data presented here are suggested as appropriate for nearly all users, while others will be of interest mainly to professional chemists interested in pursuing technical details.

An important feature included in the EVTHD is an evaluation of whether hydrocarbons detected in samples came from *Exxon Valdez* oil (EVO). The evaluation procedure was applied to the samples that contained all of the most persistent hydrocarbons present in EVO. The procedure consists of measuring how closely the pattern of hydrocarbon concentrations in a sample matches the pattern predicted by a mathematical weathering (i.e. environmentally altered) model for EVO. This procedure also provides a quantitative indication of how weathered the

EVO in a sample is, assuming EVO is really present. In addition, results of another evaluation procedure which estimates the probability that the patterns of hydrocarbon concentrations reported for a sample are consistent with a natural pattern characteristic of deeper sediments is included. These interpretive features of the EVTHD make it possible to isolate and retrieve samples that are contaminated with EVO, or contain hydrocarbons from natural source modeled.

The EVTHD interface consists of a series of screens that guide users through a sequence of decisions that determine which data and what format is selected. The first set of decisions determines the kind of data that is to be selected, i.e. which specific hydrocarbon analytes, what sample collection information, and which sample matrix (water, sediments, or tissues). The second set determines the qualifiers that are to be imposed on selected samples, i.e. from which specific locations, sampling dates, projects, etc. Once it is determined what kind of data will be selected for which kinds of samples, the data format is specified, and data that fulfill all these criteria may be examined. The criteria may be modified based on successive examinations of the data until a satisfactory data set is constructed, which may then be exported to a user-identified spreadsheet for further data analysis. This allows for the database to be explored prior to data export.

A major impediment to the use of this database is the large number of abbreviations that are incorporated into it. Nearly every kind of data is identified as an abbreviation, some of which are completely opaque. A series of tables is provided with this document that decodes all of the abbreviations used. In addition, the query-builder screen of EVTHD contains pick lists that provide the complete set of abbreviations for each field. It is therefore recommended that users un-familiar with these abbreviations use the query-builder option to identify the qualifiers imposed on data to be selected.

The authors of this effort would appreciate learning of any errors discovered by users. Please communicate these as well as other comments on the utility of the database, suggestions for improvements, or requests for individual copies, to: Bonita Nelson, Auke Bay Laboratory, 11305 Glacier Highway, Juneau Alaska, 99801-8626.

USER REQUIREMENTS

The data are grouped and queried by matrix type (sediment, tissue and water) using a series of pop-up screens that contain click boxes, hot buttons, and pull down menus (including on-line help) managed in the Window's environment. Users should be familiar with the following :

- ✓ Basic understanding of database structure and operation. Familiarity with SQL (Standard Query Language), is very helpful.

- ✓ Basic understanding of the operation of spreadsheets. This software is designed to provide users with data reports that can be viewed directly, or exported to other Windows-based software for more detailed analysis.

An understanding the motives behind the project sampling designs as well as a basic knowledge of hydrocarbon source identification procedures will be helpful for interpreting these data. Interested users should consult either principle investigators with specific questions regarding sampling designs and interpretation of analytical results or consult the final reports for these projects. Final reports are available from the Exxon Valdez Oil Spill Information Office, 645 G Street, Anchorage, AK 99501. Specific information on the procedures used to evaluate samples for the presence of EVO are found in Short et al., (1996b). Information concerning the specific methods used for hydrocarbons analysis is found in Short et al. (1996a).

The following sections review the procedures for querying the database. For users familiar with database operations, a general overview section is provided first. A more detailed set of instructions is provided for users that are less familiar with database operations. The final section is a demonstration of how to interpret the data resulting from the evaluations of the presence of EVO. The rest of this manual contains tables that can be used to decode the abbreviations used in many of the fields. In each of the following sections, helpful hints will be highlighted with :

GENERAL OVERVIEW FOR MAKING QUERIES

I. Select fields first *then* matrix type from the Field Selection Screen

1. Fields of interest are selected by clicking on boxes next to available field names. Three categories of information are available: sample collection, and analytical results for alkane and polynuclear aromatic hydrocarbons (PAH). Complete descriptions of the sample collection fields are found in Table 1. Hydrocarbon names and their abbreviated field names are found in Table 2.

2. Select matrix type (sediment, water, tissue) by clicking the appropriate hot button.

II. Select specific lines of data using the Query Screen

This screen allows the user to build conditional statements to select specific rows of data in one of two ways:

1. Clicking the "Query" button on the tool bar and selecting Query Builder. This activates the query builder, a pop-up window which prompts the user for the query conditions through a series of pick list boxes on a "Conditions" screen.

2. Typing conditional statements in the "Enter SQL Query" box using SQL (the length of the command can exceed the size of the box).

The data conforming to the conditions are returned from the database on the bottom of the Matrix Query Screen on a grid. Missing values are coded as blanks and missing dates are coded as "01/01/01". Once a query search has been activated, it can be stopped using the Windows kill process : (Ctr/Alt/Del - end task).

III. Modify data

Dry Weight

Hydrocarbon concentrations are reported in nanograms analyte per g matrix (ng/g) on a wet weight basis. They can be converted to dry weight basis by clicking on the dry weight hot button.

Method Detection Limit (MDL) Filter

After data has been returned, activating this hot button filters the data for sample and analyte specific MDL's (see p. 11), setting values below MDL = "-". This filter can be applied to data on either a dry or wet weight basis. You must select wet& dry weights and labs (and volume for the water matrix) from the fields selection screen before making the query to use this option.

IV. Save query and query results to other files

The results of the query and any modifications you have made can be saved to the clipboard and pasted into a spreadsheet or statistical package using the Windows copy and paste commands. Use the mouse to highlight the desired data in the grid, then click on Edit from the menu bar and select Copy from the pick list and paste data to new application.

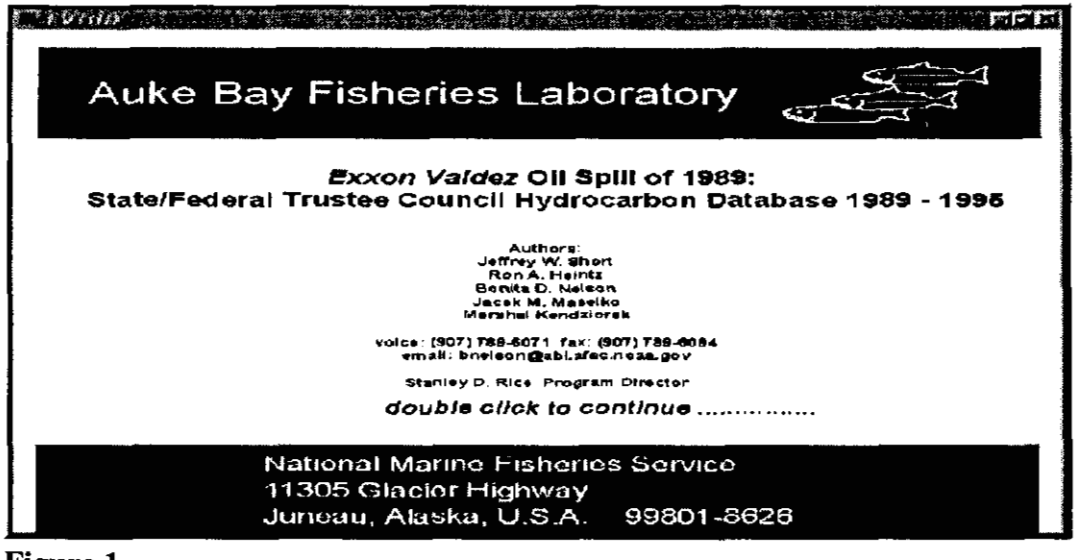

Double click on the welcome screen to begin the program (Figure 1).

Figure 1

DETAILED INSTRUCTIONS FOR MAKING QUERIES

I. Select fields then matrix type from the Field Selection Screen

The field selection screen (Figure 2) is the first screen to be activated after the welcome screen. The data are grouped into three sections (Sample Information, PAH and Alkane analytical results). Field names can be selected or deselected by clicking on the box to the left of the field name. An entire group within a category is selected by choosing the "select all" box. Complete descriptions of the sample collection fields are found in Table 1 and hydrocarbon names and their field abbreviations in Table 2.

Sample Query: What are the concentrations of naphthalene (Naph) and n-decane (C10Alk) in mussel samples collected on Knight Island (including agency, projects and date collected information). Only concentrations above the method detection limits (MDL) are desired.

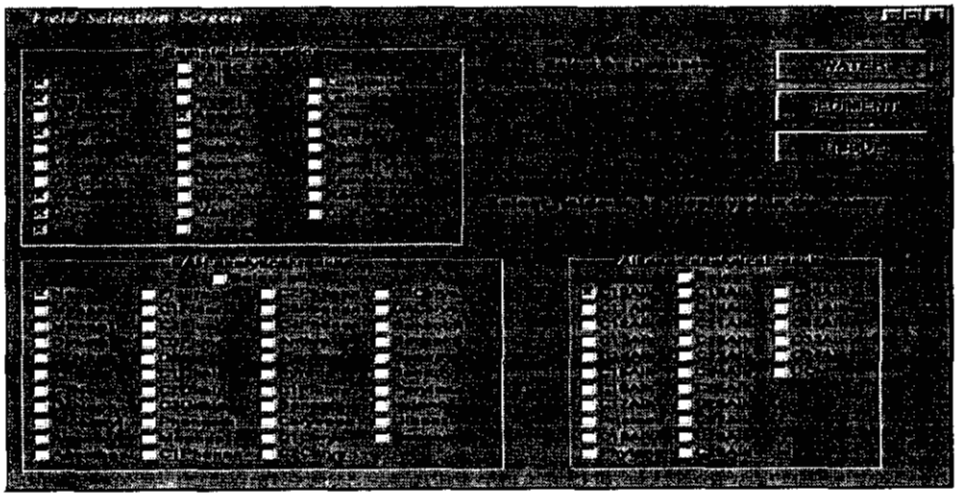

Step 1. Select appropriate* fields from the sample information and analytical results boxes.

Step 2. Click on the *tissues* hot button.

Figure 2

☞ The selection of fields chosen can be saved to a file *before* clicking on the matrix hot button and retrieved for future use by selecting File - Save from the menu bar. Saved files are retrieved using by using the File - Load menu bar options.

☞ Conditions for queries can use any fields, and are not limited to the fields checked off on the Field Selection Screen.

*In order to use the MDL option the following columns in the Sample Information box ***must*** be selected: labs, wetwt, drywt (and volume for water samples). Data are initially returned as wet weights and are converted to dry weights by choosing the dry weight hot button on the tissue query screen (next screen) after the data have been returned. Notice that the location field did not have to be selected in order to have Knight Island samples returned because these conditions can be specified using the query screen.

II. Query specific lines of data using the QUERY SCREEN

The *(Matrix)* Query Screen (Figure 3) indicates which fields were selected in the Field Selection Screen. To view all the data representing this matrix click without specifying any conditions, select the "Do SQL" button. To see a subset of the data, you must build a conditional statement.

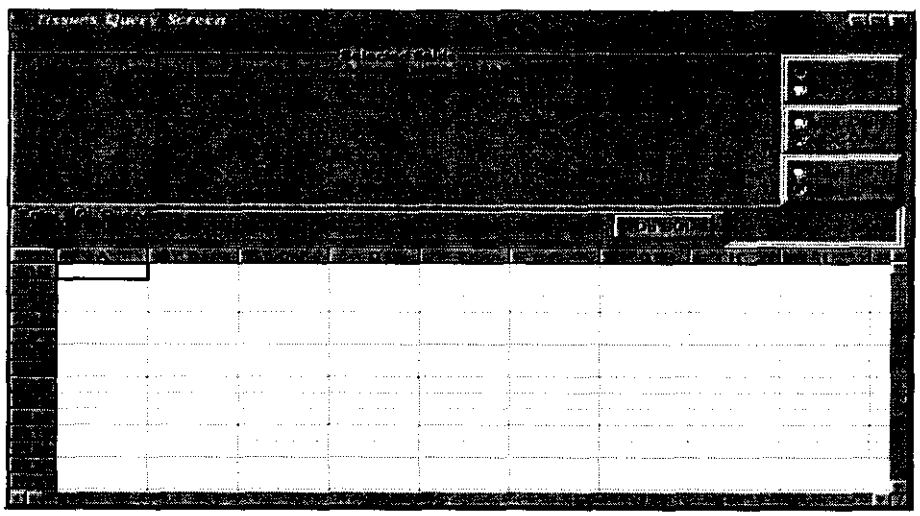

Query Screen

Figure 3

☞ If you need to change your field selections once you reach the query screen, select the Query - Select New Columns option on the Query Screen tool bar and you will return to the Field Selection Screen.

A condition statement contains a field expression (e.g. SPECABV) linked to a value expression ('MUSS') by an operator (=, >, <, >=, <=, <>). A more complicated statement can be created by linking a series of conditions with connectors (and, or). (SPECABV = 'MUSS' is the expression which represents : species = mussels).

In our example, mussels collected from Knight Island, the conditional statement must contain LOCATABV (field name for location, see Table 1) = 'KNIGI' (the abbreviation for the Knight Island see Table 4) and SPECABV = 'MUSS' (the abbreviation for mussels, see Table 8).

The condition statement can be constructed two ways: (1) clicking on Query from the menu bar and choosing the Query Builder or (2) typing in the conditional statement using SQL in the "Enter SQL Query" box and then clicking the "Do SQL" hot button.

Make the query by building the condition statement

Option 1: Building conditional statements with Query Builder option

Selecting Query Builder from the Query option on the tool bar at the top of the (*Matrix*) Query Screen initiates the query builder. A "Conditions" pop-up window (Figure 4) appears which contains a series of boxes (Connector, Field Expression, Operator, Value Expression) along the bottom. Type in an expression or use the button inside the box to choose from a pick list of valid column names, operators, or values to build the conditional statement.

You **must click "insert"** after entering each condition which causes the condition to be seen in the top box of the screen. The program automatically includes the default connector "and" between statements.

When you have finished typing in all conditions, click on OK (a hot button in the top right hand of the screen) to activate the query. Notice the default condition statement "qcerror = 'GOOD'" is automatically built into every query (see Table 1).

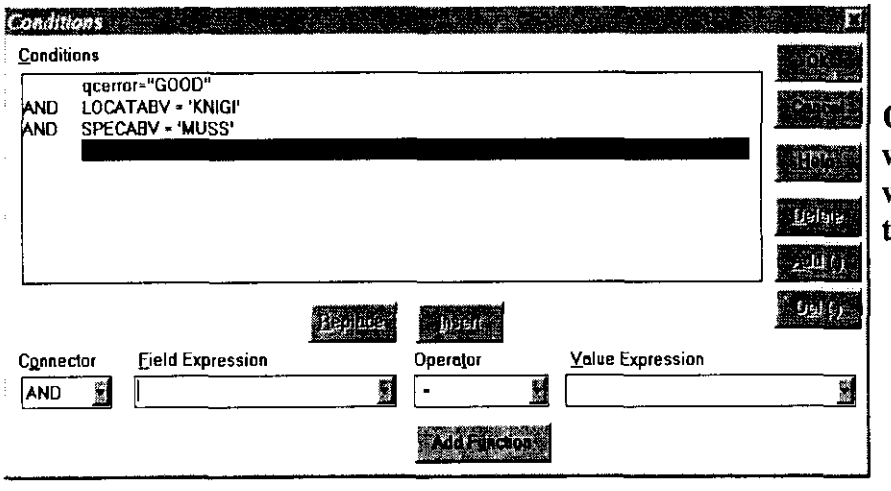

Conditions screen used when building a query with the Query Builder tool bar option.

Figure 4

The Delete, Add, Del and Add Function keys are used in conjunction with the mouse to edit queries, or to create complex nested queries.

☞ In order to specify the tissue species (such as mussels) in your query, you *must* use the field selection **SPECABV** (= 'MUSS') from the list in Table 8.

Option 2: Building conditional statements with SQL

The SQL option completes a SQL command "select ... from .... where " that began when the fields were chosen on the Field Selection Screen. You only need to complete the command by entering the conditions in the "Enter SQL Query" box, and then clicking on the "Do SQL" hot button. The SQL string comparison routines are case sensitive so value expressions must be *uppercase* and enclosed in *single* quotes and dates must be enclosed in curly braces { }. The SQL text can contain numerous comparisons, concatenated with 'and' & 'or' as well as hierarchical parentheses placed between and among the 'and' & 'or'.

Enter the SQL statement: **LOCATABV = 'KNIGI' AND SPECABV = 'MUSS'**

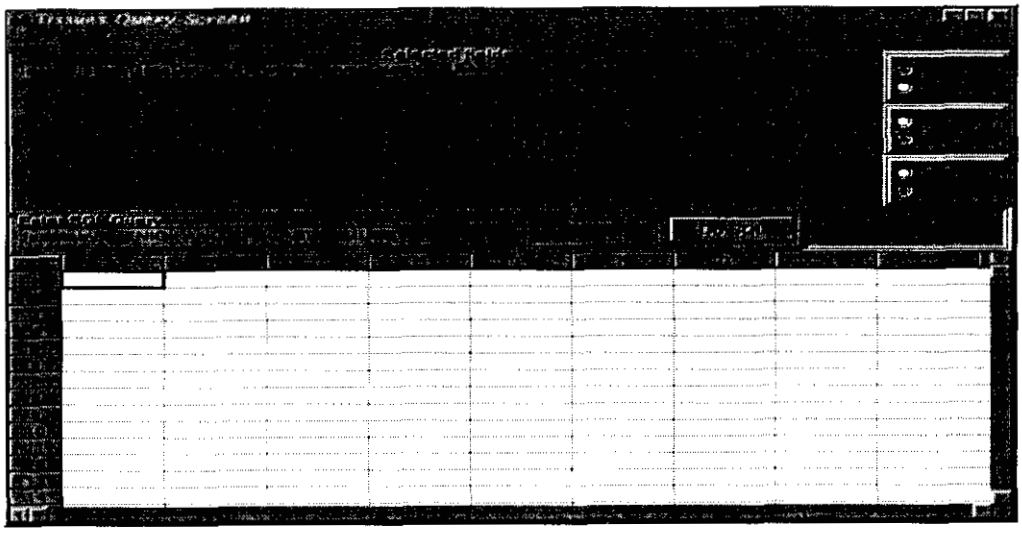

Select the "Do SQL" hot button to activate the query.

Figure 5

☞ Writing the SQL conditional statement requires the user to have an understanding of the value expressions of Table 1 and Table 2.

☞ SQL commands entered in the SQL query box, can be copied to the Windows clipboard by first highlighting the command, then clicking on Edit in the menu bar at the top of the screen and file save options.

Once the select statement has been generated using either query method, data are returned in the grid part of the query screen (Figure 6) with defaults: wet weight, MDL OFF and Deut OFF.

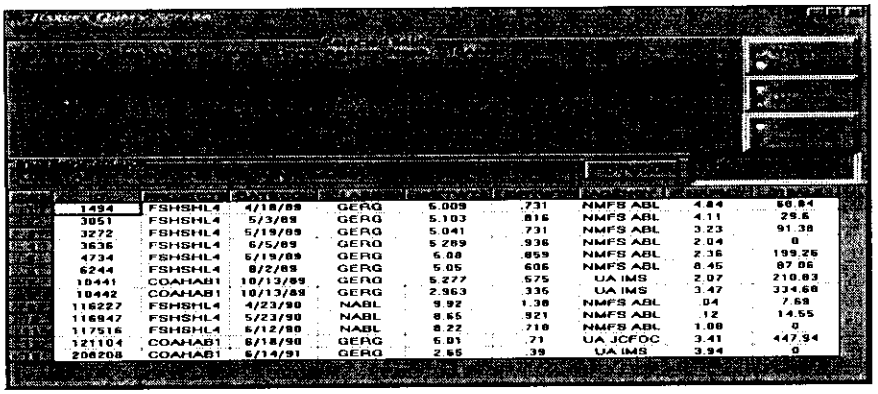

1494	FSHSHL4	4/18/89	GERG	5.009	.731	NMFS ABL	4.84	68.84
3051	FSHSHL4	5/3/89	GERG	5.103	.816	NMFS ABL	4.11	29.6
3272	FSHSHL4	5/19/89	GERG	5.041	.731	NMFS ABL	3.23	91.38
3636	FSHSHL4	6/5/89	GERG	5.289	.936	NMFS ABL	2.04	0
4734	FSHSHL4	6/19/89	GERG	5.08	.859	NMFS ABL	2.36	199.25
6244	FSHSHL4	8/2/89	GERG	5.05	.606	NMFS ABL	8.45	87.86
10441	COAHAB1	10/13/89	GERG	5.277	.575	UA IMS	2.07	210.83
10442	COAHAB1	10/13/89	GERG	2.963	.335	UA IMS	3.47	324.68
116227	FSHSHL4	4/23/90	NABL	9.92	1.38	NMFS ABL	.04	7.68
116947	FSHSHL4	5/23/90	NABL	8.65	.921	NMFS ABL	.12	14.55
117516	FSHSHL4	6/12/90	NABL	8.22	.718	NMFS ABL	1.08	0
121104	COAHAB1	6/18/90	GERG	5.01	.71	UA JCFOC	3.41	447.94
208208	COAHAB1	6/14/91	GERG	2.65	.39	UA IMS	3.94	0

Query results appear on the grid.

Figure 6

☞ The grid screen returns 9 fields of view and 14 lines of data at a time. Additional fields and lines can be scrolled through with arrow keys which appear along the margins of the grid .

III. Modify query results with Method Detection Limit (MDL) Filter

This filter is designed to identify analytical results that are below the MDL value (which is unique to each analyte, sample and lab); results below this value may be unreliable. The analyte concentrations are initially reported on a wet weight basis (ng/g wet weight), and the MDL filter can be applied to data reported on a wet or dry weight basis.

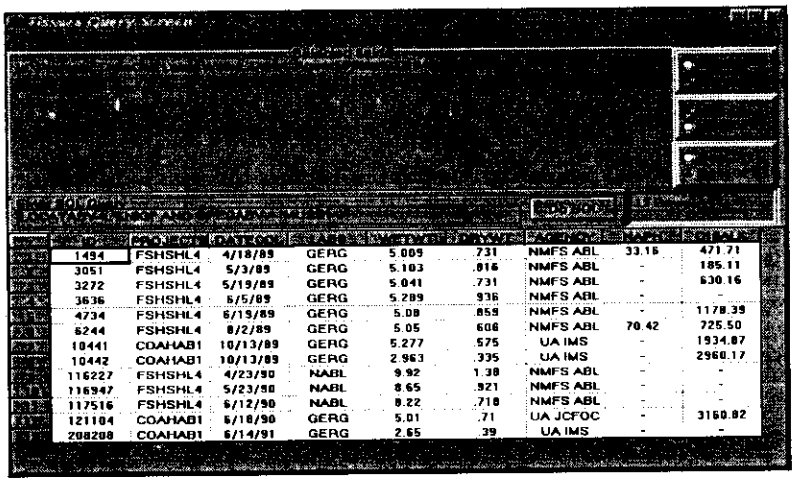

1494	FSHSHL4	4/18/89	GERG	5.009	.731	NMFS ABL	33.16	471.71
3051	FSHSHL4	5/3/89	GERG	5.103	.816	NMFS ABL	-	185.11
3272	FSHSHL4	5/19/89	GERG	5.041	.731	NMFS ABL	-	630.16
3636	FSHSHL4	6/5/89	GERG	5.289	.936	NMFS ABL	-	-
4734	FSHSHL4	6/19/89	GERG	5.08	.859	NMFS ABL	-	1178.39
6244	FSHSHL4	8/2/89	GERG	5.05	.606	NMFS ABL	70.42	725.50
10441	COAHAB1	10/13/89	GERG	5.277	.575	UA IMS	-	1934.87
10442	COAHAB1	10/13/89	GERG	2.963	.335	UA IMS	-	2960.17
116227	FSHSHL4	4/23/90	NABL	9.92	1.38	NMFS ABL	-	-
116947	FSHSHL4	5/23/90	NABL	8.65	.921	NMFS ABL	-	-
117516	FSHSHL4	6/12/90	NABL	8.22	.718	NMFS ABL	-	-
121104	COAHAB1	6/18/90	GERG	5.01	.71	UA JCFOC	-	3160.82
208208	COAHAB1	6/14/91	GERG	2.65	.39	UA IMS	-	-

☞To use this option, you must have selected wt, drywt, labs (& vol for water matrix) when selecting fields in field selection screen.

Values below MDL are reported as "-" (Figure 7).

☞ Note that once MDL filter is turned on, it cannot be switched off and the data can no longer be converted between wet and dry weight. So if the dry weight basis is desired, click dry wt. *first*, then MDL *second*.

Deuterated Recovery Filter

When groups of samples are analyzed in the laboratory, surrogate standards are included which contain known amounts of deuterated hydrocarbons. These are included in order to correct for changes in analyte concentration caused by preparation for analysis in the lab. A "perfect" analysis gives 100% recovery of deuterated surrogate samples. This filter identifies samples whose estimated recoveries range between 30 - 150% range which indicates an acceptable analysis. The deuterated hydrocarbons are identified by the "d" at the end of the analyte name. They are automatically reported when Recov. Fil option is selected from the Field Selection screen. Values outside of the acceptable range are returned as 'A'. This option is primarily used by analytical chemists only.

IV. Exporting Query Results

After viewing the data in the grid you may decide to refine your query, or save the results to some other software. Another query can be initiated at any time, and the new results will overwrite the data in the grid. To save the results, or any subset to some other software, highlight the grid area you want to save (Figure 8) and select Edit - Copy option from the menu bar. The data are now copied to the Windows clipboard and they can pasted into other software packages.

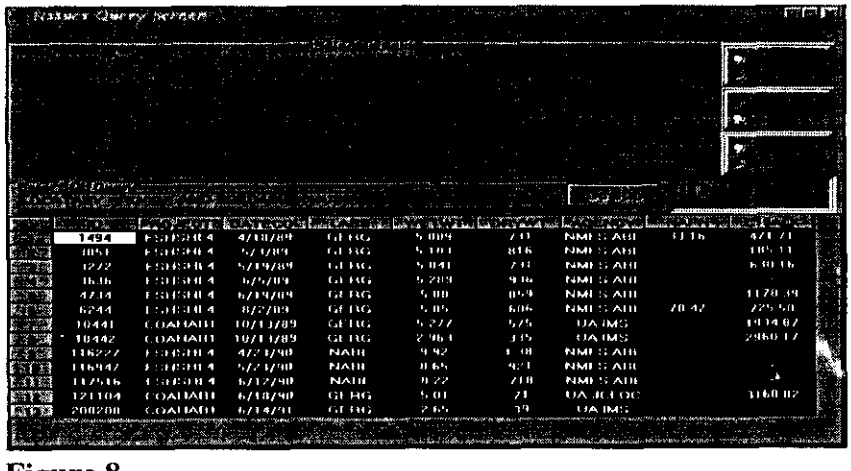

Data "painted" ready to be pasted to another software package.

Figure 8

☞ Note you can quickly select the whole grid by clicking on the button located above the row number 1 (just to the left of the column heading ID in Figure 8).

COMPLEX QUERY & INTERPRETING MODEL RESULTS

Only samples that had concentrations of 14 selected PAH (see Table 2) above MDL were evaluated for PAH source by fitting the analytical data to two different models. The two potential sources of PAH were *Exxon Valdez* oil (EVO), and naturally occurring "background". Complete description of the models used to identify sources of PAH are found Short et al. (1996b). The PAH source identification procedure produces a set of parameters (**W, OilConc, MSEoil, pOil, MSEbgrnd**, and **pBGRND**) for each sample that are reported when **Model Results** is selected from the Field Selection Screen. Samples that were fit to the PAH source models have values for each of these parameters, otherwise the value for each of them is set to missing (-99). Viewing the model results provides a means of identifying the source of the PAH in the sample.

☞ Samples that have been evaluated to determine hydrocarbon source are easily identified in queries by making sure that **W** is not equal to -99. The operator for not equal is: "<>".

Sample Query: *The following example identifies the sediment samples collected from Knight* Island that were modeled to determine the PAH source and located either above mean low tide, or deeper than 40m. You can see from the field selection screen (Figure 9) that we want to see the **id, depth, groupno** and **model results** for each of requested sediment samples .

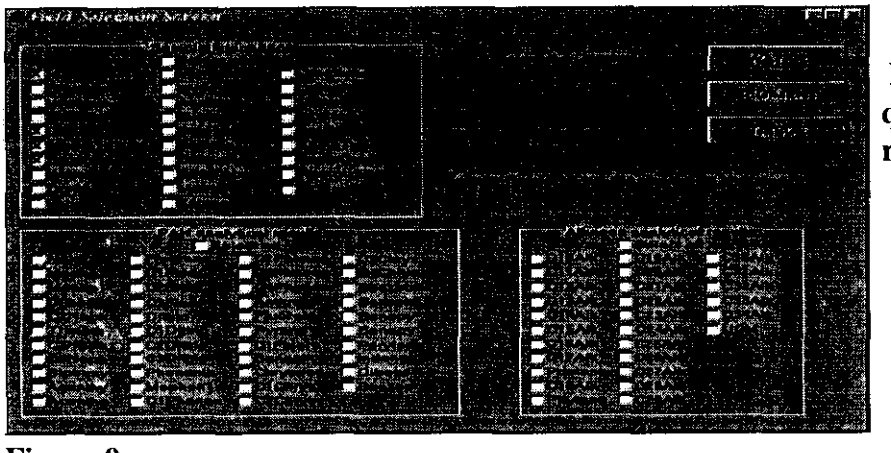

Field Selection Screen for query using oil model results.

Figure 9

The conditional statement entered into the "Enter SQL Query" box is :

LOCATABV = 'KNIGI' AND DEPTH <> -99 AND (DEPTH <0 OR DEPTH >40) AND W >-99

The database returns 7 rows of data (Figure 10), 5 rows with depths < 0 m and 2 collected from 100 m. Since the 2 deeper samples have the same **groupno** we conclude that they are replicate samples, thus their analytical results can be combined to calculate coefficients of variation for each result. Sample 116943 is also replicated, but its replicates could not be modeled.

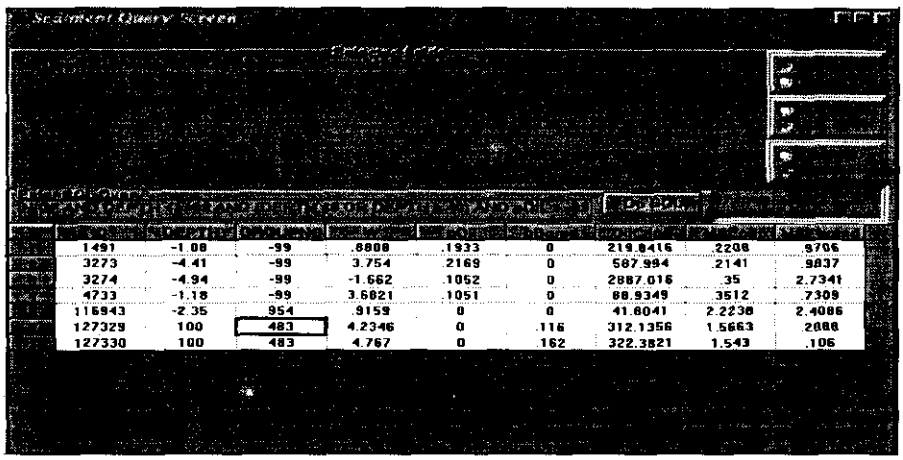

1491	-1.08	-99	.6808	.1933	0	219.8416	.2208	.9706
3273	-4.41	-99	3.754	.2169	0	587.994	.2141	.9837
3274	-4.94	-99	-1.662	.1052	0	2887.016	.35	2.7341
4733	-1.18	-99	3.6821	.1051	0	88.9349	.3512	.7309
116943	-2.35	954	.9159	0	0	41.6041	2.2238	2.4086
127329	100	483	4.2346	0	.116	312.1356	1.5663	.2888
127330	100	483	4.767	0	.162	322.3821	1.543	.106

Oil model results.

Figure 10

Viewing **pOil** and **pBgrnd** (Figure 10) reveals that the source of the PAH in 4 of the shallow samples is most likely EVO, the PAH in the 2 deep samples is most likely from "background" sources, and the source of PAH in sample 116943 is unknown.

In technical terms, the value for **pOil** is the probability of committing a Type I error: that is, the chances of being wrong when concluding that the PAH in the sample are derived a source other than EVO. This means that values of **pOil** reflect how well the pattern of PAH in the sample fit the pattern for the model of weathered oil, with the best fitting samples having a pOil equal to 1.0. The lowest value for pOil that indicates consistence with EVO depends on your willingness to commit a Type I error. The values for pBgrnd are interpreted the same way, only they reflect how well the pattern of PAH in the sample matches the model for the pattern in the "background" source.

The PAH source identification procedure for EVO produces two more values that are also important. **W** tells you how weathered the oil was when the sample was collected, and **OilConc** is an estimate of the initial concentration of the oil (micrograms of oil per gram of matrix: µg oil/g matrix) that contaminated the sample. These values only have meaning if the sample is contaminated with EVO. Weathering is a generic term for the physical processes that alter the composition of oil. Values of **W** average from near zero for un-weathered oil to larger positive values for EVO that is progressively more weathered. Highly weathered oil has almost no alkanes, and only the heaviest of the PAH remaining. Since the toxicity of oil decreases as it weathers, **W** can be used as an index of the toxicity of the oil in the sample.

MSEoil is the mean squared error between the sample and the EVO weathering model, it is compared with a distribution of **MSEoil** derived from a laboratory weathering experiment to determine **pOil.** Similarly, **MSEBgrnd** is the mean squared error between the sample and the "background" model.

USING SAVED SETTINGS AND SPECIFYING SAMPLES BY REGION

This example shows how to querying data selected from sampling locations within a geographic region, and also shows you a short-cut method of selecting the necessary columns needed for calculating total PAH values for each sample. The specific objective of the query is to compare the model results with the observation of total PAH in sediment samples collected along the southeast coast of Knight Island.

1. Select analytes to calculate total PAH

First, select the necessary analyte and sample information fields from the Field Selection Screen. EVTHD includes a field selection file that automatically selects the 40 analyte fields from the PAH analytical results section which are used to calculate the sum of the PAH values (total PAH) for the selected samples. To activate this option, select File, then Load Settings from the Field Selection Screen. Then highlight the file " totpah.sel" from the pop-up window (Figure 11).

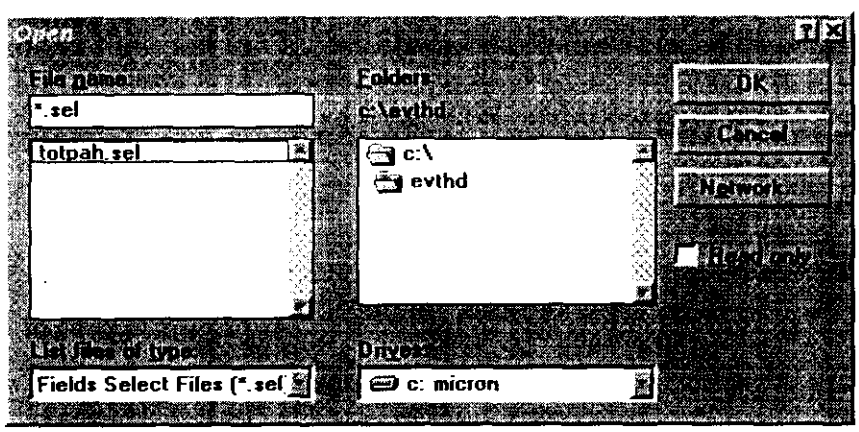

Figure 11

Pop-up window for selecting file for total PAH settings. This is activated from the Field Selection Screen

Click on the OK button and you will notice that several fields have been selected in both the Sample Information and PAH Analytical Results boxes (Figure 12).

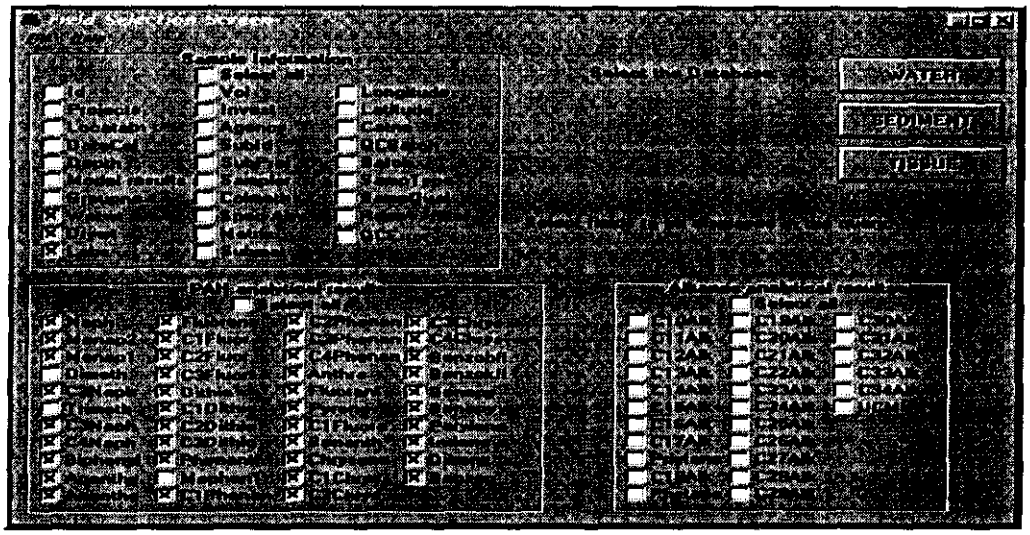

Fields automatically selected by activating the totalpah.sel file from Field Selection Screen.

Figure 12

☞ You can adjust the selections in the Sample Information Box to suit your needs, but to obtains values for total PAH consistent with values found in Trustee Reports, *you should not change the selections in the PAH Analytical Results box.*

2. Adjust the fields selected in the Sample Information box.

In this example we are also selecting the following sample fields: **id, locatabv and model results** (not shown in Figure 12).

3. Select database hot button. (This example uses the Sediment data).

4. Describe geographic region boundaries using latitudes and longitudes & activate query.

EVTHD is text based, so the most complicated regions that can be easily identified are rectangular. Regions with irregular shapes are better identified with a geographic information system (GIS).* Identify the boundaries by reading them off of a map, and enter the limits into either Query Builder or the Enter SQL Query box. Later versions will have a built in map.

*The EVOS Research and Restoration CD includes EVTHD and the Trustee GIS for identifying locations in PWS. If you have the CD the GIS can be started by selecting Map from the menu bar on the Sediment Query Screen and selecting "GIS". Queries in the Trustee GIS will provide you with a list of sample id's found in the region you defined (see documentation for the Trustee GIS for details). Highlight the id's, copy them to the Windows clipboard. Edit the id's into the following command: ID IN (id1, id2, id3, ...). Copy this command from the Windows clipboard to the "Enter SQL Query" box and click on the "Do SQL" hot button, EVTHD will return the data that you requested on the Field.

The latitudes and longitudes that bound southeast Knight Island are identified in the following query statement which should be entered into the "Enter SQL Query" box:

lat < 60.267 and lat >60.13 and long < 147.7 and long > 147.5 (Figure 13).

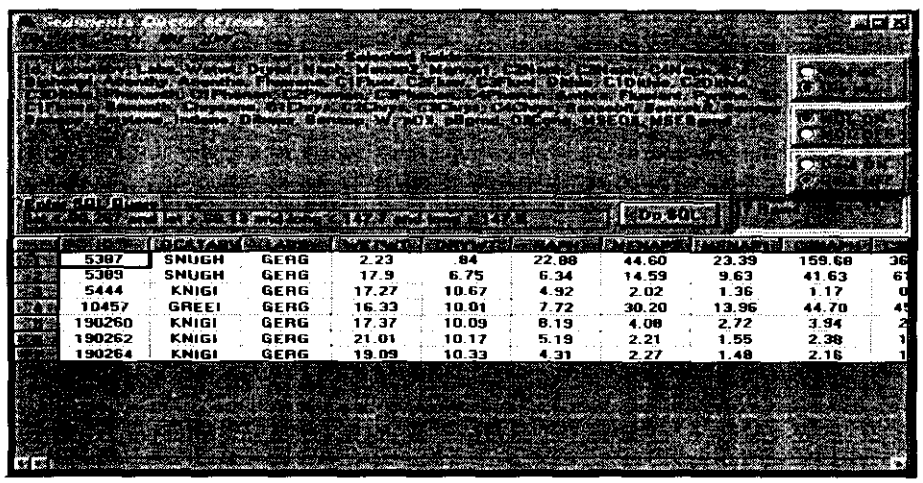

5387	SNUGH	GERG	2.23	84	22.88	44.60	23.39	159.68	36
5389	SNUGH	GERG	17.9	6.75	6.34	14.59	9.63	41.63	6
5444	KNIGI	GERG	17.27	10.67	4.92	2.02	1.36	1.17	0
10457	GREEI	GERG	16.33	10.01	7.72	30.20	13.96	44.70	4
190260	KNIGI	GERG	17.37	10.09	8.19	4.08	2.72	3.94	2
190262	KNIGI	GERG	21.01	10.17	5.19	2.21	1.55	2.38	1
190264	KNIGI	GERG	19.09	10.33	4.31	2.27	1.48	2.16	1

SQL command for area which bounds Knight Island and returned data for example.

Figure 13

5. Convert data to dry weights , select the MDL filter option and export data to a spreadsheet. EVTHD returns 7 rows of data.

6. Calculate the value for total PAH by summing the concentrations of all the analytes in your spreadsheet across each row.

The table below (Figure 14) displays a summary of the data. The analyte concentrations have been summed for each row and the results displayed in the column labeled TotPAH, the contributing analyte concentrations as well as values for **LABS**, **WETWT**, and **DRYWT** have been deleted for simplicity's sake.

ID	LOCAT ABV	Total PAH	W	POIL	PBGR ND	OIL CONC	MSE OIL	MSEB GRND
5387	SNUGH	3999.29	1.4256	0.1814	0	618.7376	0.2247	0.9281
5389	SNUGH	1000.05	3.8743	0.099	0.018	347.2358		0.3307
5444	KNIGI	53.17						0
10457	GREEI	688.05	3.6753	0.0139	0.07	221.3779	0.9299	0.2673
190260	KNIGI	94.03						0
109262	KNIGI	21.29						0
190264	KNIGI	58.61						0

Figure 14

Note that samples collected from southern Snug Harbor (SNUGH) and Green Island (GREEI) have relatively large amounts of PAH that are apparently derived from *Exxon Valdez*.

Literature Cited

Short, J.W., T.L. Jackson, M.L. Larsen, and T.L. Wade. 1996a. Analytical Methods Used for the Analysis of Hydrocarbons in Crude Oil, Tissues, Sediments, and Seawater Collected for the Natural Resources Damage Assessment of the *Exxon Valdez* Oil Spill. Pages 140 - 148 in S. D. Rice, R. B. Spies, D.A. Wolfe, and B. A. Wright, editors. Proceedings of the *Exxon Valdez* oil spill symposium. American Fisheries Society Symposium 18.

Short J. W., R.A. Heintz and B.D. Nelson. 1996b. Hydrocarbon Data Analysis, Interpretation, and Database Maintenance for Restoration and NRDA Environmental Samples Associated with the *Exxon Valdez* Oil Spill State/Federal Natural Resource Damage Assessment Final Report (Subtidal Study Number 8), National Oceanic and Atmospheric Administration, National Marine Fisheries Service, Auke Bay Laboratory, Juneau, Alaska.

Table 1. Field names and descriptions for sample collection fields in Exxon Valdez Oil Spill of 1989: State/Federal Trustee Council Hydrocarbon Database (EVTHD).

FIELD NAME	DESCRIPTION
Id	Unique identifier assigned to each sample by the database manager used to track collection and analytical information for each sample. These are assigned in blocks depending on the date of collection (except samples collected by U.S. Fish & Wildlife Service which have numbers between 20000 and 29999.)

Year of Collection	ID
1989	1000 - 20000 & 30000 - 39999
all years	20001 - 29999 (F&WS)
1990	100000 - 199999
1991	200000 - 299999
1992	300000 - 399999
1993	400000 - 499999
1994	500000 - 599999
1995	600000 - 699999

Projects Abbreviated names for *Exxon Valdez* Trustee Natural Resource Damage Assessment and Restoration projects, descriptions are found in Table 3.

Locatabv Location abbreviation of sample collection site. Table 4 provides complete names along with latitude and longitudes for each abbreviation. Note, on the "Field Selection Screen" this field is referred to as "Location".

DateCol Date sample was collected

Depth Depth, in meters, where the sample mearured are from Mean Lower Low Water (MLLW) but may be measured, or estimated by the sample collector. Depths are negative, i.e. -.66, above MLLW and positive, i.e. 1, below MLLW.

Model Results

The following field names appear in the "Selected Fields Box" when Model Results is selected on the "Field Selection Screen" (SQL commands should refer to the field names directly). The fields relate to the procedure used to evaluate samples for the presence of Exxon Valdez crude oil (EVO). Only a subset of samples that contained sufficient PAH to be analyzed by the procedure have results. The same subset of samples were also analyzed to determine how well they matched the natural PAH pattern. The specific PAH used for both models are highlighted in Table 2. Consult Short et al. (1996b) for details on the evaluation procedures. The results of the analyses are found in the fields listed below.

Table 1, continued.

FIELD NAME	DESCRIPTION
Model Results(continued)	
pOil	The probability that the hydrocarbons in the sample are derived from EVC. This number is obtained by comparing **MSEoil** to a distribution of mean squared errors for a set of experimentally weathered samples. It is a measure of the probability of Type I error when the null hypothesis is that the PAH pattern is consistent with the pattern in similarly weathered EVO. Samples with **pOil** = 1.0 are contaminated with EVO while samples with **pOil** < 0.01 are not likely to be contaminated with EVO.
pBgrnd	The probability that the hydrocarbons in the sample are derived from a natural geological source. This number is obtained by comparing **SSQbgrnd** to distribution of sums of squared errors for a set of samples collected in Constantine Harbor. Hydrocarbons in samples with **pBgrnd** = 1.0 are derived from the natural source while hydrocarbons in samples with **pBgrnd** < 0.01 are not likely to be derived from this source.
W	A value that indexes how "weathered" the oil in the sample is. Weathering refers to the process by which oil degrades. The oil in samples collected from disparate locations at different times but with equal values for **W** has degraded to the same degree. Since the toxic effects of oil persist as long as the oil is in the environment, **W** provides a measure of relative toxicity. Values for W range from near zero to 10. Lower values indicate relatively fresh and more toxic oil while greater values indicate more degraded and less toxic oil. **This value only has meaning for samples that are considered to be contaminated with EVO.**
OilConc	The estimated initial concentration of oil in the sample. The PAH evaluation technique for EVO estimates the initial concentration of oil in the sample prior to weathering, by assuming that the concentrations of some PAH are invariant with time. Assuming the sample is contaminated with EVO, the initial concentration of unweathered oil in the sample is given as micrograms of oil per gram of matrix (µg oil/g matrix).
MSEoil	The mean squared error between the sample and a hypothetical sample of oil weathered to the same value of **W**.

Table 1, continued

FIELD NAME	DESCRIPTION
Model Results (continued)	
MSEoil	This statistic measures the agreement between the sample and a hypothetical sample of oil weathered to the same state, and is compared to a distribution for **MSEoil** derived from a laboratory study (Short et al. 1996b).
MSEBgrnd	The mean squared error between the sample and the environmental sample collected from Constantine Harbor with the median value for total PAH. The PAH signature in Constantine Harbor is the archetype for the natural background pattern of PAH (Short et al. 1996b). This statistic measures the agreement between the sample and this archetype.
Groupno	Arbitrary number assigned to associate replicate samples (samples qualifying as replicates were collected at the same time and location) that can be used to evaluate data variability.
WetWt	Wet weight of the sample (g).
DryWt	Dry weight of the sample (g).
Labs	Abbreviation for the analytical laboratory conducting hydrocarbon analysis. NABL - Auke Bay Laboratory - National Marine Fisheries Service GERG - Geochemical Environmental Research Group - Texas A&M Univ.
Vol	Volume (ml) of the water sample.
Invest#	Alphanumeric identifier assigned to a sample by the field personnel.
Agency	Agency responsible for collecting the sample (Table 3).
Subid	Identifier assigned by sample collector or number assigned to samples composited after archival.
SubProj	Coastal Habitat 1 damage assessement project agency code or restoration project numerical identifier.

Table 1, continued.

FIELD NAME	DESCRIPTION
Sampler	The last name of the individual responsible for the collecting, handling and the security of the samples in the field.
ColMeth	Method used to collect the sample (Table 6).
SpecAbv	Species abbreviation used for tissue samples (Table 8).
Matrix	Sample type: seawater, sediment, tissue.
SubMat	Specific additional information about matrix (Table 7).
Long	Longitude in decimal degrees calculated for the degrees, minutes and seconds, i.e. ((LONG. Degrees)+(LONG. Minutes/60)+LONG. Seconds/3600)) assigned by sample collector.
Lat	Latitude in decimal degrees calculated from the degrees, minutes and seconds, i.e. ((LAT. Degrees)+(LAT. Minutes/60)+LAT. Seconds/3600)) assigned by sample collector.
CatNo	Alphanumeric identifier used to track groups of samples released by the database manager to a chemistry laboratory for analysis. Catalogs may be processed separately in different batches (see "QCBatch" below).
QCBatch	Identifier supplied by the analytical laboratory used to track batches of samples which were analyzed together.
Batch	An alphanumeric identifier used for tracking samples stored in the custodian's freezer. The code reflects the year (i.e. 89, 90, etc.) and the originating agency (V or R = NOAA, F = Fish&Wildlife Service).
SampType	Identifies the type of sample: ENV = environmental, EXP = laboratory.
SampQual	Describes the quality of the sample upon receipt by the custodians. Inappropriately collected, documented or damaged samples are identified with one of the following codes.

Table 1, continued.

FIELD NAME	DESCRIPTION
SampQual	This code combines the total time the sample has not been in a freezer since its collection with a letter code from the following list. 00# - Hours until sample was frozen (ex. 006 = 6h until frozen) A Archival Sample BF Arrived at archival facility broken BL Arrived at analytical facility broken D Sample questionable DE Decomposing sample F Sample not acceptable - excessive time for processing IS Insufficient sample for analysis ND Sample destroyed during analysis NO Analysis not possible for other reasons P Sample poorly labeled PQ Sample partially thawed but still cold with ice crystals Q Sample thawed in transit S Sample subsectioned immediately prior to analysis T Sample thawed, subsectioned, then frozen X Improper sample Example: A field sample that was taken 6 hours before it was frozen then thawed during a 12 hour transit to the archival facility would receive a code of Q018 (Q = sample thawed in transit and 6h + 12 h = 18 hours).
QCERROR	Identifier of reliability of the analytical results for individual samples. GOOD = No problems with analytical data BIAS = Probable problems with analytical data (Short et al. 1996b).

Table 2. Hydrocarbon names and field name abbreviations found in the Exxon Valdez Oil Spill of 1989: State/Federal Trustee Council Hydrocarbon Database (EVTHD). All hydrocarbon results for tissues and sediments are reported in concentrations of ng of hydrocarbon/g of matrix (wet weight). Results for hydrocarbon analyses of water are reported in ng hydrocarbon per liter of water (ng/L). PAH used to evaluate samples for the presence of EVO are highlighted in **BOLD**.

HYDROCARBON NAME	FIELD NAME
Polynuclear Aromatics (PAH)	
Naphthalene	Naph
2-Methyl-Naphthalene	Menap2
1-Methyl-Naphthalene	Menap1
2,6-Dimethyl-Naphthalene	Dimeth
C2-Naphthalenes	C2naph
2,3,5-Trimethyl-Naphthalene	Trimeth
C3-Naphthalenes	**C3naph**
C4-Naphthalenes	**C4naph**
Biphenyl	Biphenyl
Acenaphthylene	Acenthy
Acenaphthene	Acenthe
Fluorene	Fluorene
C1-Fluorenes	C1fluor
C2-Fluorenes	**C2fluor**
C3-Fluorenes	**C3fluor**
Dibenzothiophene	Dithio
C1-Dibenzothiophenes	**C1dithio**
C2-Dibenzothiophenes	**C2dithio**
C3-Dibenzothiophenes	**C3dithio**
Phenanthrene	Phenanth
1-Methyl-Phenanthrene	Mephen1
C1-Phenanthrenes	**C1phenan**
C2-Phenanthrenes	**C2phenan**
C3-Phenanthrenes	**C3phenan**
C4-Phenanthrenes	**C4phenan**
Anthracene	Anthra
Fluoranthene	Fluorant
Pyrene	Pyrene
C1-fluoranthenes	C1Fluora
Benzo-a-anthracene	Benanth
Chrysene	**Chrysene**
C1-Chrysenes	**C1chrys**
C2-Chrysenes	**C2chrys**

Table 2, continued.

HYDROCARBON NAME	FIELD NAME
Polynuclear Aromatics (PAH), Continued.	
C3-Chrysenes	C3chrys
C4-Chrysenes	C4chrys
Benzo-b-fluoranthene	Benzobfl
Benzo-k-fluoranthene	Benzokfl
Benzo-e-pyrene	Benepy
Benzo-a-pyrene	Benapy
Perylene	Perylene
Indeno(1,2,3-c,d)pyrene	Indeno
Dibenzoanthracene	Dibenz
Benzoperylene	Benzop
Alkanes	
n-Decane	C10alk
n-Undecane	C11alk
n-Dodecane	C12alk
n-Tridecane	C13alk
n-Tetradecane	C14alk
n-Pentadecane	C15alk
n-Hexadecane	C16alk
n-Heptadecane	C17alk
Pristane	Pristane
n-Octadecane	C18alk
Phytane	Phytane
Nonadecane	C19alk
n-Eicosane	C20alk
n-Heneicosane	C21alk
n-Docosane	C22alk
n-Tricosane	C23alk
n-Tetracosane	C24alk
n-Pentacosane	C25alk
n-Hexacosane	C26alk
n-Heptacosane	C27alk
n-Octacosane	C28alk
n-Nonacosane	C29alk
n-Triacontane	C30alk
n-Hentriacontane	C31alk
n-Dotriacontane	C32alk
n-Tritriacontane	C33alk
n-Tetratriacontane	C34alk
Unresolved Complex Mixture	UCM

Table 2, continued.

HYDROCARBON NAME	FIELD NAME
Dueterated Surrogates (Recovery Filter)	
Deuterated Acenaphthene	Acend10
Deuterated Phenanthrene	Phend10
Deuterated Chrysene	Chryd12
Deuterated Perylene	Peryd12
Deuterated Naphthalene	Naphd8
Deuterated n-Dodecane	C12Alkd
Deuterated n-Hexadecane	C16Alkd
Deuterated n-Eicosane	C20Alkd
Deuterated n-Tetracosane	C24Alkd
Deuterated Triacontane	C30Alkd
Deuterated Benzo-a-pyrene	Benad12

Table 3. Abbreviated project names (PROJECTS) and descriptions for Natural Resource Damage Assessment and Restoration Projects contributing samples to EVTHD. Detailed descriptions and listings of investigator's names and addresses can be found in the documents listed at the end of this table.

Natural Resource Damage Assessment Projects

PROJECTS	DESCRIPTION OF THE PROJECT
AIRWAT2	Petroleum hydrocarbon induced injury to subtidal marine sediment resources
AIRWAT3	Geographic and temporal distribution of dissolved and particulate petroleum hydrocarbons the water column
BIRD 1	Beached bird survey to assess injury to water birds
BIRD3	Population surveys of seabird nesting colonies in Prince William Sound (PWS) and outside coast of the Kenai Penninsula, the Barren Islands
BIRD4	Assessment of bald eagles
BIRD5	Assessment of Peale's peregrine falcons
BIRD6	Assessment of abundance of marbled murrlets
BIRD7	Assessment of fork-tailed storm petrel reproduction
BIRD8	Assessment of blacklegged kittiwakes reproduction
BIRD9	Assessment of pigeon guillemots reproduction
BIRD11	Assessment of sea ducks
BIRD12	Assessment of injury to shorebirds staging and nesting in rocky intertidal habitats
COAHAB1	Prespill/postspill concentrations of hydrocarbons in sediments and mussels
FSHSHL1	Salmon spawning area injury
FSHSHL2	Injury to salmon eggs and pre-emergent fry in PWS
FSHSHL4	Impact of oil spill on juvenile pink & chum salmon & their prey
FSHSHL11	Injury to herring
FSHSHL13	Injury to clams
FSHSHL14	Injury to crabs
FSHSHL15	Injury to shrimp
FSHSHL16	Injury to oysters
FSHSHL18	Impacts of oil spill on bottomfish & shellfish in PWS
FSHSHL22	Injury to crabs outside PWS
FSHSHL24	Demersal fish injury
FSHSHL25	Scallop mariculture injury
FSHSHL26	Sea urchin injury
MARMAM1	Assessment of humpback whales in PWS, SE Alaska and Kodiak Archipelago
MARMAM2	Assessment of killer whales in PWS, Kodiak and Southeastern Alaska
MARMAM4	Assessment of steller sea lions in Gulf of Alaska
MARMAM5	Assessment of harbor seals in PWS & adjacent areas
MARMAM6	Assessment of impacts on Sea Otter populations in spill zone
TERMAM1	Assessment of Sitka black-tailed deer in PWS
TERMAM4	Assessment of brown bear populations in PWS

Table 3, continued.

Restoration Project List

PROJECTS	DESCRIPTION OF THE PROJECT
RARCH	Effects of contamination of crude oil on archaeological sites in the Gulf of Alaska
RDH	Harlequin duck assessment
RMB	Recovery monitoring of intertidal oiled mussel beds
RSLA	Shoreline assessment
RSUB	Subtidal monitoring of the recovery of sediments & eelgrass communities

The following documents provide descriptions of all the projects listed above, these descriptions include the name of the investigators and their associated agencies, as well as sampling designs and objectives. They can be obtained from:

Oil Spill Information Office
645 G. Street
Suite 401
Anchorage, AK 99501-3451

Phone in Alaska: 1-800-478-7745
Phone outside Alaska: 1-800-283-7745
Email ospic@calvino.alaska.net
Web Site http://www.alaska.net/~ospic/

State/Federal Natural Resource Damage Assessment Plan for the Exxon Valdez Oil Spill. August 1989.

The 1990 State/Federal Natural Resource Damage Assessment Plan for the Exxon Valdez Oil Spill. Vol I: Assessment and Restoration Plan Appendices A, B, C

The 1991 State/Federal Natural Resource Damage Assessment Plan for the Exxon Valdez Oil Spill. Vol I: Assessment and Restoration Plan Appendices A, B, C

Exxon Valdez Oil Spill Restoration. Volume II. 1992 Draft Work Plan. April 1992.

Exxon Valdez Oil Spill Restoration. 1993 Final Work Plan. July 1993.

Exxon Valdez Oil Spill Restoration. Draft 1994 Work Plan. (With Brief Project Descriptions) December 1994.

Fiscal Year 1995 Work Plan. December 1994.
Draft Fiscal Year 1995 Work Plan. Supplement Volume I. Brief Project Descriptions.

Table 4. *Location abbreviations* (LOCATABV), site names, latitude and longitude for sampling sites for samples in EVTHD. Latitudes and longitudes are expressed in decimal degrees, minutes and seconds, i.e. ((Long. degress) + Long. minutes/60) + long seconds/3600)) as assigned by the sample collector.

Cr = Creek B = Bay I = Island L = Lake R = River Pa = Peninsula

LOCATABV	SITE NAME	LATITUDE	LONGITUDE
106GL	Gladhough Cr	60.88617	146.6912
107BL	Black Cr	60.90733	146.7223
115MI	Millard Cr	60.9215	146.588
116DU	Duck R	60.92472	146.5911
117IN	Indian Cr	60.95284	146.6238
11HU	Humpy Cr	60.60833	145.6733
120DO	Donaldson Cr	60.98717	146.6888
121LE	Levshakoff Cr	61.02133	146.6395
122NN	No Name Cr	61.01983	146.6097
123GR	Gregorieff Cr	61.0185	146.6018
131GO	Gorge Cr	60.67167	146.4883
133SA	Sawmill Cr	61.084	146.43
143SI	Siwash Cr	60.95833	147.6833
153ST	Stellar Cr	61.05167	146.8058
19TL	Twin Lakes Cr	60.6355	145.8052
213BE	Bench Mark Cr	60.99267	147.2043
214LO	Long Creek	61.00783	147.222
216VA	VanIhing Cr	60.99166	147.2752
21RO	Rogue Cr	60.64611	145.8086
221EI	Eickelberg Cr	60.9325	147.3283
224BA	Backyard Cr	60.90028	147.3794
229CE	Cedar Cr	60.97267	147.3703
234WE	Wells R	60.02667	147.4088
258JO	Jonah Cr	61.01222	147.6744
259JO	Johah Cr	60.00733	147.6712
264SI	Siwash R	60.95861	147.6814
265UN	Unakwik Cr	60.95028	147.6122
276BL	Black Bear Cr	60.90333	147.705
278CO	Comeback Cr	60.92283	147.7317
282GO	Good Cr	60.93567	147.7422
283BA	Bad Cr	60.92017	147.7523
303TR	Triple Cr	60.90167	147.9317
307VI	Village Cr	60.93056	148.0305
35KO	Koppen Cr	60.70417	145.8918
370CH	China Poot Cr	59.3323	151.25

Table 4, continued.

LOCATABY	SITE NAME	LATITUDE	LONGITUDE
37AL	Allen Cr	60.66917	146.0225
414HA	Harrlon Cr	60.98833	148.1907
41PA	Pass Cr	60.65983	146.2087
421MI	Mill Cr	60.95233	148.3235
424OL	Old Cr	60.90667	148.3083
425HU	Hummer Cr	60.85633	148.309
428PI	Pirate Cr	60.85667	148.3043
430ME	Meacham Cr	60.8565	148.3867
432SW	Swanson Cr	60.8425	148.406
450TE	Tebenkoff Cr	60.754 17	148.4733
454HA	Halferty Cr	60.7175	148.4139
455PA	Paulson Cr	60.70111	148.3953
469WI	Wickett Cr	60.6865	148.2833
46CO	Comfort Cr	60.706	146.075
479CU	Culross Cr	60.624	148.2033
480MI	Mink Cr	60.59167	148.2517
484EF	E. Finger Cr	60.55967	148.338
485WF	W. Finger Cr	60.591	148.3912
48BE	Beartrap R	60.78617	146.97
493MO	Most Cr	60.5175	148.2244
495CH	Chimevlky L	60.48389	148.1919
498MC	Mcclure Cr	60.4925	148.1685
506LO	Loomi Cr	60.48833	147.9697
507GU	Gumboot	60.47133	147.9902
508SO	Solf	60.4585	148.0517
510EL	Ellhansky	60.45716	148.0703
51OL	Olsen Cr	60.74117	146.1433
52CO	Control Cr	60.74183	146.2208
54CA	Carlsen Cr	60.74183	146.2208
56SM	St. Matthews	60.77433	146.2688
601PA	Paddy Cr	60.40867	148.0925
602NA	Nacktan Cr	60.42667	148.0922
603EW	Ewan Cr	60.40083	148.1706
604ER	Erb Cr	60.40083	148.1706
610KO	Kompkoff R	60.35783	148.2578
611JA	Jackpot Cr	60.355	148.2593
613JA	Jackson	60.32233	148.2723
618ES	E. Shore Chen	60.36967	147.9892
621TO	Totemoff Cr	60.3395	148.0967
623BR	Brizgaloff	60.33694	148.1006

Table 4, continued.

LOCATABV	SITE NAME	LATITUDE	LONGITUDE
628CH	Chenega	60.3325	148.0119
630BA	Bainbridge Cr	60.20528	148.2964
632CL	Claw Cr	60.21472	148.2092
633PA	Pablo Cr	60.15861	148.2178
637PC	Point Countess	60.225	148.1217
653HO	Hogg Cr	60.08972	148.1844
655JO	Johnson Cr	60.12583	148.1211
656HA	Halverson Cr	60.12833	148.107
663SH	Shelter B	60.125	147.9311
665BJ	Bjorn	60.835	147.935
666OB	O'Brien Cr	60.0775	147.9961
673FA	Falls Cr	60.98933	147.9738
677HA	Hayden Cr	60.33633	147.9055
678SB	Sleepy B	60.5095	147.8358
681HO	Hogan B	60.21	147.7581
682SN	Snug Harbor	60.26111	147.77
692HE	Herring B	60.44028	147.785
695DR	Drier B	60.35167	147.7667
699DR	Drier B	60.28333	147.8392
707MA	Macleod Cr	59.89778	147.7375
710HA	Hanning Cr	59.95	147.6889
711QU	Quadra Cr	59.97361	147.6592
739SW	Swamp Cr	60.19167	147.3039
740KE	Kelez Cr	60.20611	147.3667
744WI	Wilby Cr	60.24833	147.22
745WI	Wild Cr	60.24278	147.1972
746SC	Schuman Cr	60.24217	147.1863
747CA	Cabin Cr	60.27222	147.1847
749SH	Shad Cr	60.27833	147.1953
754DR	Dry Cr	60.30433	147.1733
758RO	Rocky B	60.33767	147.139
759RO	Rocky Cr	60.33528	147.1239
76IR	Irish Cr	60.75555	146.4319
770UD	Udall Cr	60.2625	147.0958
774RO	Rosswog Cr	60.27467	147.0265
775PA	Pautze Cr	60.29067	147.0042
788GR	Green Cr	60.28867	147.3717
806DO	Dog Salmon Cr	60.31833	146.5739
80WH	Whalen Cr	60.81833	146.1765
810GA	Garden Cr	60.3385	146.5083

Table 4, continued.

LOCATABV	SITE NAME	LATITUDE	LONGITUDE
812NU	Nuchek Cr	60.36583	146.4825
815CO	Constantine Harbor	60.37117	146.5882
827CA	Captain Cr	60.45417	146.5667
828CO	Cook Cr	60.45639	146.5342
831DO	Double Cr	60.45972	146.4481
83KE	Keta Cr	60.86806	146.1744
844MA	Makaka Cr	60.4875	146.2686
847HA	Hawkins Cr	60.51445	146.2239
849RO	Rollins Cr	60.51417	146.1144
850CA	Canoe Cr	60.5075	146.0833
851ZI	Zillesenoff	60.54972	146.0211
856WL	W. Lagoon Cr	60.54972	146.0211
857EL	E. Lagoon Cr	60.55695	146.0036
861BE	Bernard Cr	60.5555	146.9248
863OR	Orca Cr	60.58333	145.9125
87SU	Sunny R	60.88528	146.2345
89FC	Fish Cr	60.84167	146.3811
92SH	Shale Cr	60.8375	146.407
93KI	Kirkwood Cr	60.83639	146.41
99LA	Lagoon Cr	60.85833	146.5183
AGENC	Agnes Cove	59.76667	149.5733
AGULI	Aguliak I	60.3625	147.8755
ALFI	Alf I	57.39417	153.8533
ALUK	Aluklik Bay	60.02333	148.1333
AMOOP	Amook Passage	57.51667	153.8333
ANCOP	Anchor Point	59.80917	152.2531
ANTOL	Anton Larson	57.86666	152.6283
APPLI	Applegate I	60.35	146.4167
AUGUS	Augustine	59.32967	153.4782
AXELI	Axel I	60.76667	147.7833
BAINI	Bainbridge I	60.01333	148.2667
BAINP	Bainbridge P	60.14333	148.0933
BALBB	Balboa B	55.55667	160.5758
BARNC	Barnes Cove	60.30861	147.7619
BERGB	Berger B	58.33417	150.7333
BIGFI	Big Fort I.	58.50361	152.4211
BLACB	Black B	59.54111	150.215
BLACL	Black Lagoon	56.41667	158.95
BLIGI	Bligh I	60.83694	146.9169

Table 4, continued.

LOCATABV	SITE NAME	LATITUDE	LONGITUDE
BLOCI	Block I	60.51783	147.6007
BLONI	Blonde I	60.99861	147.645
BLUEF	Blue Fos B	58.44695	152.6769
BOISL	Bay of Isles	60.36333	147.7
BOSWR	Boswell R	60.41667	146.1
BUSKR	Buskin R	57.75722	152.485
CABIB	Cabin B	60.67528	147.455
CANPA	Canoe Passage	60.53333	146.1333
CCHIN	Cape Chiniak	58.51433	153.9092
CDOUG	Cape Douglas	58.88222	153.2889
CEDAB	Cedar B	60.93333	147.4333
CGULL	Cape Gull	58.235	154.1531
CHANI	Channel I	60.24028	147.3792
CHENI	Chenega I	60.26667	148.1
CHIBA	Chiginagak B	56.57	156.46
CHICI	Chicken I	60.045	148.925
CHIEC	Chief Cove	57.70889	153.8997
CHIGB	Chignik B	56.305	158.4047
CHISI	Chislwell I.	59.65222	149.5617
CHNTN	Chinitna	59.88	152.8967
CHUGI	Chugach I.	56.95	156.7667
CHUGB	Chugach B	59.18528	151.6247
CKUNM	Cape Kunmik	56.76667	157.1833
CLAMB	Clam B	60.65028	147.3681
CLAMC	Clam Cove	59.88334	152.9567
CLAMG	Clam Gulch	60.23333	151.4
CNUKS	Cape Nukshak	58.39167	153.9808
COLUG	College Fjord	60.89	147.7617
COLLF	Columbia Glacier	60.65667	147.3733
CONST	Constantine Harbor	60.34889	146.7606
COPRD	Copper R	60.36666	145.1833
CRABB	Crab B	60.07222	147.9972
CRAFI	Crafton I	60.48333	147.9333
CRESR	Cresent R	59.88	152.8967
CULLB	Culross B	60.75	148.1533
CULRI	Culross I	60.66667	148.1667
DAKAB	Dukauak B	58.04722	154.6478
DAYVI	Dayville	61.08694	146.2778
DEEPB	Deep B	60.58611	145.7833
DEERC	Deer Cove	60.24333	147.8917

Table 4, continued.

LOCATABV	SITE NAME	LATITUDE	LONGITUDE
DELEI	Delania I	60.33333	148.1167
DISCB	Discover B	58.33917	152.3433
DISKI	Diski I	60.48466	147.6512
DOUBB	Double B	60.45945	146.4692
DRIEB	Drier B	60.31333	147.82
EAGLE	Eaglek	60.815	147.7183
ELEAI	Eleanor I	60.53517	147.6083
ELIZI	Elizabeth I	59.16667	151.8333
ELLAM	Ellamar	60.88361	146.771
ELRII	Elrington I	59.96667	148.1667
ELRIP	Elrington Point	59.97167	148.1167
ESHAB	Eshamy B	60.44833	147.975
EVANI	Evans I	60.06667	147.95
EWANB	Ewan B	60.40278	148.14
FAIRI	Fairmont I	60.88	147.4583
FALLB	Falls B	60.52778	147.987
FLEMI	Fleming I	60.17305	148.0369
FOULB	Foul B	58.31667	152.7667
FOULP	Foul Passage	60.505	147.6533
FOXFA	Fox Farm	59.96667	148.1667
GALEB	Galena B	60.94333	146.64
GEOGB	Geographic B	58.06778	154.4881
GIBBO	Gibbon	60.27111	147.435
GLACS	Glacier Spit	59.86167	153.1417
GOLDC	Gold Cr	61.13472	146.4469
GOOSB	Goose B	60.70467	148.227
GOREP	Gore Point	59.195	150.9717
GRANB	Granite B.	60.41472	147.9564
GRAVB	Gravina B	60.60861	146.3031
GREEI	Green I	60.19056	147.9061
GULLI	Gull I	60.725	146.7028
HALLB	Hallo B	58.421	54.0311
HARRB	Harbor I	59.73972	149.8417
HARTB	Hartney B	60.48333	145.9
HAWKI	Hawkins I	60.51667	146.0833
HEATB	Heather B	60.985	147.0222
HELLH	Hells Hole	60.70222	146.3833
HERRB	Herring B	60.38334	147.8533

Table 4, continued.

LOCATABV	SITE NAME	LATITUDE	LONGITUDE
HERRP	Herring Point	60.44333	147.819
HINCI	HinchinbR I	59.345	146.0175
HORNC	Horn Cr	59.875	153.07
HORSB	Horseshoe B	60.01611	147.9578
IKTUB	Iktua B	60.1	147.9944
INGOI	Ingot I	60.54333	147.6483
ITALB	Italian B	60.21833	147.9014
IVANB	Ivanof B	55.80528	159.478
JAKAB	Jakalof B	59.47	151.5358
JEANC	Jeanie Cove	59.83333	147.5833
JOHNC	Johnson Cove	60.06194	147.977
JUNCI	Junction I	60.39167	147.9917
KALSB	Kalsin B	57.62722	152.34
KASHB	Kashvik B	57.90667	155.0703
KATMB	Katmai B	57.88667	155.0917
KATNM	Katmai N.M.	57.95	147.952
KIUKP	Kiukpalik	58.58556	153.5542
KIZHB	Kizhuyak B	57.73034	152.937
KNIGI	Knight I	60.13983	147.681
KOBUG	Kobugakli	57.86666	155.1333
KODIA	Kodiak	57.71833	152.4333
KUKAB	Kukak B	58.29445	154.26
KULIB	Kuliak B	58.172	154.2815
KUPRS	Kupreanof Str	57.96111	153.1294
LARSB	Larsen B	57.51667	153.9183
LATOI	Latouche I	60.0625	147.8158
LATOP	Latouche Pa	59.95	148.055
LGREI	Little Green	60.205	147.5083
LHERR	Low Herring B	60.38667	147.8156
LILJP	Ljegren Pa	60.70833	147.4022
LISMI	Lit. Smith I.	60.52167	147.433
LITTB	Little B	60.16917	147.7967
LONEI	Lone I	60.68333	147.75
LONGB	Long B	60.67667	148.28
LOUIB	Louis B	60.47167	147.6783
LUCKB	Lucky B	60.23	147.8583
MACLH	Macleod Harbor	59.71667	148.1083
MAINB	Main B	60.54361	148.0681
MALLB	Mallard B	60.29167	147.8133
MARSB	Marsha B	60.32028	147.6706

Table 4, continued.

LOCATABV	SITE NAME	LATITUDE	LONGITUDE
MCARP	McArthur Pas	59.46222	150.3797
MCCLB	McClure B	60.48333	148.185
MCDOL	McDonald's Lagoon	58.15278	152.3278
MCPHP	McPherson Pg	60.662	147.3815
MINEC	Mineral Cr	61.12917	146.4061
MISSB	Mislsak B	58.135	154.3295
MONAB	Monashka B	57.8175	152.4217
MONAC	Monashka Cr	57.8175	152.4217
MONTI	Montague I	60.04167	147.76
MONTL	L. Montague	60.00417	147.8314
MONTG	Montague Coast	59.345	147.0175
MONTP	Montague P	60.3678	147.1
MONTS	Montague Str	60.07633	147.68
MONTT	Montague Tr	59.70055	147.6364
MONTU	Montague	60.43167	147.0183
MOOSL	Moose Lips B	60.18778	147.4378
MORNC	Morning Cove	59.44972	150.3303
MUMMB	Mummy B	60.23333	147.8
MUMMI	Mummy I	60.31667	147.9167
MUSKB	Muskomee B	58.07117	153.1133
NAKEI	Naked I	60.49583	147.5922
NEARI	Near I	57.78	152.3933
NECPT	Nec Point	59.81	47.6833
NEDDL	Needle	60.1175	147.5725
NEKIT	Nekita B	58.62944	152.3542
NELSB	Nelson B	60.51667	145.8667
NEWYI	New Years I	60.31667	147.9333
NHINC	North Hinchinbrook	60.46889	146.688
NINAI	Ninagiak I	58.455	153.9981
NINIL	Ninilchik	60.325	151.6639
NORTI	North I	60.63334	145.7333
NUKAI	Nuka I	59.39	150.6217
NWBAY	Northwest B	60.54361	147.6025
OLSEN	Olsen B	60.7055	146.2168
ONEHB	One Hand B	59.21722	151.2239
OPALC	Opal Cr	60.49683	147.6958
ORCAB	Orca B	60.51667	145.8417
OUTSI	Outside B	60.39333	147.4333
PADDB	Paddy B	60.4175	148.0958

Table 4, continued.

LOCATABV	SITE NAME	LATITUDE	LONGITUDE
PASSB	Passage B	60.13334	148.0833
PAULB	Paul's B	58.34833	152.38
PBAIL	Point Bailey	57.42	152.9964
PCHAL	Port Chalmers	60.23333	147.25
PDICK	Port Dick	59.25555	151.1081
PEAKI	Peak I	60.69833	147.3967
PELLC	Pellen Cove	60.85972	147.6589
PEREI	Perevalnie I	58.63055	152.3633
PERLI	Perl I	59.12167	151.6267
PERRI	Perry I	60.66806	147.8667
PETCH	Port Etches	60.37167	146.7958
PETRP	Petrof Point	59.3775	150.765
PFIDA	Port Fidalgo	60.77472	146.5042
PGRAH	Port Grahm	59.37	151.89
PGRAV	Port Gravina	60.63334	147.25
PHELE	Point Helen	60.16333	147.7558
PLEII	Pleiades I	60.27833	148.0667
PNELJ	Port Nellie	60.61666	148.1033
POLLC	Polly Cr	60.28333	152.4467
PUALE	Paule B	57.73333	155.3967
PUFFB	Puffin B	60.73333	147.4167
PUFFC	Puffin Cr	60.18444	148.3208
PWELL	Port Wells	60.83083	148.1911
QUICC	Quicksand Cr	59.78611	149.7867
RASBS	Raspberry St	58.045	153.0417
REDRI	Red R	59.97667	152.6686
ROCKB	Rocky B	59.21056	151.3103
RUACO	Rua Cove	60.34861	147.6408
RUGGI	Rugged I	59.85833	149.3833
RUTHB	Ruth B	59.32972	153.4781
SADIC	Sadie Cove	59.465	151.3383
SALMP	Salmo Point	60.59167	145.8
SANTF	Santa Flava	57.29945	152.865
SAWMB	Sawmill B	60.05556	148.015
SAWMC	Sawmill Cr	61.08472	146.4367
SEALB	Seal B	58.45	152.2833
SEALI	Seal I	60.43	147.4067
SELDB	Seldovia B	59.42333	151.7078
SEWAR	Seward	60.1	149.4433
SGREE	S.Green I.	60.24983	147.39

Table 4, continued.

LOCATABV	SITE NAME	LATITUDE	LONGITUDE
SHARB	Sharatin B	57.79633	152.7827
SHEEB	Sheep B	60.61666	145.9833
SHEEP	Sheep Point	60.61666	145.9833
SHELB	Shelter B	60.12733	147.9169
SHOUB	Shoup B	61.12083	146.5917
SHUYI	Shuyak I	58.50889	152.6292
SIMPB	Simpson B	60.62167	145.925
SIWAB	Siwash B	60.95417	147.6806
SLEEB	Sleepy B	60.06583	147.8392
SLOPM	Slope Mt.	60.08167	152.5717
SMITI	Smith I	60.51472	147.4256
SNUGC	Snug Corner	60.745	146.6947
SNUGH	Snug Harbor	60.06694	147.8361
SPIRB	Spiridon B	57.70195	153.8836
SPIRP	Spring Point	59.875	152.86
SQUIB	Squire B	60.23222	147.9528
SQUII	Squire I	60.21667	147.9333
SQURB	Squirrel B	60.01167	148.14
STOCH	Stockdale H.	60.29417	147.2081
STORI	Storey I	60.72028	147.407
SUNNC	Sunny Cove	59.91139	149.3308
TAGNI	Tagness I	60.61833	147.3833
TAKLI	Takli I	58.06778	154.4881
TAYLB	Taylor B	59.31194	151.0217
TERRB	Terror B	57.7265	153.2165
TETRP	Tetrakof Point	58.515	152.3933
THUNB	Thunder B	59.5775	154.1039
TONSB	Tonsina B	59.21722	151.2239
TONSR	Tonsina R	58.21	151.95
TUGII	Tugidak I	56.56889	154.53
TURNA	Turnagain Arm	60.84667	148.975
TUXEB	Tuxedni B	60.16	152.6675
TWOAB	Two Arm B	59.58556	150.0672
TWOMB	Two Moon B	60.73333	146.5733
UGAKB	Ugak B	56.44278	153.0333
UGANB	Uganik B	57.51722	152.9358
UNAKW	Unakwik	60.99667	147.5444
USHAI	Ushagat I	58.9	152.2833
UYAKB	Uyak B	57.51667	153.8333
VALDA	Valdez Airport	61.13334	146.2792

Table 4, continued.

LOCATABV	SITE NAME	LATITUDE	LONGITUDE
VALDE	Valdez	61.1	146.4167
VERDC	Verdant Cove	59.69667	149.7389
WAMAI	West Amatuli	58.91667	151.95
WELLB	Wells B	60.93667	147.4822
WELLP	Wells Pass	60.755	148.1767
WESTB	West B	60.86267	146.7747
WHALB	Whale B	60.205	148.297
WIDEB	Wide B	57.43945	156.2303
WILSB	Wilson B	60.03389	147.9286
WINDB	Windy B	59.22	151.4703
WOMAB	Woman's B	57.70861	152.5539
WOODI	Wooded I	59.86666	147.4
YALIB	Yalik B	59.45472	150.6067
ZAIKB	Zaikof B	60.2675	147.0892

Table 5. Abbreviations for agencies (AGENCY) responsible for collecting EVTHD sample information.

AGENCY	AGENCY NAME
ADEC	Alaska Department. Of Environmental Conservation
ADFG	Alaska Department. of Fish and Game
FWS	U. S. Fish & Wildlife Service
NBS	National Biological Service
NMFS ABL	NMFS*-Auke Bay Laboratory (Juneau, AK)
NMFS ECD	NMFS*-Environmental Conservation Division (Seattle, WA)
NMFS KOD	NMFS*-Kodiak Laboratory (Alaska)
NMFS MML	NMFS*-Marine Mammal Laboratory (Seattle, WA)
NPS	National Park Service
UA IAB	Univ. of Alaska Fairbanks - Institute of Arctic Biology
UA IMS	Univ. of Alaska Fairbanks -Institute of Marine Science
UA JCFOS	Univ. of Alaska Fairbanks - Juneau Center for Fisheries and Ocean Science
UAF	Univ of Alaska Fairbanks

* NMFS National Marine Fisheries Service

Table 6. Abbreviations used to describe sample collection methods (COLMETH) for samples in EVTHD.

COLMETH	METHOD
BSEI	Beach Seine
CAMU	Caged Mussel
COCU	Cookie Cut-spatula
CORE	Core Sample
CSEI	Cliff Seine
DCAP	Died in Capativity
DIVE	Diver
DNET	Dip Net
FDEA	Found Dead
FORC	Forceps
GNET	Gillnet
GRAB	Grab Sampler
HAND	Taken by Hand
POT	Underwater Pot
PSEI	Purse Seine
PUMP	Pump
RAKE	Rake
SEIN	Seine (General)
SHOT	Shotgun
SHOV	Shovel
SPEA	Spear
SPOO	Spoon
SSAM	Special Hydrocarbon
STRA	Sediment Trap
SUBM	Submersible
TPDR	Tongue Depressor
TRAW	Trawl
VGRB	Van Veen Grab (Dredge)

Table 7. Submatrix abbreviations (SUBMAT) used to more clearly define types of tissues sampled and reported in EVTHD. Only abbreviations are shown, many other entries in this field completely describe the submatrix.

SUBMAT	TYPE OF SUBMATRIX
EGG C	Egg Contents
EGG S	Egg Shell
GUT C	Gut Contents
HEPAT	Hepatopancreas
INTESTIN	Iintestines
OVARYC	Ovary Contents
RUMENCON	Rumen Contents
SED/FIL	Sediment Trap Filtrate
STOM OIL	Stomach Oil
STOMCON	Stomach Contents
SUBSTRAT	Substrate

Table 8. Species abbreviations (SPECABV), common and Latin names for organisms whose tissues were sampled for hydrocarbons and reported in EVTHD. Table is sorted by SPECABV.

SPECABV	COMMON NAME	SPECIES
ANMU	Anciet Murrelet	*Synthliboramphus antiquus*
BACA	Barnacle	*Balanus cariosus*
BAEA	Bald Eagle	*Haliaeetus leucocephalus*
BAGO	Barrow's Goldeye	*Bucephala islandica*
BLKI	Black Leg Kittiwake	*Rissa tridactyla*
BLOY	Am. Blk. Oyster	*Haematopus bachmani*
BLSC	Black Scoter	*Melanitta nigra*
BLTU	Black Turnstones	*Arenaria melanocephala*
BRBE	Brown Bear	*Ursus arctos*
CLAM	Clam	Bivalvia (Class)
CLIN	Nattall's Cockle	*Clinocardium nuttalii*
COGO	Common Goldeneye	*Bucephala clangula*
COLO	Common Loon	*Gavia immer*
COMU	Common Murre	*Uria aalge*
CSCA	Scallop Chlamys	Chlamys Ssp.
CSHR	Coonstripe Shrimp	*Pandalus hypsinotus*
DROC	Dusky Rock	*Sebastes ciliatus*
DSOL	Dover Sole	*Microstomus pacificus*
DUNG	Dungeness Crab	*Cancer magister*
EELG	Eel Grass	*Zostera marina*
FISH	Unidentified Fish	
FLAT	Unidentified Flatfish	
FSOL	Flathead Sole	*Hippoglossoides elas*
FTSP	Forked Tail Storm Petrel	*Oceanodroma furcata*
FUCU	Fucus	Fucus Spp.
GARI	Bivalve	*Garia californica*
GURC	Green Sea Urchin	*Strongylocentrotus droebachiensis*
GW	Gray Whale	*Eschrichtius robustu*
HADU	Harlequin Duck	*Histrionicus histrionicus*
HASE	Harbor Seal	*Phoca vitulina*
HERR	Pacific Herring	*Clupea harengus*
HP	Harbor Porpoise	*Phocoena phocoena*
HUMI	Bivalve	*Humilaria kennerleyi*
KCRA	Red King Crab	*Paralithodes camtschatica*
KIMU	Kittlitz Murrele	*Brachyramphus brevirostris*
KW	Killer Whale	*Orcinus orca*
LIMP	Limpet	Acmaeidae (Family)
LISP	Periwinkle Snail	Littorina Spp.

Table 8, continued.

SPECABV	COMMON NAME	SPECIES
MAMU	Marbled Murrelet	*Brachyramphus marmoratus*
MCLA	Macoma Clam	*Macoma balthica*
MUSS	Pacific Blue Mussel	*Mytilus trossulus*
MW	Minke Whale	*Balaenoptera acutorostrata*
OYST	Pacific Oyster	*Crassostraea gigas*
PCLA	Little Neck Clam	*Protothaca staminea*
PCOD	Pacific Cod	*Gadus macrocephalus*
PEFA	Peregrine Falcon	*Falco peregrinus*
PIGU	Pigeon Guillemot	*Cepphus columba*
PINK	Pink Salmon	*Oncorhynchus gorbuscha*
PRIC	Prickleback	*Anoplarchus purpurescens*
PSCA	Weather Scallop	*Patinopecten caurinus*
RCLA	Pacific Razor Clam	*Siliqua patula*
ROSA	Rock Sandpiper	*Calidris ptilocnemis*
SBTD	Sitka Deer	*Odocoileus hemionus*
SCLA	Butter Clam	*Saxidomus giganteus*
SCUO	Tidepool Sculpin	*Oligocottus maculosus*
SEOT	Sea Otter	*Enhydra lutris*
SL	Sea Lion	*Eumetopias jubatus*
SNAI	Unidentified Snail	
SSHR	Spot Shrimp	*Pandalus platyceros*
SSHT	Sidestrip Shrimp	*Pandalopsis dispar*
SURF	Surfbird	*Aphriza virgata*
SUSC	Surf Scoter	*Melanitta perspicillata*
TANN	Tanner Crab	*Chionoecetes bairdi*
WGRE	White Spotted Greenling	*Hexagrammos stelleri*
WWSC	White Winged Scoter	*Melanitta fusca*
XIPH	Black Prickelback	*Xiphister atropurpureus*

MACHINE REQUIREMENTS FOR EVTHD

- ✓ IBM or compatible personal computer: 386 processor
- ✓ Windows version 3.1 or Windows 95
- ✓ 8 Mbytes of RAM
- ✓ VGA video display minimum
- ✓ 12 Mbytes free space on hard disk drive
- ✓ Mouse

INSTALLATION INSTRUCTIONS FOR EVTHD

WINDOWS 3.1

1) Boot up your computer
2) Insert EVTHD PROGRAM DISK 1 into your disk drive, note which drive you used.
3) Select "File" from the Program Manager menu bar.
4) Select "Run..." from the "File" pick list.
5) If EVTHD PROGRAM DISK 1 is in the A: drive, type "A:Setup" in the box, and hit "ENTER", otherwise enter the appropriate drive letter.
6) Setup will initialize. Installation of all 4 disks should take about 8 minutes.
7) Accept the default path by clicking on "Continue", or enter a new path first.
8) Exchange disks with the one in the drive, when prompted by Setup.
9) Once the installation is complete you should reboot your computer.

WINDOWS 95

1) Boot up your computer
2) Insert EVTHD PROGRAM DISK 1 into your disk drive, note which drive you used.
3) Select the "Start" button
4) Select "RUN" from the pick list.
5) Type in the phrase "A:setup" and then select "OK", if the EVTHD PROGRAM DISK 1 is in the A: drive, otherwise insert the appropriate letter. You may get the following warning message " can not copy file a:\ DDEML.DL since the destination file already use" when loading disk 1. This just refers to a driver file many Windows 95 applications already have installed, therefore disregard this warning and proceed with the installation
6) Setup will initialize. Installation of all 4 disks should take about 8 minutes.
7) Accept the default path by clicking on "Continue", or enter a new path first.
8) Exchange disks with the one in the drive, as prompted by Setup.
9) Once the installation is complete you should reboot your computer.

After installation, EVTHD can be found in the folder labeled EVTHD. Open the folder and select the hydrocarbon icon labeled EVTHD.

PART II

Identification of *Exxon Valdez* Oil in Sediments and Tissues from Prince William Sound and the Northwestern Gulf of Alaska Based on PAH Weathering

Identification of *Exxon Valdez* Oil in Sediments and Tissues from Prince William Sound and the Northwestern Gulf of Alaska Based on PAH Weathering

JEFFREY W. SHORT* AND RON A. HEINTZ

National Marine Fisheries Service, NOAA, Alaska Fisheries Science Center, Auke Bay Laboratory, 11305 Glacier Highway, Juneau, Alaska 99801-8626

Keywords: petroleum; weathering; *Exxon Valdez*; PAH; fingerprinting; oil spill

November 1996

We used a first-order loss-rate kinetic model of polynuclear aromatic hydrocarbon (PAH) weathering to evaluate 7767 environmental samples collected for the *Exxon Valdez* oil spill (EVOS) of March 1989 for the presence of spilled oil. The model was developed from two successive experiments with gravel coated with Alaska North Slope crude oil and washed for 6 months. The 14 most persistent PAH of 44 analyzed by GC/MS were included in the PAH-weathering model. Parameters include loss-rate constants related to the energy required for PAH to escape from petroleum through the Arrhenius equation, and a quantitative index of weathering. The model accounts for 91% of the temporal variability of modeled PAH concentrations; the remaining variability is ascribed to relatively small interferences of tetramethylnaphthalenes and di- and trimethylfluorenes.

We applied the weathering model to analytical results from field samples collected for the EVOS by comparing the fit of model-predicted versus measured PAH concentrations, with a probability distribution of fits derived from the experimental weathering results. Only 1541 field samples contained sufficient PAH for valid application of the model; three-fourths fit the model at $\alpha \geq 0.01$ type I error, 9% fit an alternate model characterized by the absence of weathering, 17% fit neither model, and a few fit both models. The 1164 total samples that fit the weathering model account for 86% of all the PAH concentrations detected in all 7767 samples. We conclude that first-order loss-rate kinetics accounts for PAH weathering in the laboratory and for the dominant PAH weathering processes in the EVOS, and that the rate of weathering is determined mainly by the ratio of surface area to volume of petroleum in the environment.

Introduction

Identification of a petroleum pollution source based on chemical analysis of environmental samples is complicated by time-varying compositional changes (weathering) following introduction into the environment. The effects of weathering processes such as evaporation, dissolution, microbial degradation, and photo-oxidation that cause the composition of petroleum to vary in the environment seem difficult to predict because they are sensitive to a plethora of varying environmental conditions. Compositional changes caused by weathering have, therefore, constrained identification methods to those that are based on stable and persistent parameters derived from chemical analysis of environmental samples (*1*), or that explicitly account for the compositional changes, e.g. by comparison of analytical results from environmental samples with results from petroleum samples that have been artificially weathered to varying degrees (*2*).

The above weathering processes imply first-order (FO) loss-rate (LR) kinetics for the disappearance of polynuclear aromatic hydrocarbons (PAH) from petroleum. Evaporation and dissolution involve FOLR kinetics explicitly, with rate constants determined by the enthalpy of vaporization through the Arrhenius equation. Similar FOLR disappearance kinetics have recently been demonstrated for microbial oxidation of petroleum PAH (*3*), where PAH dissolution is promoted by biosurfactants secreted by microbes (*4*) that increase the effective surface area of the petroleum phase. The disappearance kinetics that characterize dissolution and microbial oxidation are, therefore, probably similar to evaporation qualitatively, and the distribution pattern of PAH that results from the combined effects of these processes characteristically include preferential losses of PAH that have lower molecular weight and

contain fewer alkyl substituents (*1*, *5–9*). In contrast, the kinetics of PAH photo-oxidation may be second order and autocatalytic (*10*). Photo-oxidation of PAH probably begins with photolytic generation of mainly benzylic free radicals (*11*), which would result in preferential losses of PAH that contain more numerous alkyl substituents. However, at low ambient light fluxes PAH photo-oxidation rates may be small compared with rates for evaporation and dissolution.

If the dominant PAH weathering processes include evaporation, dissolution, and microbial oxidation, but not photo-oxidation, then similar overall FOLR kinetics for PAH disappearance from petroleum result. Although the absolute concentrations of PAH constituents of petroleum may depend in a complicated way on the environmental history of a sample, the similar FOLR kinetics imposes constraints on relative PAH concentrations in weathered samples of petroleum. These constraints may provide a basis for identification of a major petroleum source in environmental samples if alternative sources can be distinguished with confidence.

We report here our experimental validation of a FOLR kinetic model to describe the disappearance of PAH from gravel coated with experimentally-weathered petroleum, and our subsequent evaluation of this model as a basis for identifying petroleum spilled from the T/V *Exxon Valdez* in environmental samples of sediments and tissues. We measured PAH concentration changes of the petroleum over 6 months of exposure to flowing, intermittently brackish water, and fit the results to a FOLR kinetic model. We developed a least-squares parameter estimation procedure for the model; these parameters include relative kinetic constants for disappearance of each of 14 PAH analytes monitored, and a metric for each

gravel sample collected, indicating the extent of weathering. We used these results to develop a probability-based method to distinguish between PAH derived from petroleum released into the area affected by the T/V *Exxon Valdez* oil spill (EVOS) of 24 March 1989 and PAH in Prince William Sound (PWS) and the northern Gulf of Alaska from alternative sources.

The EVOS provided a unique opportunity to evaluate the petroleum identification procedure we derived. Photo-oxidation was probably suppressed by the low sun angle and persistent cloud cover characteristic of the affected area, compared with more temperate regions. The EVOS area was nearly pristine before the spill (*12, 13*), and PAHs from natural sources were mainly confined to subtidal sediments in that area (*14–16*), so PAH interferences from sources other than the EVOS were often minimal in environmental samples. Moreover, the PAH pattern that characterizes the dominant natural source of PAH in marine sediments of PWS is temporally invariant and thus apparently not subject to weathering (*13*). This natural and stable PAH source provides an alternative pattern that may be used to evaluate the discriminating power of our identification method. Finally, the number of environmental samples collected and analyzed by consistent GC/MS methods (*17*) was exceptionally large (7767 analyses), and the analytical methods and spilled petroleum are directly comparable with those used for the weathering experiment we performed to evaluate the kinetic model. Therefore, the EVOS may be considered an especially large-scale field test for our kinetic model.

Model Description and Parameter Estimation

Suppose the rate of loss to the environment of a PAH (denoted as P) dissolved in petroleum follows FOLR kinetics, so that

$$-\frac{d[P]}{dt} = k(t)[P] \quad (1)$$

The time dependence of the LR constant, $k(t)$, derives from the variable exposure conditions of the petroleum in the environment. Writing $k(t)$ as $k\,f(t)$ and integrating eq 1 gives

$$\ln\left(\frac{[P]_0}{[P]}\right) = k\int_0^t f(t)dt = kw \quad (2)$$

where the value of the integral in eq 2 is indicated by a weathering parameter, w, which summarizes the exposure history of the petroleum volume element sampled.

Equation 2 may be simultaneously applied to J different PAH in each of I different samples as

$$\ln\left(\frac{[P_{ij}]_0}{[P_{ij}]}\right) = k_j w_i \quad (3)$$

where j specifies the PAH and i specifies the sample. Note that each k_j is the same for all samples, and that each w_i is the same for all the PAH in a sample. If the initial concentrations $[P_{ij}]_0$ in an environmental sample are known, the parameters k_j and w_i may be estimated from measurements of the $[P_{ij}]$ in the samples (see below).

The initial PAH concentrations $[P_{ij}]_0$ in an environmental sample may be estimated from the initial amount and composition of the petroleum in the sample. The initial amount

of petroleum introduced into unit mass of the sampled environmental matrix can be determined if there are temporally invariant analytes contained in the petroleum, denoted here as j^+ (and assuming the analyte set is restricted to PAH). Denoting the proportion of the jth PAH in the unweathered petroleum as π_j, then the concentration c_i of unweathered petroleum originally introduced into the ith sample is determined as the ratio of $[P_{ij+}]$ (= $[P_{ij+}]_0$) to π_{j+}. The mean of these ratios may be used as an estimator of c_i,

$$\hat{c}_i = \frac{1}{n_{j+}} \sum_{j+ \in J} \frac{[P_{ij+}]}{\pi_{j+}} \tag{4}$$

where n_{j+} indicates the number of temporally invariant PAH included in the sum. Because $[P_{ij}]_0 = \hat{c}_i \pi_j$, eq 3 may be expressed as

$$d_{ij} = \ln \frac{\hat{c}_i \pi_j}{[P_{ij}]} = k_j w_i \tag{3a}$$

Note that the quantity indicated by d_{ij} may be determined entirely from measurements of PAH concentrations in the unweathered petroleum and in an environmental sample.

Error minimization of $e_{ij} = d_{ij} - \hat{k}_j \hat{w}_i$ by least-squares leads to

$$\hat{k}_j = \frac{\sum_{i=1}^{I} \hat{w}_i d_{ij}}{\sum_{i=1}^{I} \hat{w}_i^2}; \qquad \hat{w}_i = \frac{\sum_{j=1}^{J} \hat{k}_j d_{ij}}{\sum_{j=1}^{J} \hat{k}_j^2} \tag{5}$$

It can be shown that eqs 5 imply that the vector $\hat{\mathbf{k}}$ of elements $\hat{k}_j$ may be identified with the dominant eigenvector of the matrix **D′D**, where the elements of **D** are d_{ij} (see appendix). Imposition of the normalization condition $\sum \hat{k}_j^2 = 1$ removes the indeterminacy implied by eq 3, so that $\hat{\mathbf{k}}$ may be identified with the first principal component of **D′D**, with corresponding eigenvalue $\lambda_1 = \sum \hat{w}_i^2$. Thus, a principal component analysis of **D′D** provides least-square estimates of k_j, and the $\hat{w}_i$ may then be calculated from eqs 5 and the d_{ij}. In this context, the ratio of the dominant eigenvalue λ_1 to the sum of the eigenvalues (i.e. the trace of **D′D**) may be interpreted as the proportion of data variability explained by the model. Also, $\exp\pm(\sum_{j>1}^{J} \lambda_j)/IJ)^{1/2}$ provides a measure of the root-mean-square fit of predicted and observed PAH concentrations.

The distribution of $\sum_j e_j^2$ provides a basis for evaluating the probability that PAH in an environmental sample is consistent with weathered *Exxon Valdez* oil (EVO) as the PAH source. Given $\hat{\mathbf{k}}$ and $\hat{w}_i$ derived from PAH measurements of experimentally weathered EVO samples, predicted PAH concentrations may be calculated for sample i by eq 3a. The agreement of predicted and measured PAH concentrations in the ith sample may be expressed as the mean of the squared differences of logarithms of measured PAH and predicted PAH, or mean square error (MSE_i):

$$\frac{1}{J}\sum_{j=1}^{J}\left[\ln\left(\frac{[\hat{P}]_{ij}}{[P]_{ij}}\right)\right]^2 \quad = \quad \frac{1}{J}\sum_{j=1}^{J}\left(d_{ij} - \hat{d}_{ij}\right)^2 \quad = \quad MSE_i \tag{6}$$

The quantity $MSE_{i'}$ may be similarly calculated for PAH of uncertain origin in an environmental sample i', and compared with the MSE_i distribution developed by the bootstrap method applied to PAH measurements of experimentally weathered EVO samples. An

estimate of the probability that the PAH in the environmental sample i' is consistent with the experimentally weathered petroleum may then be made on the basis of this comparison.

If PAH concentrations can be predicted on the basis of alternative PAH sources, the same approach may be used to estimate the probability that PAH in an environmental sample is consistent with the alternative PAH source, provided the alternative mean square error distribution is available. In particular, if the alternative PAH source is not subject to weathering, so that relative PAH concentrations do not change with time, then PAH proportions of the sum of the PAH measured provides a basis for prediction. Equation 6 may be used to calculate the alternative mean square error MSE_i', which can be compared with the MSE_i' distribution calculated by the bootstrap method from known samples containing PAH from only the alternative source. An estimate of the probability that the PAH in the environmental sample is consistent with the alternative PAH source may then be made on the basis of this comparison.

Methods

Petroleum Sources and Composition. The petroleum spilled from the T/V *Exxon Valdez* was produced from the Alaskan North Slope (ANS) oil fields in 1989, and the petroleum used in the weathering experiment was produced from the same fields in 1992 and 1993. The PAH analytes we considered are listed in Table 1, with proportions of these PAH analytes in unweathered petroleum from the cargo of the T/V *Exxon Valdez* as determined by the hydrocarbon analysis methods used herein (*17*). Also in Table 1 are the PAH analytes we selected for modeling, based on analyte persistence above method detection limits (MDL; see

below) during the experimental weathering period. The proportions of selected PAH in unweathered EVO given in Table 1 are taken as the π_j in developing the weathering model.

Petroleum Weathering Experiments. Petroleum produced from the ANS was experimentally weathered by continuously washing petroleum-coated gravel for 6 months. The petroleum was heated at 70 °C overnight to 80% initial mass to remove volatiles, then sprayed onto tumbling gravel. Four different loadings of petroleum on gravel were prepared in 1992 and three in 1993, when the weathering experiment was repeated. The 1992 loadings were 55.2, 622, 3130, and 4510 μg petroleum/g gravel, and were 281, 717, and 2450 μg petroleum/g gravel in 1993. Each 11-kg preparation of petroleum-coated gravel was weathered by continuously washing it in a polyvinyl chloride (PVC) tube with alternating fresh and 30‰ seawater, switching every 6 h, at flow rates of 150 mL/min. Water temperatures ranged from 12 °C at the beginning of the weathering period to 2 °C in midwinter. Further details on the methods used to determine petroleum loadings on gravels, gravel preparation, and weathering apparatus and procedures have been presented previously (*18*).

Gravel samples were composited for PAH analysis from 8–15 replicate preparations of each petroleum loading. At each sampling, equal numbers of gravel pieces were removed from each replicate PVC tube, mixed, and stored at -20 °C until analysis. Gravel samples were collected 5, 62, 90, and 180 days after the columns were filled in 1992, and 3, 41, 68, and 181 days after the columns were filled in 1993. Duplicate composite samples were collected at day 62 in 1992; otherwise, single composite samples were collected. Of the 32

composite samples, 6 were not used to develop the weathering model because one or more of the PAH analytes selected for modeling were below MDL.

The PAH content of samples was determined by a GC/MS method. The analytes include unsubstituted and alkyl-substituted homologues of 2- to 4-ring PAH, and dibenzothiophene homologues (Table 1). PAH were extracted with dichloromethane, purified by alumina/silica gel column chromatography followed by size-exclusion high-performance liquid chromatography. Purified PAH were separated by GC and measured by MS operated in the selected ion monitoring mode. Concentrations of PAH in the dichloromethane extracts were determined by the internal standard method based on a suite of deuterated-PAH internal standards. Four quality control samples were analyzed with each batch of 12 samples, including 2 reference samples, a method blank, and a method blank spiked with certified hydrocarbon standards obtained from the National Institute of Standards and Technology (NIST). Method detection limits of hydrocarbon analytes were determined experimentally (*19*), and were generally 1 ng/g. At the Auke Bay Laboratory (ABL), the accuracy of this analysis is better than about ±15% based on comparison with NIST values, and precision expressed as coefficient of variation is about 25% for the analytes in the weathering model, based on reference sample results (see data analysis). Additional details of the method used have been presented elsewhere (*17*).

***Exxon Valdez* Oil Spill Study Area.** The EVOS introduced some 35,500 metric tons of ANS petroleum into PWS, which traveled about 750 km southwest along the Kenai peninsula and through Shelikov Strait before dispersing into the northern Gulf of Alaska, oiling about 1750 km of shoreline along the way (*20*). The path followed by the spilled

petroleum conformed with the Alaska Coastal Current (ACC) (Figure 1), which flushes PWS through Hinchinbrook Entrance and exits through Montague Strait (*21*). Sea-surface temperatures of the affected area typically range from near 0 to 16 °C annually. The ACC transports sediments burdened with PAH from natural sources into PWS (*16*). The pattern of relative PAH concentrations characteristic of sediments transported by the ACC into PWS has been consistently found at intertidal stations near Hinchinbrook Entrance (*13*, *16*), and has often been found subtidally within PWS (*13–16*). At Constantine Harbor off Hinchinbrook Entrance, concentrations of selected PAH in intertidal sediments have been constant at least since 1977, and probably much longer (*13*).

After the EVOS, 3433 samples of sediments, 2150 samples of mussels (*Mytilus trossulus*), and 2184 samples of other tissues were collected and analyzed for PAH to support the natural resource damage assessment efforts of the state and federal governments. ABL staff collected most of these sediments and mussels, using dichloromethane-rinsed apparatus, and stored them in pre-cleaned glass jars fitted with polytetrafluoroethane cap-liners at −20 °C until analysis. Procedures used to collect the remaining samples were usually similar. The PAH analysis methods used (*17*) were identical with those summarized above for the petroleum weathering experiment.

Database Archive. All of the hydrocarbon analysis results for this report are contained in the EVOS of 1989 State/Federal Trustee Council Hydrocarbon Database (EVTHD) at the ABL and available on internet at www.xxx.xxx.xxx.gov. Results of all sampling information and hydrocarbon analyses were entered into a data repository before being reviewed by the principal investigators responsible for the sample collections. Data in

this repository, named PWSOIL, were transferred to EVTHD after principal investigators reviewed database sampling information and analytical results for consistence with their project records. Only data for environmental samples were transferred; experimentally manipulated samples, method blanks, spiked samples, samples with incomplete information, and duplicate analyses were not included with EVTHD. We treat hydrocarbon results incorporated into EVTHD below MDL as zero for the purposes of this report.

Data Analysis

Petroleum Weathering Experiments. We could not apply the weathering model to all the PAH initially present in EVO because progressively more PAH were below MDLs as the petroleum weathered during the weathering experiment. We therefore applied the weathering model to the most broadly persistent PAH selected from the five most prominent PAH-homologue groups in EVO: naphthalenes, fluorenes, dibenzothiophenes, phenanthrenes, and chrysenes. Nine of the selected PAH were present above MDL in all 32 samples collected during the petroleum weathering experiments and provided 288 observations of PAH for the model. Another 5 PAH were simultaneously present in 26 of the 32 samples, and the 14 PAH simultaneously present in these 26 samples provided 364 observations of PAH. This combination of 14 PAH in 26 samples provided the maximum number of simultaneous PAH observations possible. We therefore applied the weathering model to the $J = 14$ PAH (identified in Table 1) simultaneously present in $I = 26$ of the 32 samples collected during the petroleum weathering experiment.

We calculated the initial oil concentration parameter ($\hat{c}_i$) for each sample based on the modeled chrysene homologues, which are persistent in weathered crude oil (*5*). The sum of chrysene, C-1 chrysene, and C-2 chrysene concentrations did not change significantly with time in 1992 or 1993 (repeated measures ANOVA; $P > 0.05$), therefore these homologues were used to estimate $\hat{c}_i$ from eq 4. Gravimetric determinations of petroleum initially applied to the gravel used in the weathering experiments were linearly related to $\hat{c}_i$ ($r^2 = 0.86$, $P = 0.02$), and were about 60% lower after correcting for volatility losses. We calculated $\hat{w}_i$ for the 26 samples and relative $\hat{k}_j$ for the 14 PAH from the 364 PAH observations obtained from the petroleum weathering experiment by principal component analysis of the matrix **D'D**, after transformation of PAH observations to the matrix elements d_{ij} of **D**.

Bootstrapped distributions of the MSE_i and $\hat{k}_j$ were simultaneously constructed by Monte Carlo simulation. One of the 26 samples was randomly removed, and a new matrix **D*** was calculated from the PAH observations of 26 random selections with replacement from the 25 remaining samples. New LR constants were calculated by finding the eigenvector $\hat{\mathbf{k}}^*$ of **D*'D***, and the MSE_i was calculated for the removed sample from eq 6 using $\hat{\mathbf{k}}^*$. This process was repeated 500 times, and the 14 $\hat{k}_j^*$ and MSE_i were recorded for each iteration. The distribution of the 14 $\hat{k}_j^*$ is presented as the range of the central 95% of the bootstrap results for each $\hat{k}_j$. The frequency distribution of MSE_i is used to estimate the probability that PAH in environmental samples are consistent with PAH from weathered ANS petroleum.

Characterization of PAH in Sediments from Natural Sources. We based our model of relative PAH concentrations that characterize the natural PAH source on samples collected from Constantine Harbor. The relative PAH concentration pattern and its error

distribution are derived from 15 intertidal sediment samples collected during six samplings in 1989 and 1990. Because total PAH (TPAH, i.e., the sum of the PAH analyzed) did not vary significantly (ANOVA, $P > 0.23$) among these samples (*13*), the sample with the median value of TPAH was arbitrarily selected as representative of the characteristic PAH pattern, and an error distribution for this pattern was generated by comparing the remaining samples with this representative sample as follows. The same 14 PAHs used in the weathering model were each converted to proportions by dividing each PAH concentration for a sample by the TPAH of the sample. We denote these PAH proportions in the median sample $\tilde{i}$ and a different sample i as $p_{\tilde{i}j}$, and p_{ij}, respectively, and calculate MSE_i' for discrepancies among these proportions as

$$\frac{1}{14}\sum_{j=1}^{J}\left(\ln[p_{\tilde{i}j} \,/\, p_{ij}]\right)^2 \quad = \quad MSE_i' \tag{7}$$

A bootstrapped distribution for MSE_i' was constructed by iterating the following procedure 500 times. One of the 15 samples from Constantine Harbor was randomly removed, and the remaining 14 samples were sampled with replacement 15 times. The sample of the resulting set with the median TPAH value was selected as a new representative of the characteristic PAH pattern. The PAH proportions of TPAH for the new median sample and for the sample initially removed were respectively denoted as $p^*_{\tilde{i}j}$ and p^*_{ij}, and these proportions were used in eq 7 to calculate a new observation of MSE_i'. The collection of 500 such observations was taken as the empirical error distribution for MSE_i'.

Hypothesis Testing. We used the bootstrapped error distributions for the weathering model and the natural sediment PAH source as the basis for distinguishing PAH sources in environmental samples. All the environmental samples with concentrations of the 14 selected PAH above MDL were consecutively fit to both models, and *MSE* and *MSE'* were calculated for each sample by eq 6 and 7 respectively. The probability that the source of PAH in the *k*th sample was consistent with ANS petroleum, denoted here as $Pr_{oil}(k)$, was determined by subtracting from 1 the percentile of values $\leq MSE_k$ in the cumulative frequency distribution of MSE_i for the weathering model. The null hypothesis that the PAH pattern in the *k*th sample was consistent with ANS petroleum was rejected when $Pr_{oil}(k) < \alpha$, where α specifies the probability of type I error. Similarly, $Pr_{ns}(k)$, the probability that the pattern of PAH in the *k*th sample was consistent with the natural sediment source, was derived by comparing MSE_k' to the cumulative frequency distribution of MSE_i'. The null hypothesis that the *k*th sample is consistent with the natural sediment pattern was rejected when $Pr_{ns}(k) < \alpha$. Note that the two models must be considered as separate alternatives rather than simultaneously [(as by, *e.g.*, SIMCA (*22*) methods], because the models are not isolinear and, therefore, cannot be combined into the same principal component matrix.

Results

Weathering Model Parameters. The eigenvector of $\hat{k}_j$ calculated as the first principal component of the matrix **D'D** accounts for 86% of the total variability in the PAH data from the petroleum weathering experiments. The mean unexplained variability per sample and per analyte is 0.161, indicating that most of the PAH values predicted by the weathering model

are within −33% and +49% of observed values from the petroleum weathering experiments. Three analytes, C4-naphthalene and C2- and C3-fluorene, together account for 73% of the magnitude of the second principal component of the $\mathbf{D}'\mathbf{D}$ matrix, and the second principal component accounts for an additional 8% of the total variability in the PAH data from the petroleum weathering experiments. The mean variability of logarithmically-transformed data per sample and per analyte that is not explained by the first two principal components is 0.069, which implies a mean coefficient of variation of 26% for the untransformed data, consistent with analytical precision. The first two principal components, therefore, account for all the data variability except analytical error; the first component accounts for 91% [i.e. (86/0.94)%] of the explainable data variation. Thus, the second principal component summarizes the discrepancies between the weathering model and the data after discounting variability due to analytical error.

The values of $\hat{k}_j$ increase with decreasing alkyl-substitution and number of aromatic rings (Table 2). The largest values of $\hat{k}_j$ are for C3-naphthalene, C1-dibenzothiophene, and C1-phenanthrene, whereas the smallest values are for C3- and C4-phenanthrene and the three chrysene homologues. The proximity to zero of the $\hat{k}_j$ of these latter five analytes indicates that the duration of the weathering experiments was insufficient for appreciable weathering loss to occur. Also in Table 2 are the ranges for the most central 95% of the bootstrap estimates of the $\hat{k}_j$ as a measure of dispersion of the estimates. This dispersion is proportionally least for those analytes that changed most in concentration during the weathering experiments.

The values for $\hat{w}_i$ increase linearly with time during the petroleum weathering experiments, and increase faster at lower petroleum loadings (Figure 2). In the 1992 experiment, these linear trends are significant ($P < 0.027$) for all but the lowest petroleum loading ($P < 0.09$). Values for $\hat{w}_i$ range above 7 for the most heavily weathered, lowest petroleum-loaded gravel at 85 days exposure but do not exceed 3.5 for the most heavily loaded gravel at 175 days. The weathering rate, $d\hat{w}_i/dt$, increases linearly with decreasing petroleum loading ($r^2 = 0.98$; $P < 0.01$) in the 1992 weathering experiments. Similar trends occur in the 1993 experiment, but the more limited 1993 data preclude a meaningful statistical summary.

The distribution of MSE_i derived from the fit of the bootstrapped iterations of the weathering model and the PAH data from the petroleum weathering experiments (see eq 6) is strongly leptokurtic (Figure 3). The MSE_i ranges from 0.0086 to 1.47, with a median of 0.145. The 95th and 99th percentiles occur at $MSE_i = 0.57$ and 0.98, respectively, and the latter value is used below to evaluate samples from the EVOS. This corresponds with accepting a type I error probability of 0.01 when evaluating the null hypothesis that PAH patterns of environmental samples are consistent with weathered EVO. A comparison of observed and predicted PAH proportions that correspond with the median MSE_i for a weathered ($\hat{w}_i = 3.95$) example is depicted in Figure 4B, where the PAH proportions of the unweathered EVO are also presented for further comparison (Figure 4A).

Characterization of PAH in Sediments from Constantine Harbor. The PAH of Constantine Harbor intertidal sediments are proportionally lower in naphthalenes and dibenzothiophenes, and higher in phenanthrenes and chrysenes compared with EVO (Figure

4C). The distribution of MSE_i' derived from application of eq 7 to the bootstrapped iterations of the Constantine Harbor samples is less strongly leptokurtic than the MSE_i distribution of weathered EVO (compare Figures 3 and 5). The MSE_i' of the logarithmically-transformed PAH data ranges from 0.0066 to 0.37, with a median of 0.056, and this median is equivalent to a coefficient of variation of 24% for untransformed data, consistent with analytical precision. The 95th and 99th percentiles occur at $MSE_i' = 0.28$ and 0.34, respectively, and the latter value is used below to evaluate samples from the EVOS. This corresponds with accepting a type I error probability of 0.01 when evaluating the null hypothesis that PAH patterns in environmental samples are consistent with PAH from the natural source.

Classification of Sediment Samples from the EVOS. The results of our classification procedure indicate that although EVO did not contaminate most of the EVOS sediment samples collected, EVO was the source of most of the PAH detected. Concentrations of the 14 PAH included in the weathering model are above MDL in 996 of the 3433 sediment samples analyzed for the EVOS. Of these 996 samples, 618 have $MSE_k < 0.98$ and $MSE_k' > 0.34$, which we accepted as consistent with weathered EVO (Figure 6A). The sum of all the PAH concentrations detected above MDL in these 618 samples is more than 86% of the total sum of all PAH concentrations detected in all the sediment samples analyzed.

The sediment samples we classified as contaminated by EVO may also contain PAH from other contamination sources. The median MSE_k of the 618 EVO-contaminated samples was 0.34, or more than twice the median MSE_i derived from the bootstrap distribution of the petroleum weathering experiments. The larger value of the median MSE_k may be caused by PAH from other sources that alter the relative PAH proportions of sediment samples and

consequently fit the weathering model less well. This is most evident for samples that contain relatively low total PAH concentrations. Of the 618 EVO-contaminated samples identified, the median MSE_k for the 255 of these samples that have total PAH concentrations less than 750 ng/g (dry weight) is 0.47, compared to a median of 0.25 for the remaining 363 samples that have total PAH concentrations greater than 750 ng/g. The distribution of the MSE_ks for these 363 samples is strongly leptokurtic, and similar to the MSE_i distribution derived by bootstrapping results of the petroleum weathering experiments.

Most of the EVO-contaminated sediments we identified were collected from the inter- and shallow-subtidal within the EVOS impact area (Figure 1). Epibenthic surface depth was reported for 546 EVO-contaminated sediment samples; 93% of these were collected above 20 m subtidal depth within the EVOS area. Another 5.3% were collected from subtidal depths below 20 m within the EVOS area, and 1.7% were collected outside the EVOS area.

Of the 996 sediment samples we evaluated, 110 samples had $MSE_k > 0.98$ and $MSE_k' < 0.34$, which we accepted as consistent with PAHs derived from the natural PAH source (Figure 6A). The sum of all the PAH concentrations detected above MDL in these 110 samples is less than 0.06% of the total sum of all PAH concentrations detected in all the sediment samples analyzed. The median MSE_k' of the 110 EVO-contaminated samples was 0.17, or more than three times the median MSE_i' derived from the bootstrap distribution of the intertidal Constantine Harbor sediments. As with the EVO-contaminated sediments, this larger value of the median MSE_k' may be caused by PAH from other sources that alter the relative PAH proportions of environmental sediment samples and thereby fit the Constantine Harbor pattern less well.

Most of the sediments we identified as contaminated by PAH from the natural source were collected from deeper-subtidal depths within the EVOS impact area (Figure 1). Over 80% of these sediments collected within the EVOS area were from subtidal depths below 20 m. In contrast, most of the sediments collected east of the EVOS area that we identified as contaminated by PAH from the natural source were from the Constantine Harbor intertidal, which was used to define this PAH pattern.

Of the remaining sediment samples we evaluated, 30 fit both the weathering model and the Constantine Harbor PAH pattern, and 238 fit neither. The 30 samples that fit both patterns at the $\alpha = 0.01$ type I error rate (i.e. $MSE_k < 0.98$ and $MSE_k' < 0.34$) account for 0.02% of the total sum of all PAH concentrations detected in all the sediment samples analyzed. At $\alpha = 0.05$ type I error rate, no sample fit both patterns simultaneously. The 238 samples that fit neither PAH pattern ($MSE_k > 0.98$ and $MSE_k' > 0.34$) include 41 samples of sediment trap filtrates that were contaminated during sample collection (*23*), and 5 samples of EVO that were so diluted for analysis that C-1 dibenzothiophenes were detected just above MDL but well below concentrations predicted by the weathering model, which caused the poor fit to the weathering model. The PAH in the remaining samples of this category account for 0.31% of the total sum of all PAH concentrations detected in all the sediment samples analyzed, and may include mixtures of PAH from natural sources, the EVOS, and other, unknown sources.

Most of the 2437 other sediment samples that could not be evaluated contained low PAH concentrations. These samples could not be evaluated because 1 or more of the 14 PAH used in the weathering model were below MDL. The sum of the all the PAH concentrations

detected above MDL in these samples is 11.5% of the total sum of all PAH concentrations detected in all the sediment samples analyzed (Figure 6A). However, most of these PAH were in a few samples that were visibly contaminated with EVO but were over-diluted for PAH analysis, which resulted in concentration estimates for some of the 14 modeled PAH below sample mass-adjusted MDLs. For example, the sample mass analyzed for 19 of these samples was ≤50 mg, but the PAH concentrations detected above MDL in these samples account for 8.3% of the total sum of all PAH concentrations detected in all the sediment samples analyzed. The remaining 2418 samples account for 3.2% of the total sum of PAH concentrations detected.

Classification of Mussel Samples from the EVOS. As with sediments, the results of our classification procedure indicate that although EVO did not contaminate most of the mussel samples collected, EVO was the source of most of the PAH detected. Concentrations of the 14 PAH included in the weathering model are above MDL in 452 of the 2150 mussel samples analyzed for the EVOS. Of these mussel samples, the $MSE_k < 0.98$ and the $MSE_k' > 0.34$ for 435 samples, which we accepted as consistent with weathered EVO (Figure 6B). The sum of the all the PAH concentrations detected above MDL in these 435 samples is >84% of the total sum of all PAH concentrations detected in all the mussel samples analyzed. The median MSE_k of the 435 EVO-contaminated mussel samples was 0.25, about 75% more than the median MSE_i derived from the bootstrap distribution of the petroleum weathering experiments. As with the 363 EVO-contaminated sediment samples above, the distribution of the MSE_ks for these 435 mussel samples is strongly leptokurtic, and similar to the MSE_i distribution derived by bootstrapping results of the petroleum weathering experiments. In

contrast with sediment samples, the median MSE_k for sets of EVO-contaminated mussels varies little, regardless of the minimum PAH content of the sample set.

The smaller median MSE_k for mussels compared with sediments suggests that mussels were less subject to PAH contamination from sources other than the EVOS. In particular, the smallest MSE_k' of mussels is 0.57, which indicates that the Constantine Harbor sediment-PAH pattern is absent entirely in mussels, and also that no mussel simultaneously fit the weathering model and the Constantine Harbor pattern. However, 17 mussel samples fit neither PAH pattern ($MSE_k > 0.98$ and $MSE_k' > 0.34$), and these account for 0.95% of the total sum of all PAH concentrations detected in all the mussel samples analyzed (Figure 6B).

All but three of the EVO-contaminated mussel samples we identified were collected from within the EVOS impact area: two had ambiguous location information reported, and one was reported as collected from eastern PWS.

As with sediments, most of the 1699 other mussels that could not be evaluated contained low PAH concentrations. The sum of all the PAH concentrations detected above MDL in these samples is 15.0% of the total sum of all PAH concentrations detected in all the mussel samples analyzed (Figure 6B).

Classification of Other Tissue Samples from the EVOS. Samples of other tissues are classified as EVO-contaminated by the weathering model less frequently than sediments and mussels. Concentrations of the 14 PAH in the weathering model are above MDL in 93 of the 2184 other tissue samples analyzed for the EVOS. Of these 93 samples, the $MSE_k <$ 0.98 and the $MSE_k' > 0.34$ for 80 samples, which we accepted as consistent with weathered EVO (Figure 6C). The sum of all the PAH concentrations above MDL in these 80 samples is

34% of the total sum of all PAH concentrations detected in all the other tissue samples analyzed. Most of these 80 samples were from external surfaces of oiled animals. Another 12 samples did not fit either model ($MSE_k > 0.98$ and the $MSE_k' > 0.34$) and account for another 42% of detected PAH, most (>90%) of which is due to three stomach content samples from bald eagles. One sample fit both models. The remaining 23% of detected PAH is distributed among the 2090 samples of other tissues that could not be evaluated, usually at concentrations near MDLs.

Time-Dependence of the Weathering Parameter in EVO-Contaminated Sediments and Mussels. The weathering parameter $\hat{w}_i$ was only weakly correlated with the sample collection date of sediment or mussel samples identified as EVO-contaminated by the weathering model ($r^2 = 0.045$, $P < 0.001$; Figure 7). Values of $\hat{w}_i$ ranged from near zero to >7 during each of the 6 years following the EVOS, which together with the small proportion of variation in $\hat{w}_i$ explained by the sample collection dates indicates that the effect of time on weathering rate varies considerably.

Discussion

Assessment of First-Order Weathering Kinetics for Experimentally Weathered EVO. The principal component analysis of the logarithmically-transformed PAH results from the petroleum weathering experiments indicate three factors that determine the observed PAH variability. These three factors are FOLR kinetics, analytical error, and remaining variability summarized by the second principal component, which we denote as process error. Because performance of any model is constrained by the analytical error, that error must be estimated

in order to evaluate model performance. We accept the results of laboratory analysis of reference samples as the basis for analytical error estimation because these samples include matrix effects and the large number of repetitive analyses available for these analyses records analytical variability over a period of years. Because the squared coefficient of variation for PAH in reference sample results is equivalent to the variance of logarithmically-transformed PAH results, these variation coefficients may be used to calculate the approximate analytical error variance expected. On this basis, the meaningful principal components are limited to the first two: FOLR kinetics and process error.

Comparison of the eigenvalues of the first two principal components shows that the process error component is at most a minor perturbation of the FOLR process. The process error component may indicate incorrect specification of the weathering model (i.e. PAH do not weather according to FOLR kinetics), or alternatively may indicate systematic experimental errors; its composition suggests the latter rather than the former. The three largest PAH constituents of the process error component, C4-naphthalenes and C2- and C-3 fluorenes, could be due to unknown analytical interferences, or to composition differences between EVO and ANS petroleum. The composition constants π_j in our weathering model are derived from EVO, but the ANS petroleum we used was produced 3 years after the EVOS, and may have somewhat different PAH composition due to variable contributions from different ANS oil fields (*24*). The weathering model accounts for 94% of the PAH variability when the composition constants π_j are derived from the composition of the ANS petroleum initially applied to the petroleum weathering gravels, and the remaining variability is due to

analytical error. We therefore conclude that, within the limitations imposed by analytical and systematic errors, PAH variability for the weathering experiments follows FOLR kinetics.

PAH vaporization from petroleum may be considered as an endothermic chemical reaction that involves breaking the cohesive bonds between PAH solutes and the petroleum solvent. The physical rate-limiting step (RLS) implied by FOLR kinetics is the energy required to overcome the attractive van der Waals forces between the petroleum phase and departing PAH molecules that constitute these bonds. This energy requirement is approximately equal to the enthalpy of vaporization, which is proportional to molecular surface area. The Arrhenius rate equation gives the relation between rate constant k, activation energy E_a, and temperature as $k = A \exp-(E_a/RT)$. The linearity of a plot of ln k versus E_a derived from observations of aqueous dissolution rates of PAH from petroleum is evidence of a similar RLS for PAH vaporization and aqueous dissolution. An Arrhenius plot ln k_j versus estimates of total molecular surface area (TSA), used here as a surrogate for enthalpies of vaporization (which are not available for PAH vaporization from petroleum), is approximately linear ($r^2 = 0.75$, $P < 0.005$; Figure 8). This linearity corroborates initial separation of PAH from the petroleum phase as the RLS, regardless of the nature of the phase receiving the PAH lost from the petroleum. This also explains why the weathering model performs equally well with EVO in subtidal sediments where the receiving phase is aqueous, and with intertidal sediments and mussels, where the receiving phase may at times be the atmosphere.

An Arrhenius plot of logarithms of FOLR constants reported for a petroleum-weathering field experiment conducted at higher temperatures [Table 3 in (*3*)] is also linear (r^2

= 0.90, $P < 0.001$; Figure 8), but has a significantly ($P < 0.001$) less slope, which implies less variability with TSA among these rate constants compared with ours. The linearity corroborates the proposed RLS, but the smaller slope is due to expected temperature effects on the rate constants implied by the Arrhenius rate equation. Differences among rate constants increase with decreasing temperature when E_a is independent of temperature, and these differences are exacerbated in this case by incipient crystallization of PAH in petroleum at temperatures near 0 °C, which would increase vaporization enthalpies of larger PAH compared with warmer temperatures. These differences indicate that the relative LR constants presented herein should not be applied to appreciably different (i.e., $\lesssim$10 °C) thermal environments without correction for these temperature effects, for which accurate data on enthalpies of vaporization of PAHs from petroleum as a function of temperature would be helpful.

The FO weathering model may be used to predict relative PAH concentrations that evaporate into the atmosphere or that dissolve into aqueous solution. From eq 3, the instantaneous rate of decrease of a PAH P_j from weathering petroleum is $-\mathrm{d}P_j/\mathrm{d}w = k_j P_j$, and is proportional with the instantaneous increase in the concentration of P_j in the receiving phase. This ensures that PAH concentrations of the receiving phase are correlated with PAH concentrations initially present in the petroleum. Predicted correlation coefficients for aqueous PAH concentrations dissolved from initially unweathered EVO and PAH concentrations initially present in unweathered EVO (proportional to π_j) exceed 0.9, and are consistent with correlation coefficients based on dissolved PAH concentrations measured in seawater 1–2 weeks following the EVOS (*25*). The high correlation is because variability

among π_j is substantially greater than variability among the k_j, and the most rapidly dissolving (or evaporating) PAH tend also to be the most abundant initially present in EVO.

The Weathering Model and PAH Source Identification. Our weathering model is related to currently accepted protocols for oil-spill source identification based on PAH analysis (*26*, *27*). The protocols currently adopted in the United States and in Europe compare normalized PAH results for samples and suspected sources, and patterns that match within constraints imposed by analytical precision and by weathering effects are accepted as evidence implicating the suspected source. The constraints imposed by weathering effects include decreasing trends in pattern discrepancies with increasing PAH boiling points (*27*) or with increasing alkyl-substitution within homologous PAH series (*26*). Those normalized PAHs identified as unaffected by weathering can be included in multivariate statistical comparisons with corresponding results from suspected oil-spill sources to evaluate whether discrepancies that remain among these analytes can be ascribed to analytical precision. The identification procedure thus employs two criteria: patterns of normalized PAH that match within the constraints of analytical precision for analytes that are not affected by weathering, and patterns of PAH weathering losses that conform with specified trends.

Our weathering model may be regarded as an alternative formulation of the above protocols. It provides an explicit mathematical specification of the PAH weathering-loss trends, and the PAHs included in the matching procedure are extended to weathered PAH. The weathering model reduces to a simple comparison of relative PAH concentrations in a sample i and in a suspected source oil as w_i approaches zero. As w_i increases, progressively more PAH are significantly affected by weathering, depending on comparison of the product

k_j w_i and analytical precision for the jth PAH expressed as a coefficient of variation. The European protocol (*27*) makes greater use of the information produced by the chemical analysis, because all the resolvable isomer peaks are considered individually, in contrast to summation of isomer peaks for each homologue reported, as was done here. Although this is a substantial advantage of the European protocol, our model could be adapted to such protocols as a possible refinement.

An advantage unique to the weathering model is its provision for more precise definition of weathering. The weathering parameter w_i defines weathering by indexing the relative abundance of a set of PAH with known LR constants, so that comparisons between samples can be unambiguously controlled for weathering, which leads to a distribution for MSE_i that is independent of weathering state. Given a distribution for MSE_i derived from laboratory observations, source identifications can be evaluated by estimates of the probability of committing type I error. In our model, a type I error is an erroneous rejection of the null hypothesis that the pattern of PAH in a sample is consistent with EVO.

By quantifying the weathering state, w_i also provides an index of the potential toxicity remaining in the oil of a sample. Lower values of w_i indicate progressively greater relative abundances of the PAHs that are most readily lost to the environment, and PAHs are the most toxic components (in absolute terms) of petroleum (*28*). The value of w_i is thus inversely related to the toxic burden remaining in an oil sample. In this regard, w_i is an especially appropriate parameter for bioremediation studies, where the objective is to find biological conditions that accelerate dw_i/dt.

Although we used chrysenes to determine the parameter c_i of unweathered petroleum originally introduced into the *i*th sample, other temporally-invariant constituents of petroleum could also be used. The low estimates of k_j we obtained for C3- and C4-phenanthrenes indicate that these could have been included in eq 4 to estimate c_i, but were not because the chrysenes were chosen *a priori* for this purpose. Alternatively, other persistent constituents such the alicyclic hopanes or stearanes could be used.

Successful application of our weathering model requires careful consideration of the interaction among (a) the PAH set selected for inclusion in the model, (b) the detection limit definition chosen, and (c) the effects of these choices on the scaling of w_i. Detection limit stipulation is critical because the value calculated for the fit of the model to the data (i.e., MSE_i) will increase dramatically if contributions from analytes well below detection limits are included, since the discrepancy between observed and predicted analyte concentrations may be orders of magnitude at concentrations sufficiently below detection limits. Thus, once weathering proceeds to the point where concentrations of one or more of the analytes in the weathering model are below detection limits, application of the model may be compromised. The choice of analytes included in the model, together with the detection limits used, therefore determine the range of weathering states covered by the model. The model may consequently fail to apply to samples that contain very high concentrations of petroleum if it is very weathered, because the dilution necessary for valid analysis of the most abundant analytes included in the model may cause the most weathered analytes to fall below the detection limits applied.

The choice of analytes included in the model also affects the ability of the model to distinguish among initial stages of petroleum weathering, because most of the information regarding w_i is contained in the measurements of the most rapidly lost analytes. Consequently, a model that includes rapidly lost analytes (e.g., naphthalene) will distinguish among earlier weathering stages better one that does not, but the latter will be applicable over a broader range of weathering states, because its constituent analytes are more persistent. Also, the weathering states that correspond to a particular value of w_i will not be the same for these two models, owing to the normalization condition $\sum \hat{k}_j^2 = 1$. This condition causes the results for w_i to be a function of the analytes included in the model, so w_is based on different analyte sets cannot be directly compared.

The ratio of surface area to volume of petroleum in a sample is an important factor affecting the relation of w_i and time. As demonstrated in Figure 2, dw_i/dt decreases as the film thickness of petroleum applied to the gravel substrate increases; this behavior is consistent with the RLS for PAH-loss from petroleum discussed above. This implies that a variety of weathering states may be observed shortly following an oil spill, depending on the surface area to volume ratio of the petroleum sampled. Also, relatively unweathered petroleum may persist for prolonged periods in the field if the surface area exposed to wind or water currents is small relative to the petroleum volume associated with the matrix sampled, hence the weak correlation of w_i and time (Figure 7).

Assessment of First-Order Weathering Kinetics for Petroleum Spilled from the T/V *Exxon Valdez*. The applicability of the laboratory-derived weathering model to field results from an oil spill may be assessed by (a) comparing the error distributions derived from

applying the weathering model to laboratory results *versus* field results, and (b) comparing the geographic distribution of samples identified as contaminated by EVO with the geographic boundaries of the area contaminated by the EVOS.

The error distributions that result from applying the weathering model to field samples of mussels and sediments confirm that the dominant weathering processes of this oil spill followed FOLR kinetics. The median MSE_k of 0.25 for EVO-contaminated field mussels means that most of the PAH concentrations predicted by the weathering model fall within -40% to +65% of observed concentrations. The corresponding range for the laboratory weathering experiments is -33% to +49%, which indicates that the weathering model is almost as successful at predicting PAH concentrations in field mussels as it is at predicting PAH concentrations in experimentally-weathered petroleum. The greater disparity between observed and predicted PAHs in mussels compared with experimentally-weathered petroleum is probably due to the combined effects of small interferences from other hydrocarbon sources in the environment or introduced during sample collection or storage, small PAH composition differences between the petroleum used for the weathering experiment and the petroleum spilled, and composition differences induced by the differences in the thermal histories of the spilled petroleum and the petroleum used for the weathering experiments. These effects may collectively be regarded as small perturbations compared with the much larger PAH concentration changes that result from FO weathering processes.

The similarly leptokurtic distributions of the MSE_ks of mussels and the MSE_fs of experimentally-weathered petroleum, together with the fact that the distribution for mussels includes nearly all the mussels that meet the MDL requirements of the weathering model,

corroborates the similarity of the underlying weathering processes for EVO in mussels in the field and on gravel in the weathering experiments. The 17 mussels that were modeled as not consistent with EVO at the 1% type I error rate is probably the result of truncation of the MSE_i distribution after the median value is increased to 0.25. The MSE_k distribution based on all the mussels that meet the weathering model requirements is, therefore, generally consistent with expectations based on the weathering model, with small allowance for environmental perturbations.

The similarity of the error distributions derived from mussels and from the more contaminated sediments indicates that the weathering model applies equally well for these matrixes. The median MSE_k for mussels is almost identical with the median for sediments identified as EVO-contaminated at total PAH concentrations >750 ng/g, and both distributions are similarly leptokurtic. Thus, with few exceptions, sediment samples that are sufficiently contaminated by EVO that other hydrocarbon sources are negligible in comparison, display patterns of relative PAH concentrations consistent with FOLR kinetics. That the same model produces similar results for such disparate environmental matrixes further validates the kinetics of the underlying weathering processes assumed by the model. Following the EVOS, PAH losses due to weathering followed FOLR kinetics regardless of the great variability of environmental conditions among intertidal mussels, intertidal sediments, subtidal sediments, and EVO-contaminated sediments in transport from the intertidal to the subtidal, at geographic locations of very different aspects. This generality derives from the simple notion that the rate of PAH loss from petroleum is determined by the energy required for PAH molecules to escape from petroleum.

The effects of PAH interferences on the weathering model can be assessed by constructing hypothetical mixtures of PAHs from EVO and alternative sources, and calculating the increase in MSE_i' that results from application of the EVO-weathering model. For example, eq 6 may be applied to PAH of a synthetic sample for which a proportion (1 - q) of the total PAH is from EVO and the remaining proportion q is from an alternative PAH source (such as that apparent in the intertidal sediments at Constantine Harbor). The change of the MSE_i' as q increases may be used to assess the sensitivity of the weathering model to interference from the alternative PAH source. This procedure may be bootstrapped at fixed values of q to generate a distribution of $MSE_i'^{(q)}$ from mixtures of Constantine Harbor and experimentally-weathered EVO samples, analogous to the generation of the distribution for MSE_i from experimentally-weathered EVO samples. The median value of the $MSE_i'^{(q)}$ distribution is comparable with the median of the MSE_i distribution of the weathering model for $q \lesssim 0.2$, which indicates that the weathering model is not sensitive to mixtures that contain as much as 20% of the total PAH from the natural source (Figure 9). Similarly, the median value of the $MSE_i'^{(q)}$' distribution is comparable with the median of the MSE_i' distribution of the natural source model for $q \lesssim 0.05$ which indicates that the natural source model is not sensitive to mixtures that contain as much as 5% of the total PAH from EVO.

We conclude from these exercises on synthetic mixtures of PAH sources that the models we have presented are most validly applied to samples that contain PAH from a single predominant source. This is the usual case for more heavily contaminated samples collected during catastrophic events such as major oil spills, where the PAH contribution from the catastrophic source predominates. It is also the usual case for pristine environments that

contain PAH from a single natural source, or from multiple sources but in contributions of constant proportions (provided no weathering occurs). However, the validity of these models is compromised as PAH contributions from a suspected predominant source approach contributions from alternative sources, because of the difficulty in distinguishing larger MSE_k values that result from mixtures, and larger MSE_k values that result from stochasticity. Stochastic consequences may be important in this context because of the relatively low precision of the underlying analytical measurements.

The geographic distribution of the samples we identified as contaminated by EVO is generally consistent with the trajectory of the spilled petroleum, indicating an absence of spurious identifications generated by the weathering model. This is supported by the low frequencies of mussel or sediment samples identified as EVO-contaminated that were collected outside the trajectory of the spilled petroleum, or that were collected at sediment epibenthic depths below about 20 m. Also, no mussel or sediment sample collected just before landfall of the spilled EVO was identified as EVO-contaminated.

The EVOS provided a unique opportunity to assess the weathering model because the most heavily contaminated compartments of the affected area were among those least affected by PAH inputs from alternative sources before the spill. Before the EVOS, the PAHs characteristic of EVO were rarely detected in mussels outside Port Valdez in PWS (*12*, *13*). Sediment PAH concentrations derived from natural sources decrease with progressively shallower epibenthic depths, so that total PAH concentrations from these sources rarely exceed 100 ng/g in intertidal sediments and 200 ng/g in subtidal sediments to 20 m depth (*14*, *16*). Weathered EVO was most prevalent in these two environmental compartments: mussels, and

sediments at less than 20 m epibenthic depth. As a result, PAH concentration patterns characteristic of weathered EVO are ubiquitous in mussels that contain sufficient PAH to be evaluated by the weathering model, and common in sediments that have total PAH concentrations exceeding about 750 ng/g. Note that a subtidal sediment sample that contains 750 ng/g total PAH with 200 ng/g from natural sources and 550 ng/g from EVO would most likely be classified as EVO by the weathering model procedure, based on the sensitivity of the model to mixtures from these sources discussed above. Interference from natural sources on the EVO identification procedure we present herein is, therefore, probably negligible in mussels, and also in sediments that contain more than about 750 ng/g total PAH.

The absence of PAH from natural sediment PAH sources in mussels, together with the observation that the PAH pattern that characterizes these sources does not weather, places strong constraints on the nature of these sources. These sources have been identified with natural petroleum seeps along the southern coast of Alaska at Katalla and elsewhere (*16*), but this identification is not obviously consistent with the absence of weathering and with the absence of these PAH in mussels, which implies that these PAH are sequestered in such a way that biological availability is precluded. The absence of weathering and of biological availability is most clearly evident at Constantine Harbor, where concentrations of PAH most susceptible to weathering have not changed in intertidal sediments during a 15-year monitoring period, and were rarely detected in adjacent mussels simultaneously collected. The pattern of PAH concentrations of unburned coal is difficult to distinguish from petroleum in sediments (*29*), and because PAH sequestered in microscopic coal particles is consistent with the absence of weathering and with the absence of these PAH in mussels, coal has been

suggested as an alternative source (*13*, *14*). Coal as a possible source has been dismissed based on the apparent absence of inventoried coal deposits in Alaska [(*30*); although cited in (*31*), this reference does not appear to address this issue] to account for the characteristic PAH pattern that is observed in submarine sediments east of Katalla (*31*). However, absence of proof is not equivalent to proof of absence, and undiscovered coal deposits in Alaska (or discovered deposits in the Alsek river drainage of Canada) remain plausible sources, so this dismissal is premature. Conversely, before a petroleum seep source is accepted, the absence of weathering and of bioavailability must be explained, because these are not consistent with the environmental behavior of petroleum.

Acknowledgments

The research described in this paper was supported by the *Exxon Valdez* Oil Spill Trustee Council. However, the findings and conclusions presented by the authors are their own and do not necessarily reflect the views or position of the Trustee Council.

Literature Cited

(1) Wang, Z.; Fingas, M.; Sergy, G. *Environ. Sci. Technol.* **1994**, *28*, 1733–1746.

(2) Killeen, T. J.; Eastwood, D.; Hendrick, M. S. *Talanta* **1981**, *28*, 1–6.

(3) Venosa, A. D.; Suidan, M. T.; Wrenn, B. A.; Strohmeier, K. L.; Haines, J. R.; Eberhart, B. L.; King, D.; Holder, E. *Environ. Sci. Technol.* **1996**, *30*, 1764–1775.

(4) Singer, M. E.; Finnerty, W. R. In *Petroleum Microbiology*; Atlas, R. M., Ed.; Macmillan publishing Co.: New York, 1984.

(5) Roques, D. E.; Overton, E. B.; Henry, C. B. *J. Environ. Qual.* **1994**, *23*, 851–855.

(6) Michel, J.; Hayes, M. O. In *Proceedings of the 1993 International Oil Spill Conference*; American Petroleum Institute: Washington, DC, 1993.

(7) Kennicutt, M. C., II. *Oil Chem. Pollut.* **1988**, *4*, 89–112.

(8) Boehm, P. D.; Steinhauer, M. S.; Green, D. R.; Fowler, B.; Humphrey, B.; Fiest, D. L.; Cretney, W. J. *Arctic* **1987** *40* (Suppl. 1), 133–148.

(9) Humphrey, B.; Boehm, P. D.; Hamilton, M. C.; Norstrom, R. J. *Arctic* **1987** *40* (Suppl. 1), 149–161.

(10) Majewski, J.; O'Brien, J. *Environmental Letters* **1974**, *7* (2), 145–161.

(11) Hansen, H. P. *Rapp. P.-v. Reun. Cons. int. Explor. Mer* **1977**, *171*, 101–106.

(12) Karinen, J. F.; Babcock, M. M.; Brown, D. W.; MacLeod, W. D., Jr.; Ramos, L. S.; Short, J. W. *Hydrocarbons in Intertidal Sediments and Mussels from Prince william Sound, Alaska, 1977–1980: Characterization and Probable Sources;* U.S. Department of Commerce, Auke Bay Lab: Juneau, AK, 1993; NOAA Tech. Memo. NMFS-AFSC-9.

(13) Short, J. W.; Babcock, M. M. *Am. Fish. Soc. Symp.* **1996**, *18*, 149–166.

(14) O'Clair, C. E.; Short, J. W.; Rice, S. D. *Am. Fish. Soc. Symp.* **1996**, *18*, 61–93.

(15) Short, J. W.; Sale, D. M.; Gibeaut, J. C. *Am. Fish. Soc. Symp.* **1996**, *18*, 40–60.

(16) Page, D. S.; Boehm, P. D.; Douglas, G. S.; Bence, A. E.; In *Third ASTM Symposium on Environmental Toxicology and Risk Assessment: Aquatic, Plant, and Terrestrial;* April 25–28, 1993, Atlanta, GA; American Society for Testing and Materials: Philadelphia, PA, 1993.

(17) Short, J. W.; Jackson, T. J.; Larsen, M. L.; Wade, T. L. *Am. Fish. Soc. Symp.* **1996**, *18*, 140–148.

(18) Marty G. D.; Short, J. W.; Dambach D. M.; Willits, N. H.; Heintz, R. A.; Rice, S. D.; Stegeman, J. J.; Hinton, D. E. Submitted, *Can. J. Zool.*

(19) Glaser, J. A.; Forest, D. L.; McKee, G. D.; Quave, S. A.; Budde, W. L. *Environ. Sci. Technol.* **1981**, *15*, 1426–1435.

(20) Wolfe, D. A.; Hameedi, M. J.; Galt, J. A.; Watabayashi, G.; Short, J.; O'Claire, C.; Rice, S.; Michel, J.; Payne, J. R.; Braddock, J.; Hanna, S.; Sale, D. *Environ. Sci. Technol.* **1994**, *28*, 561A–568A.

(21) Niebauer, H. J.; Royer, T. C.; Weingartner, T. J. *J. Geophys. Res.* **1994**, *99*, 14,113–14,126.

(22) Wold, S.; Sjöström, M. In *Chemometrics: Theory and Application*; Kowalski, B. R., Ed.; ACS Symposium Series 52; Washington, DC, 1977.

(23) Sale, D. M.; Gibeaut, J. C.; Short, J. W. *Nearshore Transport of Hydrocarbons and Sediments Following the Exxon Valdez Oil Spill, Exxon Valdez Oil Spill State/Federal Natural Resource Damage Assessment Final Report (Subtidal Study Number 3B)*; Alaska Department of Environmental Conservation: Juneau, AK, 1995.

(24) Bence, A. E.; Burns, W. A. In *Exxon Valdez Oil Spill: Fate and Effects in Alaskan Waters*; Wells, P. G.; Butler, J. N.; Hughes, J. S., Eds.; American Society for Testing and Materials: Philadelphia, PA, 1995; special technical publication 1219.

(25) Short, J. W.; Harris, P. M. *Am. Fish. Soc. Symp.* **1996**, *18*, 17–28.

(26) ASTM. In *Annual Book of ASTM Standards, Section 11: Water and Technology* **1996**, *11.02* Water (II), 835–845.

(27) NORDTEST. *Nordtest method*; NT Chem 001, Ed. 2; NORDTEST: Espoo, Finland, 1991.

(28) National Research Council. *Oil in the Sea: Inputs, Fates, and Effects*; National Academy Press: Washington, DC, 1985 (p. 372).

(29) Tripp, B. W.; Farrington, J. W.; Teal, J. M. *Mar. Pollut. Bull.* **1981**, *12*, 122–126.

(30) Tysdal, R. G.; Case, J. E. *Geologic Map of the Seward and Blying Sound Quadrangles, Alaska. Miscellaneous Investigations Series Map I-1150*; U.S. Geological Survey: Washington, DC, 1979. [Referred to in (*31*).]

(31) Page, D. S.; Boehm, P. D.; Douglas, G. S.; Bence, A. E.; Burns, W. A.; Mankiewicz, P. J. *Environ. Toxicol. Chem.* **1996**, *15*, 1266–1281.

(32) Pearlman, R. S.; Yalkowsky, S. H.; Banerjee, S. *J. Phys. Chem. Ref. Data* **1984**, *13*, 555–562.

Appendix

Least-square estimation of w_i and k_j

Least square (LS) estimates of w_i and k_j satisfy the following conditions:

$$\frac{\partial}{\partial k_j}\{\text{trace}[(\mathbf{D} - \hat{\mathbf{w}}\hat{\mathbf{k}})'(\mathbf{D} - \hat{\mathbf{w}}\hat{\mathbf{k}})]\} = 0 \qquad \textbf{(A1)}$$

and

$$\frac{\partial}{\partial w_i}\{\text{trace}[(\mathbf{D} - \hat{\mathbf{w}}'\hat{\mathbf{k}})'(\mathbf{D} - \hat{\mathbf{w}}'\hat{\mathbf{k}})]\} = 0 \qquad \textbf{(A2)}$$

where $\hat{\mathbf{w}}'$ is a column vector with elements $\hat{w}_i$ and $\hat{\mathbf{k}}$ is a row vector with elements $\hat{k}_j$. Because the elements of $\mathbf{D}$ are measured constants here, and because trace $\mathbf{D}'\hat{\mathbf{w}}'\hat{\mathbf{k}}$ = trace $\hat{\mathbf{k}}'\hat{\mathbf{w}}\mathbf{D}$, these two conditions lead to

$$2\frac{\partial}{\partial k_j}(\text{trace } \mathbf{D}'\hat{\mathbf{w}}'\hat{\mathbf{k}}) = \frac{\partial}{\partial k_j}(\text{trace } \hat{\mathbf{k}}'\hat{\mathbf{w}}\hat{\mathbf{w}}'\hat{\mathbf{k}}) \qquad \textbf{(A3)}$$

and

$$2\frac{\partial}{\partial w_i}(\text{trace } \mathbf{D}'\hat{\mathbf{w}}'\hat{\mathbf{k}}) = \frac{\partial}{\partial w_i}(\text{trace } \hat{\mathbf{k}}'\hat{\mathbf{w}}\hat{\mathbf{w}}'\hat{\mathbf{k}}) \qquad \textbf{(A4)}$$

Noting that

$$\text{trace } \mathbf{D}'\hat{\mathbf{w}}'\hat{\mathbf{k}} = \sum_{j=1}^{J}\left(\hat{k}_j\sum_{i=1}^{I} d_{ij}\hat{w}_i\right) \qquad \textbf{(A5)}$$

and

$$\text{trace } \hat{\mathbf{k}}'\hat{\mathbf{w}}\hat{\mathbf{w}}'\hat{\mathbf{k}} = \left(\sum_{i=1}^{I}\hat{w}_i^2\right)\left(\sum_{j=1}^{J}\hat{k}_j^2\right) \qquad \textbf{(A6)}$$

the differentiations indicated in eqs A3 and A4 produce the following equations for the LS estimates of the parameters $\hat{k}_j$ and $\hat{w}_i$, respectively:

$$\hat{k}_j = \frac{\sum_{i=1}^{I} \hat{w}_i d_{ij}}{\sum_{i=1}^{I} \hat{w}_i^2} \tag{A7}$$

and

$$\hat{w}_i = \frac{\sum_{j=1}^{J} \hat{k}_j d_{ij}}{\sum_{j=1}^{J} \hat{k}_j^2} \tag{A8}$$

Equations A7 and A8 imply that $\hat{\mathbf{k}}'$ is an eigenvector of $\mathbf{D}'\mathbf{D}$ as follows: given

$$e_{ij} = d_{ij} - \hat{w}_i \hat{k}_j \; ; \qquad \sum_{j=1}^{J} e_{ij} \hat{k}_j = \sum_{j=1}^{J} d_{ij} \hat{k}_j - \hat{w}_i \sum_{j=1}^{J} \hat{k}_j^2 = 0$$

by eq A7, so

$$\hat{\mathbf{E}} \hat{\mathbf{k}}' = \mathbf{0}^{I \times 1} \tag{A9}$$

Also,

$$\sum_{i=1}^{I} \hat{e}_{ij} \hat{w}_i = \sum_{i=1}^{I} \left(d_{ij} - \hat{w}_i \hat{k}_j \right) \hat{w}_i = \sum_{i=1}^{I} d_{ij} \hat{w}_i - \hat{k}_j \sum_{i=1}^{I} \hat{w}_i^2 = 0 \tag{A10}$$

by eq. 17, so

$$\hat{\mathbf{w}} \hat{\mathbf{E}} = \mathbf{0}^{1 \times J} \tag{A11}$$

Now

$$\mathbf{D}'\mathbf{D} = (\hat{\mathbf{w}}'\hat{\mathbf{k}} + \hat{\mathbf{E}})'(\hat{\mathbf{w}}'\hat{\mathbf{k}} + \hat{\mathbf{E}}) = \hat{\mathbf{k}}'\hat{\mathbf{w}}\hat{\mathbf{w}}'\hat{\mathbf{k}} + \hat{\mathbf{k}}'\hat{\mathbf{w}}\hat{\mathbf{E}} + \hat{\mathbf{E}}'\hat{\mathbf{w}}'\hat{\mathbf{k}} + \hat{\mathbf{E}}'\hat{\mathbf{E}}$$

Multiplication of $\mathbf{D}'\mathbf{D}$ on the right by $\hat{\mathbf{k}}'$, and using eqs A9 and A11 gives

$$\mathbf{D}'\mathbf{D}\,\hat{\mathbf{k}}' = \hat{\mathbf{k}}'\sum_{i=1}^{I}\hat{w}_i^2 \qquad \textbf{(A12)}$$

if $\sum k_j^2 = 1$, showing that $\hat{\mathbf{k}}'$ is an eigenvector of $\mathbf{D}'\mathbf{D}$, associated with the following eigenvalue:

$$\lambda_1 = \sum_{i=1}^{I}\hat{w}_i^2 \qquad \textbf{(A13)}$$

This eigenvalue λ_1 is the dominant eigenvalue of $\mathbf{D}'\mathbf{D}$, because the remaining eigenvectors of $\mathbf{D}'\mathbf{D}$ form a basis for the error space of $\hat{\mathbf{E}}$, the elements of which are minimized by the LS procedure. The constraint $\sum k_j^2 = 1$ means that the k_j are all relative to an arbitrary scaling factor.

TABLE 1.

PAHs determined in environmental samples collected for the EVOS, and PAH proportions in petroleum spilled from the T/V *Exxon Valdez* in Prince William Sound on 24 March 1989. The 14 polynuclear aromatic hydrocarbons that persisted above method detection limits (MDL; see text) during the 6-month weathering experiments are indicated by *, and the corresponding proportions by weight ($\times 10^3$) are taken as the π_j for the weathering model. Also listed are PAH abbreviations used in the figures of this report, and coefficients of variation for the analysis of these PAH in reference samples at the Auke Bay Laboratory (N = 102). ND = not determined, concentration below MDL in reference sample.

PAHs	Abbreviation	$\pi_j(\times 10^3)$	Coefficient of Variation (%)
Naphthalene		0.724	7.41
2-Methylnaphthalene		1.33	6.62
1-Methylnaphthalene		1.02	6.17
Biphenyl		0.183	12.0

C-2 Naphthalenes		3.15	19.4
Acenaphthylene		0.0139	8.99
Acenaphthene		0.0174	20.0
*C-3 Naphthalenes	C3naph	2.35	11.3
*C-4 Naphthalenes	C4naph	0.598	23.8
Fluorene		0.0911	17.7
C-1 Fluorenes		0.225	27.8
*C-2 Fluorenes	C2fluor	0.191	34.2
*C-3 Fluorenes	C3fluor	0.151	50.7
Dibenzothiophene		0.195	16.3
*C-1 Dibenzothiophenes	C1dithio	0.417	16.7
*C-2 Dibenzothiophenes	C2dithio	0.570	19.1
*C-3 Dibenzothiophenes	C3dithio	0.481	35.4
Phenanthrene		0.255	13.4
Anthracene		<0.001	19.1
*C-1 Phenanthrene/Anthracenes	C1phenan	0.755	20.1
*C-2 Phenanthrene/Anthracenes	C2phenan	0.892	12.0
*C-3 Phenanthrene/Anthracenes	C3phenan	0.558	15.5
*C-4 Phenanthrene/Anthracenes	C4phenan	0.166	41.1
Fluoranthene		0.00909	18.5
Pyrene		0.0147	12.6
C-1 Fluoranthene/Pyrenes		0.0716	16.8

Benz-a-anthracene		<0.001	20.0
*Chrysene	Chrysene	0.0492	20.5
*C-1 Chrysenes	C1chrys	0.0802	23.3
*C-2 Chrysenes	C2chrys	0.106	38.4
C-3 Chrysenes		0.0362	43.2
C-4 Chrysenes		<0.001	ND
Benzo-(b+k)-fluoranthene		0.00644	19.8
Benzo-e-pyrene		0.0119	21.6
Benzo-a-pyrene		<0.001	19.7
Perylene		<0.001	19.7
Indeno[1,2,3-cd]pyrene		<0.001	21.2
Dibenzo-a,h-anthracene		<0.001	43.0
Benzo-ghi-perylene		<0.001	23.9

TABLE 2.

Loss-rate (LR) constants $\hat{k}$ derived from principal component analysis of PAH data for the petroleum weathering experiment. Parentheses contain the range of the central 95% of results from bootstrap iterations of LR constant estimates (see text).

PAH	$\hat{k}$
C-3 Naphthalenes	0.659 (0.653, 0.706)
C-4 Naphthalenes	0.148 (0.040, 0.215)
C-2 Fluorenes	0.118 (0.003, 0.188)
C-3 Fluorenes	0.082 (0.013, 0.147)
C-1 Dibenzothiophenes	0.433 (0.392, 0.462)
C-2 Dibenzothiophenes	0.188 (0.144, 0.258)
C-3 Dibenzothiophenes	0.056 (0.019, 0.119)
C-1 Phenanthrene/Anthracenes	0.512 (0.456, 0.585)
C-2 Phenanthrene/Anthracenes	0.126 (0.086, 0.181)
C-3 Phenanthrene/Anthracenes	-0.027 (-0.068, 0.011)
C-4 Phenanthrene/Anthracenes	-0.024 (-0.055, 0.005)
Chrysene	0.041 (0.015, 0.064)

C-1 Chrysenes	-0.051 (-0.068, -0.034)
C-2 Chrysenes	0.036 (0.007, 0.076)

Figure Legends

FIGURE 1. Map of the northern Gulf of Alaska showing the area affected by the Exxon Valdez oil spill of 24 March 1989 (shaded region). Arrows indicate the path of the Alaska Coastal Current, which flushes Prince William Sound (PWS) and transports sediments from the Copper River and eastward into PWS.

FIGURE 2. Regression relations of weathering parameters (w) and time (days) at four loadings of petroleum on gravel used in the petroleum weathering experiments. Petroleum loadings are expressed as ng total PAH per g gravel.

FIGURE 3. Bootstrapped frequency and cumulative distribution of MSE_i derived from the fit of the bootstrapped iterations of the weathering model to the PAH data from the petroleum weathering experiments. The arrow indicates the MSE_i at the 99th percentile of the cumulative distribution, which is used as a critical value to evaluate the probability that PAH patterns of environmental samples are consistent with weathered EVO.

FIGURE 4. (A) Normalized PAH proportions of unweathered EVO. (B) Predicted and observed normalized PAH proportions of weathered EVO for the case $\hat{w}_i = 3.95$ and $MSE_i = 2.03$, the median of the bootstrap MSE_i distribution. (C) Normalized PAH proportions of sediments from Constantine Harbor, where thin vertical bars indicate the range of the central 95% of results from the bootstrap distribution about the median

indicated by the thick vertical bars. In each case, normalization means that the presented PAH proportions sum to unity.

FIGURE 5. Bootstrapped frequency and cumulative distribution of MSE_i' derived from the fit of the bootstrapped iterations of PAH data from intertidal sediments of Constantine Harbor. The arrow indicates the MSE_i' at the 99th percentile of the cumulative distribution, which is used as a critical value to evaluate the probability that PAH patterns of environmental samples are consistent with the natural PAH source evident at Constantine Harbor.

FIGURE 6. Source classification of PAH in environmental samples as a proportion of samples collected (solid bars) and as a proportion of the sum of the PAH concentrations detected above MDL (shaded bars) for (A) sediments, (B) mussels, and (C) other tissues. The numbers of samples are listed above the solid bars indicating proportions of samples. Sources include EVO = petroleum spilled from the T/V *Exxon Valdez*, Constantine Harbor = the natural sediment PAH source represented by PAH at Constantine Harbor, Neither = other unknown sources (or possibly mixtures of EVO and the natural sediment source), Both = samples that are ambiguously classified, and Not Considered = samples in which one or more of the PAH used in the weathering model are below MDL. For source classification criteria, see text.

FIGURE 7. Weathering parameter $\hat{w}_i$ for EVO-contaminated sediments and mussels versus sample collection time t (in total days) after the EVOS, 1989 to 1995. The linear regression is $\hat{w}_i = 3.557 + 0.000645t$, $r^2 = 0.045$, $P < 0.001$.

FIGURE 8. Arrhenius plot of logarithms of rate-loss constants ($\hat{k}$) from (A) the petroleum weathering experiment and from (B) an independent field experiment (*3*), vs total molecular surface area (TSA) for selected PAH. The selected PAH are identified by abbreviations listed in Table 1, and include the least persistent PAH of the petroleum weathering experiment. Estimates of TSA are presented as nm^2 based on (*32*) for unsubstituted homologues, with 0.20, 0.19, and 0.10 nm^2 added respectively for 1, 2, and each successive carbon of an alkyl substituent [based on average TSA increases due to methyl substitution in (*32*)]. The TSA for dibenzothiophene is estimated as that of fluorene increased by 0.011 nm^2 to account for the longer carbon-sulfur bonds. The TSA is used here as an approximate surrogate measure of vaporization enthalpy. Both sets of rate-loss constants are normalized so that $\Sigma k_j^2 = 1$.

FIGURE 9. Effect of hypothetical mixtures of PAH from EVO and the natural sediment PAH source on the median value of mean square errors (*MSE*) distributions describing the fit of such samples to (A) the EVO weathering model, and (B) the natural sediment PAH source represented by PAH at Constantine Harbor. The abscissa is the proportion $(1 - q)$ of total PAH derived from EVO that is combined with the complementary proportion q derived from the natural sediment source. Random

pairwise combinations according to these proportions of samples from the experimental weathering samples and the Constantine Harbor sediment samples were evaluated by eq 6 & 7 to generate a bootstrapped distribution of the $MSE^{(q)}$, and the median value of these distributions is given as the ordinate.

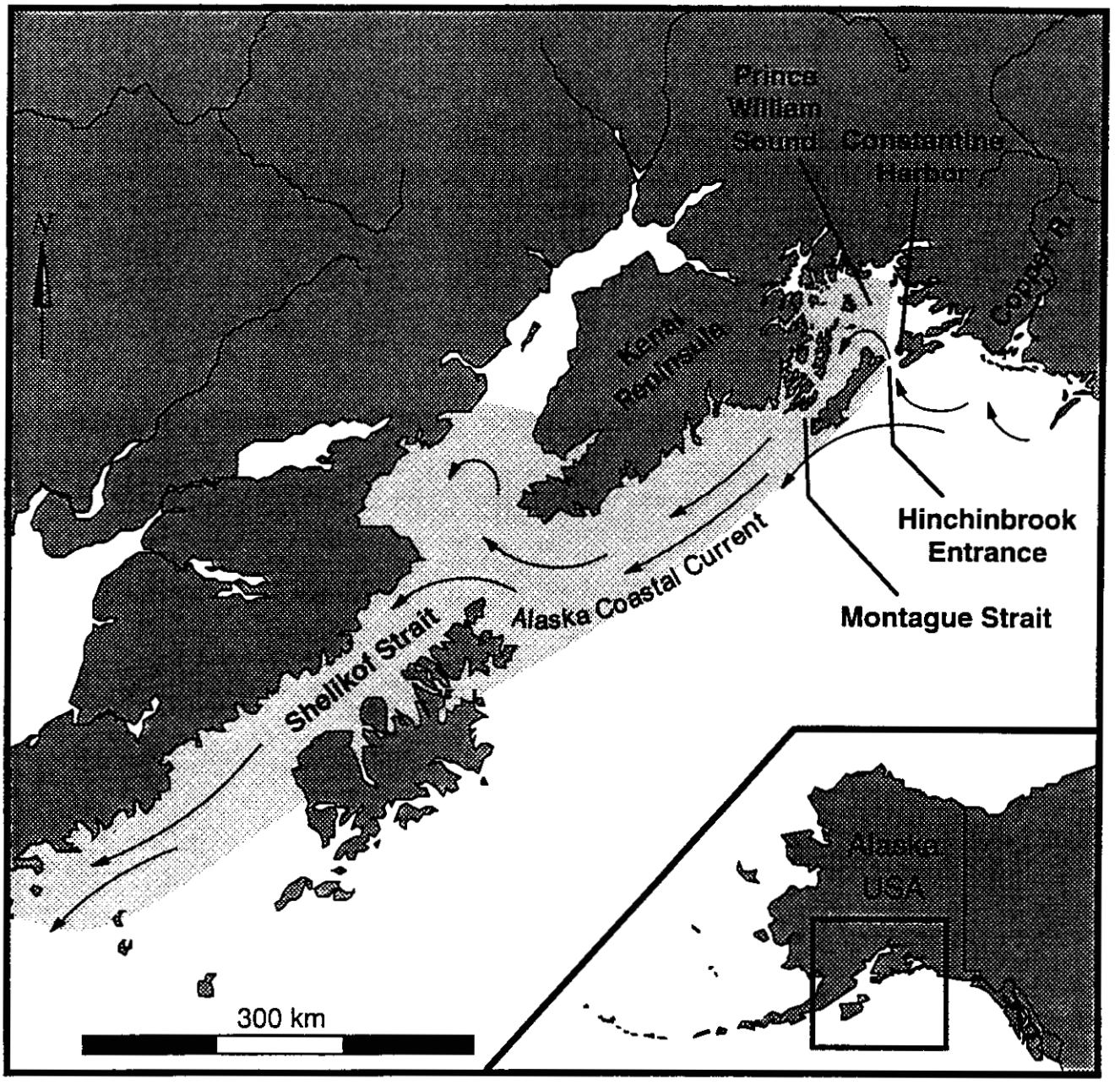

FIGURE 1. The path followed by the spilled *Exxon Valdez* petroleum conformed with the Alaska Coastal Current (ACC).

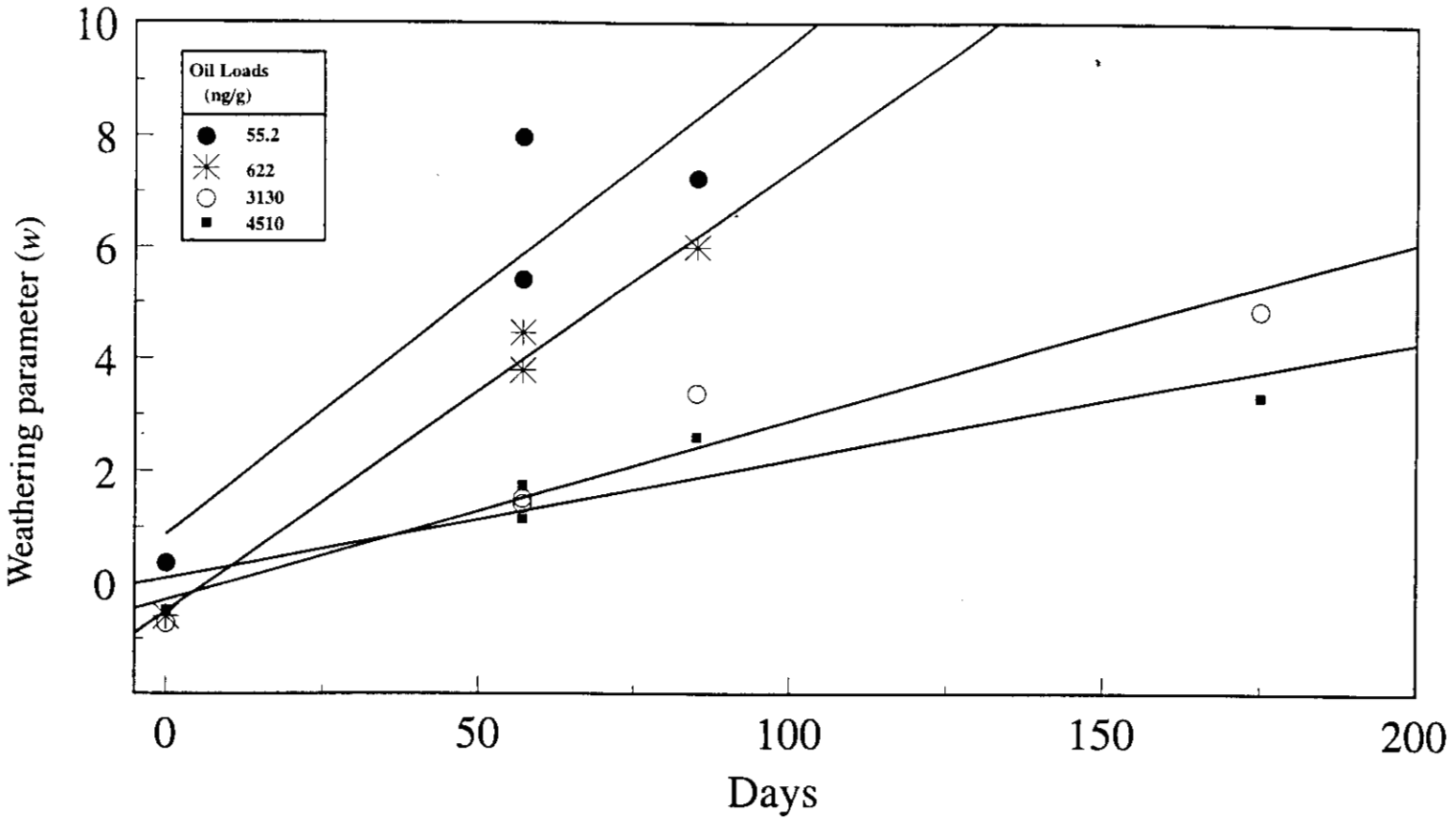

FIGURE 2. Regression relations of weathering parameters (*w*) and time (days) at four loadings of petroleum on gravel used in the petroleum weathering experiments. Petroleum loadings are expressed as ng total PAH per g gravel.

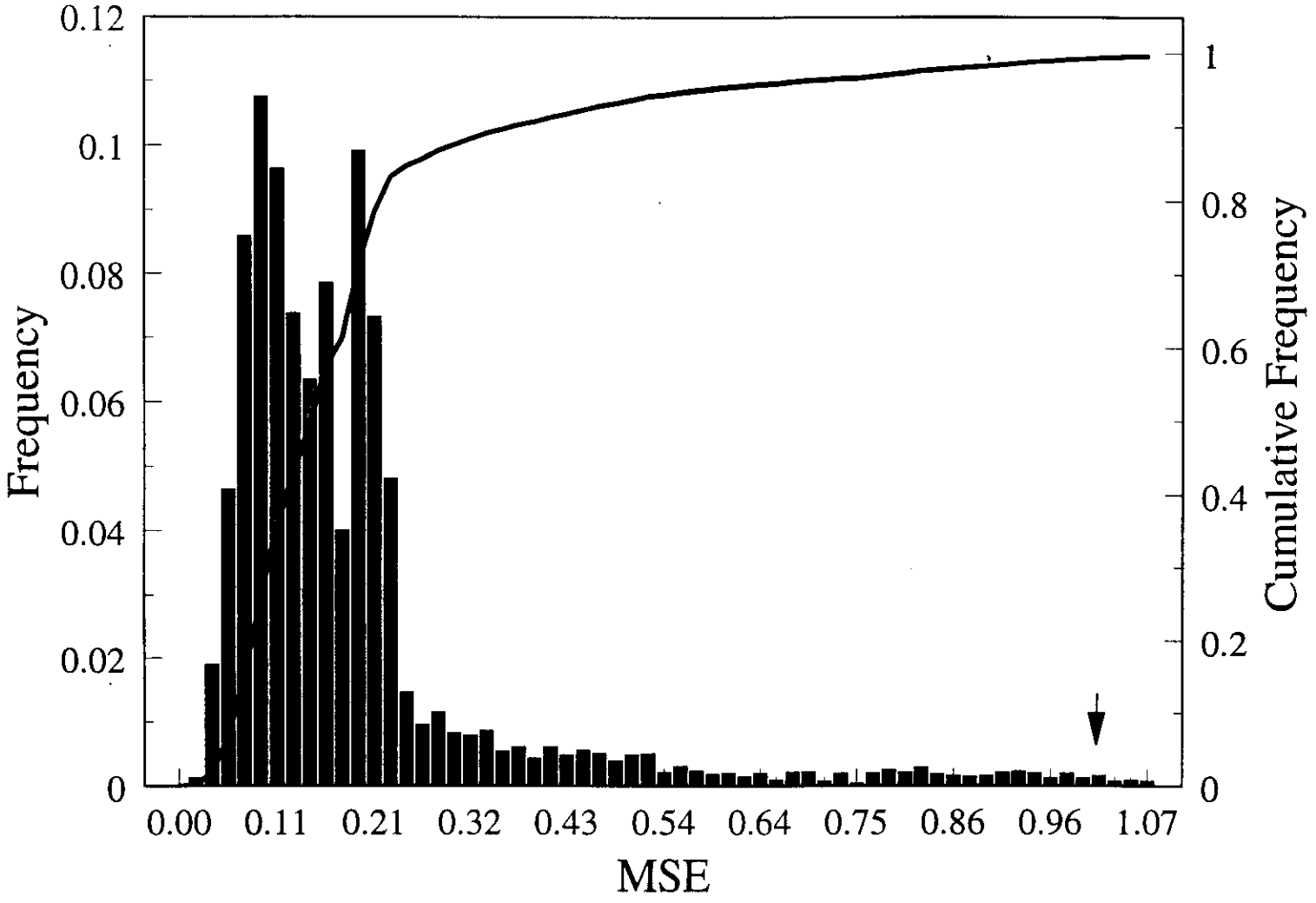

FIGURE 3. Bootstrapped frequency and cumulative distribution of MSEi derived from the fit of the bootstrapped iterations of the weathering model to the PAH data from the petroleum weathering experiments. The arrow indicates the MSEi at the 99th percentile of the cumulative distribution, which is used as a critical value to evaluate the probability that PAH patterns of environmental samples are consistent with weathered EVO.

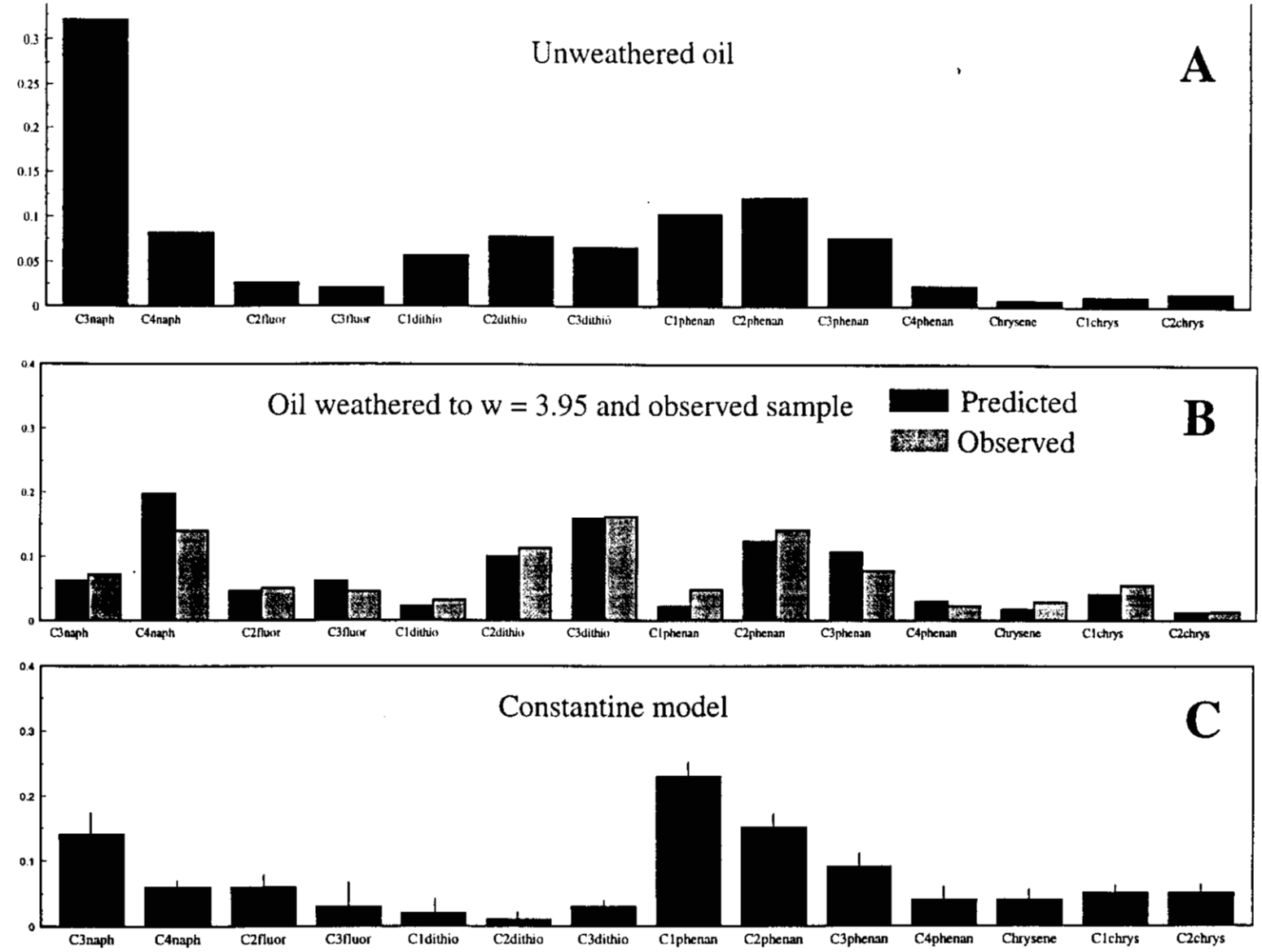

FIGURE 4. (A) Normalized PAH proportions of unweathered EVO. (B) Predicted and observed normalized PAH proportions of weathered EVO for the case i = 3.95 and MSEi = 2.03, the median of the bootstrap MSEi distribution. (C) Normalized PAH proportions of sediments from Constantine Harbor, where thin vertical bars indicate the range of the central 95% of results from the bootstrap distribution about the median indicated by the thick vertical bars. In each case, normalization means that the presented PAH proportions sum to unity.

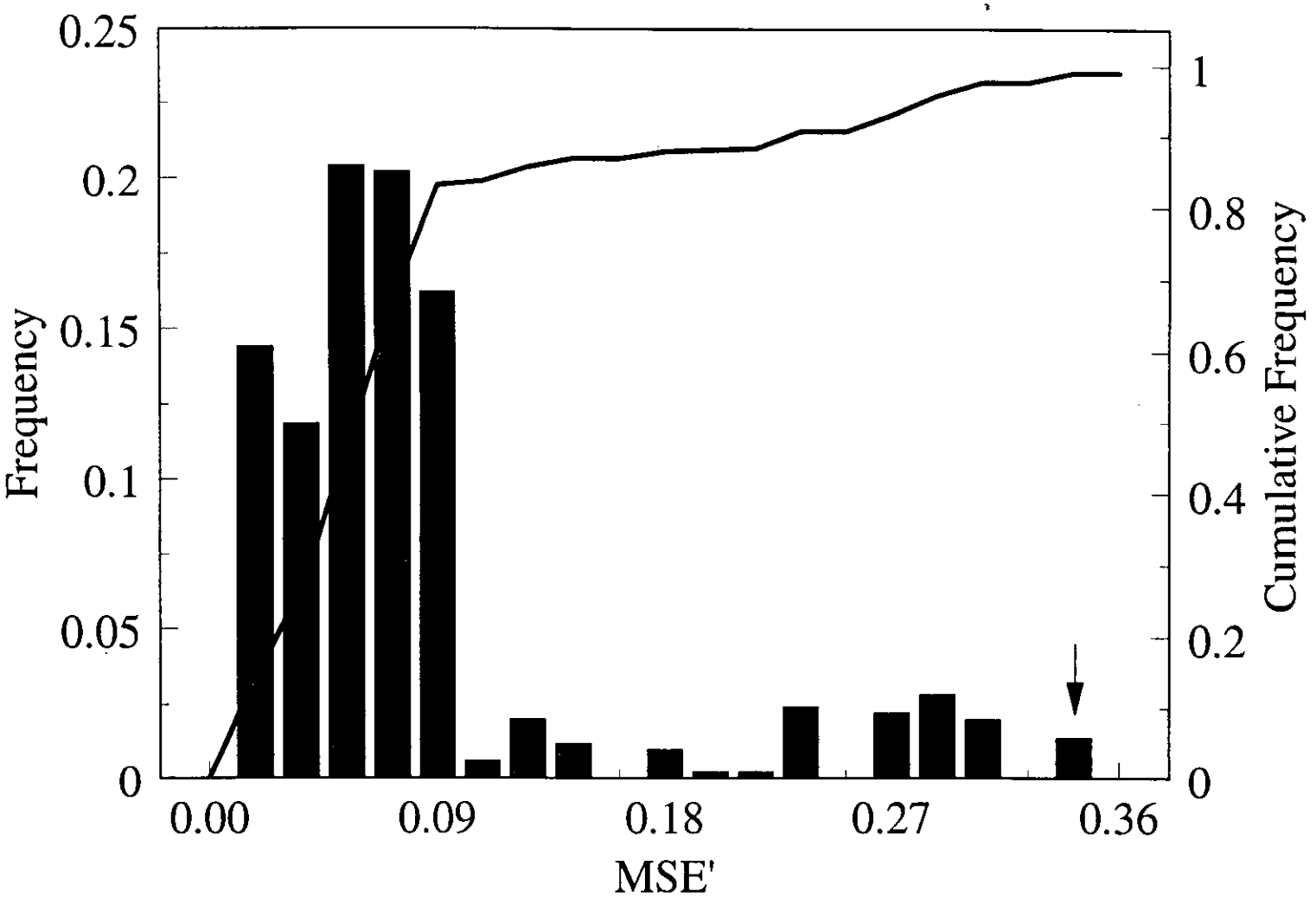

FIGURE 5. Bootstrapped frequency and cumulative distribution of MSEi derived from the fit of the bootstrapped iterations of PAH data from intertidal sediments of Constantine Harbor. The arrow indicates the MSEi at the 99th percentile of the cumulative distribution, which is used as a critical value to evaluate the probability that PAH patterns of environmental samples are consistent with the natural PAH source evident at Constantine Harbor.

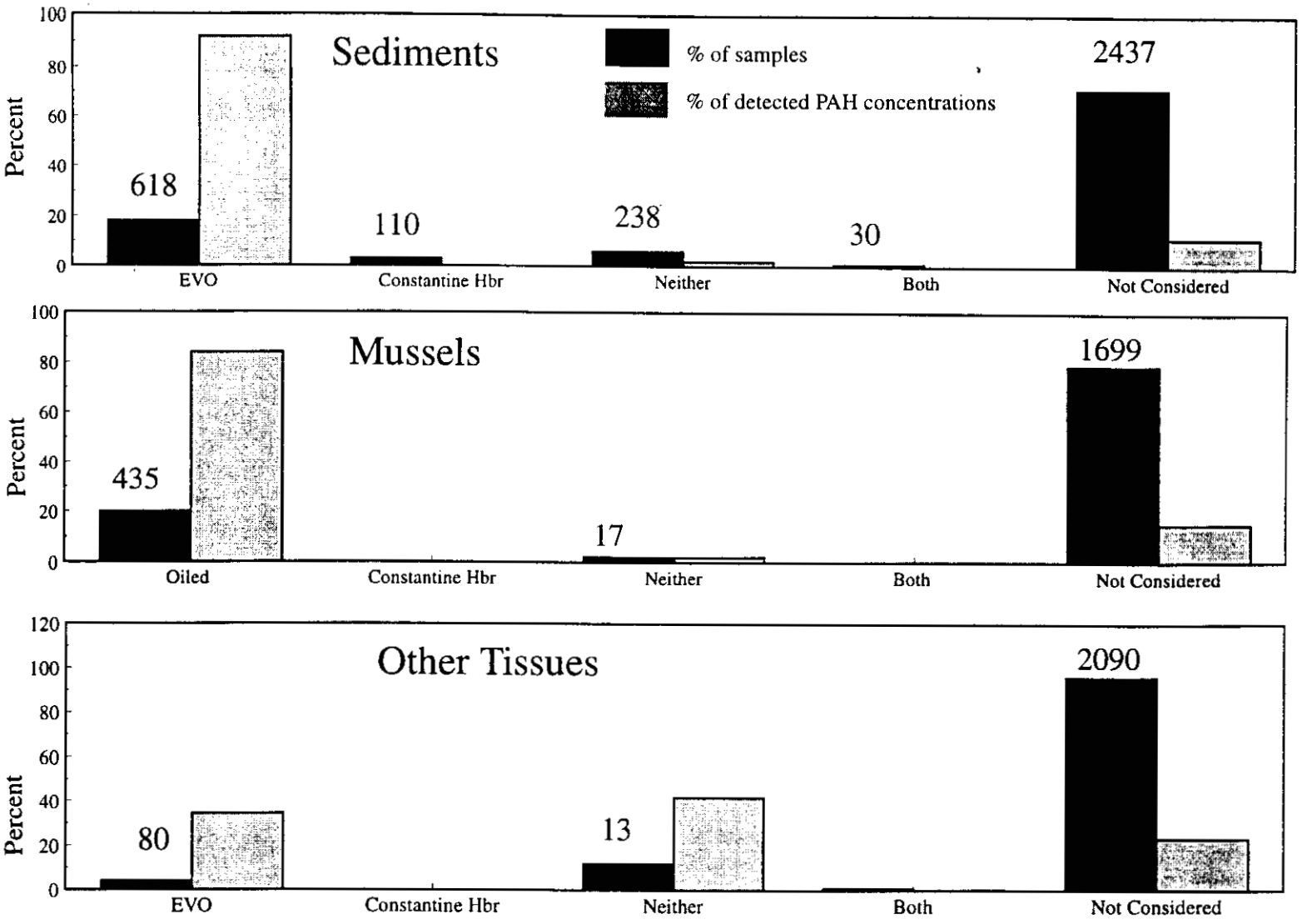

FIGURE 6. Source classification of PAH in environmental samples as a proportion of samples collected (solid bars) and as a proportion of the sum of the PAH concentrations detected above MDL (shaded bars) for (A) sediments, (B) mussels, and (C) other tissues. The numbers of samples are listed above the solid bars indicating proportions of samples. Sources include EVO = petroleum spilled from the T/V Exxon Valdez, Constantine Harbor = the natural sediment PAH source represented by PAH at Constantine Harbor, Neither = other unknown sources (or possibly mixtures of EVO and the natural sediment source), Both = samples that are ambiguously classified, and Not Considered = samples in which one or more of the PAH used in the weathering model are below MDL For source classification criteria, see text.

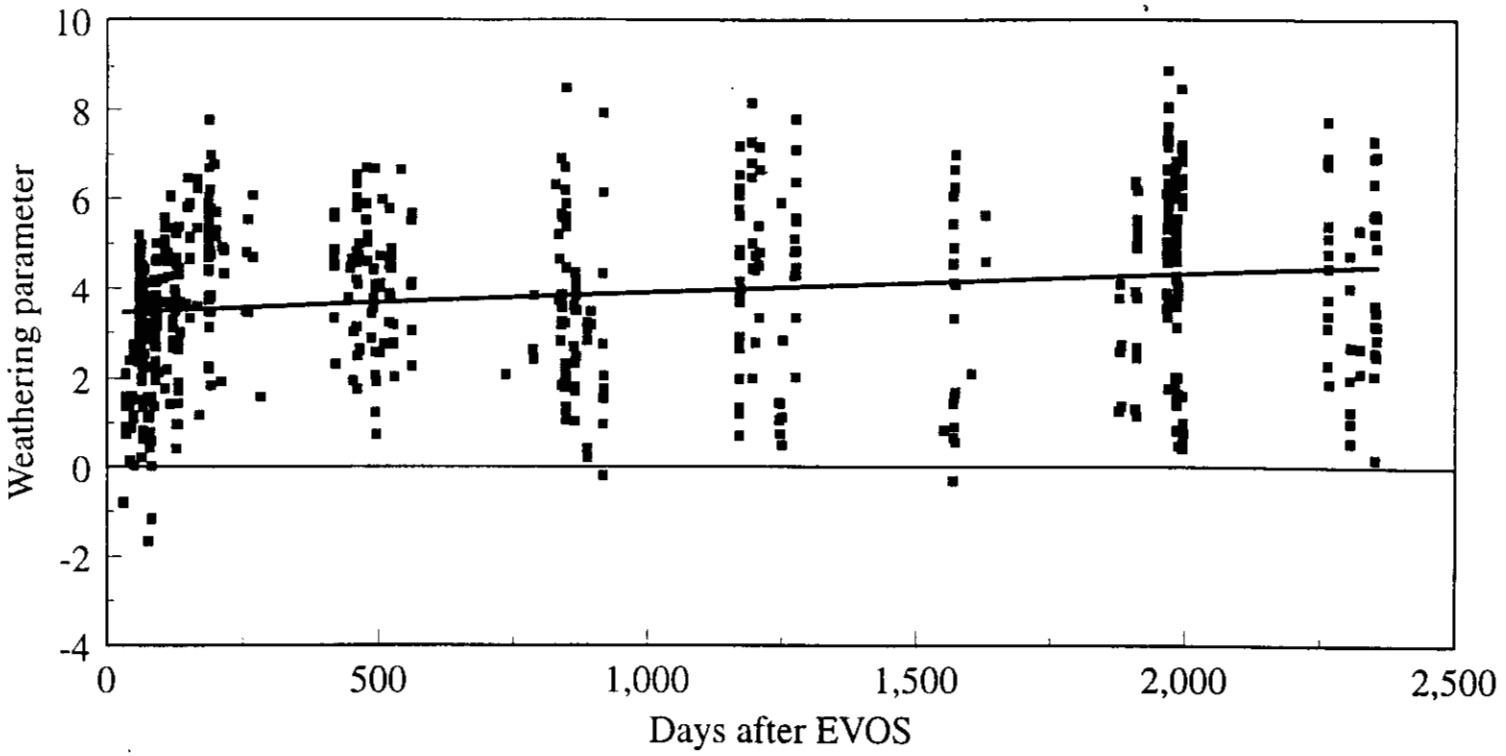

FIGURE 7. Weathering parameter i for EVO-contaminated sediments and mussels versus sample collection time t (in total days) after the EVOS, 1989 to 1995. The linear regression is $i = 3.557 + 0.000645t$, $r2 = 0.045$, $P < 0.001$.

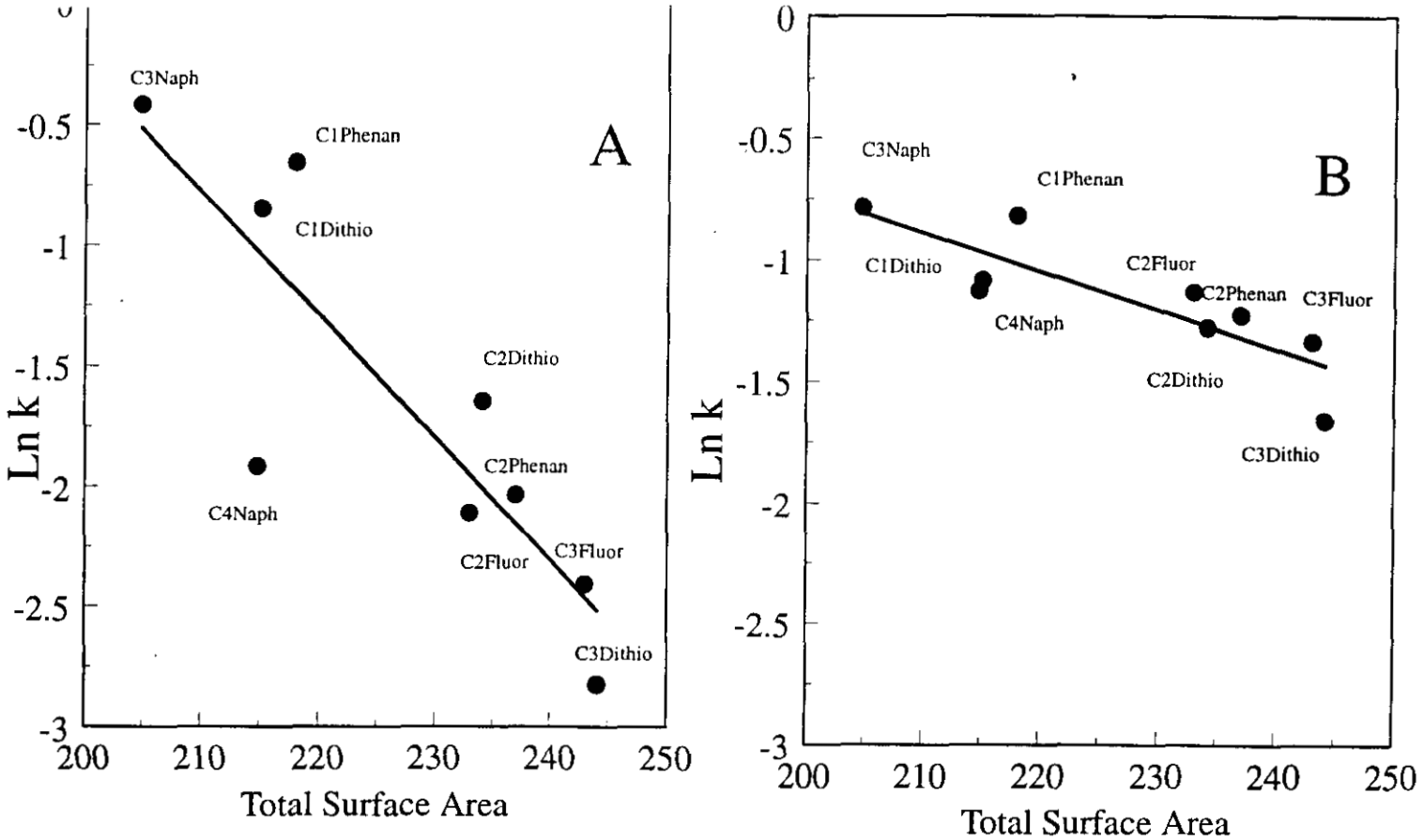

FIGURE 8. Arrhenius plot of logarithms of rate-loss constants () from (A) the petroleum weathering experiment and from (B) an independent field experiment (3), vs total molecular surface area (TSA) for selected PAH. The selected PAH are identified by abbreviations listed in Table 1, and include the least persistent PAH of the petroleum weathering experiment. Estimates of TSA are presented as nm2 based on (32) for unsubstituted homologues, with 0.20, 0.19, and 0.10 nm2 added respectively for 1, 2, and each successive carbon of an alkyl substituent [based on average TSA increases due to methyl substitution in (32)]. The TSA for dibenzothiophene is estimated as that of fluorene increased by 0.011 nm2 to account for the longer carbon-sulfur bonds. The TSA is used here as an approximate surrogate measure of vaporization enthalpy. Both sets of rate-loss constants are normalized so that kj2 = 1.

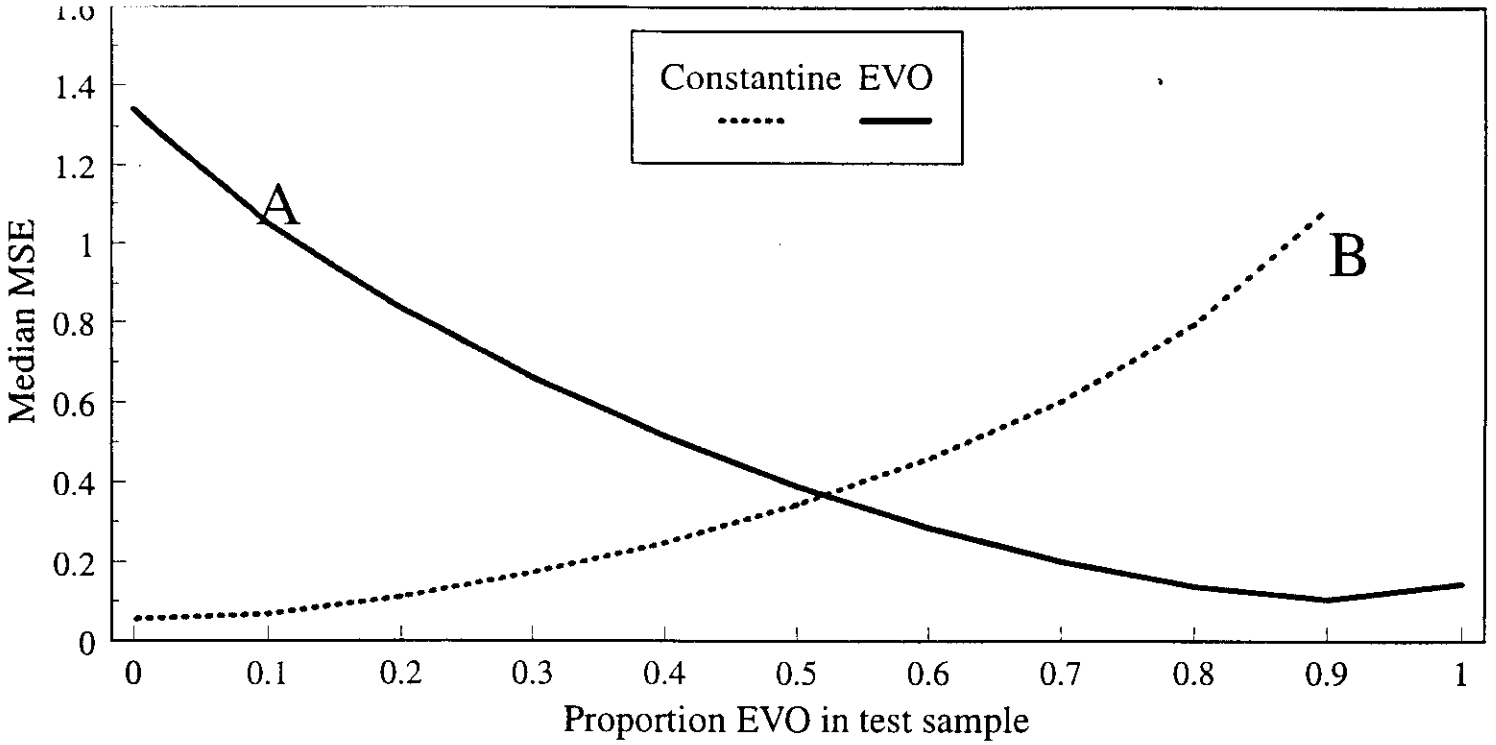

FIGURE 9. Effect of hypothetical mixtures of PAH from EVO and the natural sediment PAH source on the median value of mean square errors (MSE) distributions describing the fit of such samples to (A) the EVO weathering model, and (B) the natural sediment PAH source represented by PAH at Constantine Harbor. The abscissa is the proportion (1 q) of total PAH derived from EVO that is combined with the complementary proportion q derived from the natural sediment source. Random pairwise combinations according to these proportions of samples from the experimental weathering samples and the Constantine Harbor sediment samples were evaluated by eq 6 & 7 to generate a bootstrapped distribution of the MSE(q), and the median value of these distributions is given as the ordinate.

Part III

Descriptive Documentation for Identification of Biased Sediment and Mussel Tissue Samples in the *NRDA* Hydrocarbon Database

Exxon-Valdez Natural Resource Damage Assessment Project

Subtidal 8

DESCRIPTIVE DOCUMENTATION

FOR

IDENTIFICATION OF BIASED SEDIMENT AND MUSSEL TISSUE SAMPLES IN THE *NRDA* HYDROCARBON DATABASE

Prepared by

J. Short and R. Heintz

Auke Bay Laboratory
Alaska Fisheries Science Center
National Marine Fisheries Service, NOAA

IDENTIFICATION OF BIASED SEDIMENT AND MUSSEL TISSUE SAMPLES IN THE *NRDA* HYDROCARBON DATABASE

The credibility of chemical data derived from an environmental sampling program depends, in part, on the agreement of results among replicate samples, and on confirmation of the general absence of contaminant levels in samples of known uncontaminated sites. Contaminant levels determined by chemical analysis that vary by orders of magnitude among replicate samples, or that occur sporadically among control site samples, may be rightly regarded with skepticism, especially if the outlier samples responsible for these deviations are associated with artificial predictor variables, such as the person who collected the samples, or particular batches of samples analyzed, or the analytical facility, etc. On the other hand, the underlying distribution of contaminants in the sampled environment may be such that levels measured in replicate samples may fail to agree within orders of magnitude in some proportion of the replicated samples. However, in this latter case the outlier samples will be distributed approximately randomly among artificial predictor variables, especially if the data set contains a relatively large number of replicated samples.

The following procedure has been developed to determine whether outlier hydrocarbon data from Exxon-Valdez NRDA samples of sediments or of marine mussel tissue are approximately randomly

distributed among certain artificial predictor variables. The purpose of this procedure is to identify artificial predictor variables that are associated with an improbably large number of outlier samples on the hypothesis of random distribution, so that data from all the samples, whether replicated or not, associated with the identified variable may be used with appropriate caution.

The success of the following procedure depends critically on the relatively large number of samples analyzed and replicated, the relatively large number of chemical analytes simultaneously measured in each sample, and on rigorously consistent definitions of outlier samples. As of October 23, 1992, the Exxon-Valdez NRDA Hydrocarbon Database contained chemical analysis data for 2,698 sediment samples, which includes 1,902 samples that are replicated; and 941 mussel tissue samples, which includes 430 samples that are replicated. Each sample has been analyzed for 63 unique aromatic and alkane hydrocarbon classes simultaneously. These large numbers of analyte classes and of replicated samples make it possible to identify associations of outlier samples at a high level of confidence.

The procedure described below consists of two parts, which are described sequentially. Part I describes the methods for identifying outlier samples, and Part II describes the methods used to examine the distribution of identified outlier samples among artificial predictor variables. Finally, a brief summary

of results is presented in Part III. The artificial predictor variables considered include the identification number of the catalogue (i.e., batch of samples), and the project responsible for sample collection. Individual samples suspected of systematic bias on the basis of these methods are identified in the **QCERROR** column of the **RECOVERY** table in the NRDA hydrocarbon database. Inclusion of samples identified as biased by these methods in a data set may substantially reduce the power of subsequent statistical tests by inflating the estimate of the sample variance, and by distorting the apparent underlying distribution of the hydrocarbon data.

PART I. IDENTIFICATION OF OUTLIER SAMPLES

A. Structure of the data

Samples were assigned to catalogs under a stratified random system where the stratum was priority level; samples with high priority were analyzed first. Priority levels were assigned by investigators and batches with similar priority levels usually consisting of combinations of control and "oiled" samples. No samples were analyzed in more than one catalog, but different matrices could be included in a catalog. Some samples could be associated into replicate groups according the following criteria for replicate: samples collected on the same date under the same project at the same location within an area of less than 1 m^2.

Each investigator contributing samples to the database was asked to identify samples meeting these criteria for replicate groups. Catalogs could contain all or a portion of the samples from a replicate group. Control sample locations were obtained by polling the investigators. All control locations were selected a priori by the investigators.

Outlier samples fail to conform with one or both of the following expectations. First, hydrocarbon concentrations in replicate groups are expected to be more or less similar. Second, samples collected from a priori control sites were not expected to contain hydrocarbons characteristic of Exxon-Valdez crude oil.

B. Replicate Sample Outliers (Type I Deviants)

A sample was considered an outlier if more than 9 of its 63 hydrocarbon classes were simultaneously very different, when compared with respective concentrations in the remaining samples of the replicate group. These outlier samples are referred to as Type I deviants.

The first step in identifying deviant samples in a replicate group is to identify replicate groups that contain outlier samples. For each hydrocarbon, the logarithm of the squared range of values for the hydrocarbon for each replicate group is plotted against the logarithm of the median value for that group. (Replicate groups that have zero range for the hydrocarbon

considered are not included because the samples in the group obviously do not deviate, failing to meet the criterium for a deviant replicated sample.) The log-log plot accounts for the expected increase in the variance of each hydrocarbon at higher concentration. A linear regression line is calculated for this plot, and the replicate groups associated with the highest 5% of positive deviations from the regression line are identified and given a score of 1, indicating that the replicate group's range for a hydrocarbon concentration was deviant. Only positively deviant replicates on the plot are identified because these have the largest ranges; the negatively deviant replicates are those that agree most closely for the hydrocarbon under consideration. Thus, 63 regressions are calculated and replicate groups had scores ranging from 0 to 63. The score indicated the number of times the replicate group had deviant hydrocarbon ranges. These deviant ranges arise from high hydrocarbon observations in some of the samples included in the group.

Replicate groups with a score greater than 9 were subsequently examined to determine which samples in the group were outliers. In order for a sample to be an outlier it had to have at least 10 hydrocarbon observations that were simultaneously "very different". A hydrocarbon observation was considered "very different" if it met two criteria: 1) its magnitude had to be greater than 10 times the method detection limit (MDL) for that analyte, and 2) the magnitude must have been 3 times the magnitude of the highest remaining observation in the replicate

group. If an observation met these criteria, then the sample was given a score of 1. If a sample accumulated a score greater than 9 (the sample contains more than 9 "very different" observations) then that sample was considered an outlier and flagged.

The reason a sample required 10 or more simultaneous outlier hydrocarbon observations to be identified as a Type I deviant follows. Each sample will contain some number **n** of outlier hydrocarbon measurements. If the distribution of these outliers were random among samples, then each hydrocarbon observation has a 5% probability of being identified as an outlier in each sample. The probability, **P**, that a sample will contain **n** deviant observations simultaneously under these assumptions is:

$$1. \quad P = \binom{k}{n} (0.05)^n (0.95)^{k-n}$$

where **k** = 63 is the number of hydrocarbon classes examined for each sample. According to Eq. 1, the probability that more than 9 hydrocarbon observations are simultaneously deviant within a sample is less than 0.2% (**k** = 63, **n** = 10). This means that the above procedure will mis-identify less than 0.2% of the samples as outliers, if instances of outlier hydrocarbon observations are really randomly distributed among samples.

All samples satisfying the above criteria are identified as Type I deviants and flagged in the database. The process is reiterated without the flagged samples until no more Type I deviant samples are identified. Reiteration is necessary because outlier samples causing the largest ranges are discovered first, and bias the slope of the log-log regression line to obscure less dramatic outliers.

C. Control Site Sample Outliers (Type II Deviants)

A second group of outlier samples, termed Type II deviants, is identified by failure to conform with the expectation that samples collected from a priori control sites are not expected to be contaminated with petroleum hydrocarbons. This expectation is based on a hydrocarbon survey of Prince William Sound conducted in 1977 - 1980, which showed intertidal sediments and mussels to be generally free of petroleum hydrocarbons except in localized areas of vessel traffic (Karinen et al, 1992). Control site samples were collected from control sites picked a priori by the principal investigator (PI) for each project. Petroleum hydrocarbon contamination was be considered present in a control site sample if more than 5 hydrocarbon observations in the following hydrocarbon analyte classes were present at greater than 5 times their respective MDLs: fluorenes, dibenzothiophenes, phenanthrenes, chrysenes, and phytane. Any sample collected from an a priori control site that met this criterium was identified as a Type II deviant and flagged.

PART II.

DISTRIBUTION OF OUTLIER SAMPLES AMONG CATALOGS AND PROJECTS

The distribution of type I deviant samples among catalogs and projects is examined based on an approach that is analogous with eq. 1. Given **j** Type I deviant among a total of **J** samples initially considered, the probability **P** that a project or catalog containing **L** samples of which **m** are deviant is:

$$2. \quad P = \binom{L}{m}\left(\frac{j}{J}\right)^{m}\left(1-\frac{j}{J}\right)^{L-m}$$

assuming the underlying distribution of deviant samples among catalogs or projects is random. These probabilities are first calculated for each project, and the plausibility of the observed probabilities was evaluated using a chi-square test. An estimate of chi-square is calculated as:

$$3. \quad \chi^2 = \sum_{i=1}^{h} \frac{((j/J)L_i - m_i)^2}{(j/J)L_i}$$

where **h** is the number of projects considered. If this estimate is higher than the critical value of chi-square at $\alpha = 0.05$ and **h**-2 degrees of freedom, then all the deviant samples associated in the least probable project are flagged as systematically deviant. A new estimate of chi-square is calculated for the

remaining projects, where both **j** and **J** are reduced by the **m** and **L**, respectively, of the excluded project. The new estimate of chi-square is compared with the critical value, and the process is reiterated until the chi-square estimate is less than the critical value. This process is repeated using catalogs. Catalogs that contain improbably large numbers of Type I deviant samples are listed as Type I catalogs (no projects have yet been identified that contain an improbable number of Type I deviant samples).

A similar process is performed on the Type II deviant samples with some modifications. Type II deviant samples are believed to have come from uncontaminated sites, yet they apparently contain hydrocarbons characteristic of petroleum. Improbable associations of Type II deviant samples with samples sites, sample depths, projects, and catalogs, in that order, are examined using the chi-square procedure described in the preceeding paragraph. Some sites and depths, but no projects, have been found to be associated with an improbably large number of Type II deviant samples. Type II deviant samples associated with these identified sites and depths are therefore excluded, and the distribution of the remaining Type II deviant samples among projects and catalogues are examined. Catalogs containing improbably large numbers of Type II deviant samples were listed as Type II catalogs.

PART III. FINAL DATA EVALUATION

Type I Deviants: Examination of replicate group similarity among the sediment samples, using the methods described above, reveals 122 outlier samples. The chi-square analysis identifies 7 catalogs with disproportionate numbers of deviant samples.

Type II Deviants: Examination of the samples taken from control sites reveal that 6 sites (Simpson Bay, Longb, Maclh, Mcclb, Dayvi, and Ugakb) and the 100 m depth contour contain disproportionate numbers of contaminated samples; these sites and depths may have been contaminated prior to the Exxon-Valdez oil spill. The control site sample analysis also reveal 15 catalogs that appear to contain disproportionate numbers of contaminated samples. Samples from replicate groups or control sites do not appear to be biased by the project that collected them.

Tables 1 and 2 summarize the results of these analyses for the sediment and mussel data, respectively. Note that many catalogs do not contain control site samples, and others contain large numbers of unreplicated samples. Catalogs may therefore be classified according to the number of replicated samples and control site samples they contain. Catalogs in the group most amenable to evaluation using the methods described above include samples from at least 5 replicate groups that are replicated outside the catalog, and at least 5% of the samples in the catalog are from control sites; these catalogs are identified as

"fully evaluatable" in tables 1 and 2. A second group of catalogs meet only one of these criteria, and are identified as "partially evaluatable". A third group of catalogs meet meet none of these criteria, and are identified as "marginally evaluatable". Among the sediment samples, 28 catalogs are fully evaluatable, 29 catalogs are partially evaluatable, and 17 catalogs are marginally evaluatable.

Conclusions

Sediments:

Samples in catalogs that contain improbably large numbers of both Type I and Type II deviant samples are considered biased. These samples are labeled "biased" in the **QCERROR** column of the **SAMPLE** table in the database. Four fully evaluatable catalogs meet these criteria: 6471, 6472, 6476, and 6699. Samples in two partially evaluatable catalogs are also labeled as "biased", those in catalogs 6470 and 6474. In catalog 6470, there are too few replicated samples to evaluate, but 8 of 8 control site samples are Type II deviant. In catalog 6474, there are no control site samples, but 22 of 44 samples are Type I deviants, which is extremely improbable.

Samples in remaining catalogs are labeled as either "suspect" or as "good" in the **QCERROR** column of the **SAMPLE** table in the database. Samples in catalogs that contain improbably large

numbers of either Type I or Type II deviant samples are labeled "suspect", otherwise they are labeled "good".

Of the 2,698 sediment samples processed, 252 were labeled "biased", 466 "suspect" and 1980 "good". Samples labeled "biased" should be used with extreme caution for statistical analyses. Samples labeled "suspect" should be used with some caution because there is reason to believe they are biased, but the results are not definitive. Samples labeled "good" do not appear biased on the basis of the methods and criteria described above, although this may be a result of insufficient replicate and control site samples in the catalog.

Mussels:

No biases have been detected in the mussel sample data. There are 12 catalogs in common between the sediment and mussel data. Of these, only catalog 6116 contained suspect data. Catalog 6116 appeared on the Type II list after analyzing the sediment data, and there are no control samples of mussel tissue in the catalog. Mussel samples associated with this catalog are labeled "suspect". All other mussel samples are labeled "good".

Literature Cited

Karinen, J F, Babcock M M, Brown D B, MacLeod W D, Ramos L S, Short J W. 1992. Hydrocarbons in Intertidal Sediments and Mussels from Prince William Sound, Alaska, 1977-1980: Characterization and Probable Sources. NOAA Tech. Memo., in review.

Table 1. Number of samples in each catalog and number of Type I and II deviants, level of evaluability and final QCERROR CODE for catalogs containing sediment samples

Catno	Number of samples in catalog	Number of unreplicated samples in catalog	Number of Type I deviants in catalog	Number of groups in catalog	Number of groups replicated outside catalog	Number of control samples in catalog	Number of Type II deviants in catalog	How catalog is listed	Are there 5% controls?	Level of evaluatability	QCERROR code
6116	18	8	1	10	10	1	1	II	YES	FULL	SUSPECT
6168	52	37	0	15	15	7	1		YES	FULL	GOOD
6472	43	20	15	22	22	12	12	I,II	YES	FULL	BIASED
6477	40	24	2	16	16	4	0		YES	FULL	GOOD
6478	44	15	2	28	28	7	0		YES	FULL	GOOD
6548	38	13	2	18	14	4	0		YES	FULL	GOOD
6549	46	18	3	16	10	5	1		YES	FULL	GOOD
6582	41	0	6	18	7	6	0	I	YES	FULL	SUSPECT
6584	43	0	0	22	22	12	0		YES	FULL	GOOD
6588	44	0	0	26	25	3	0		YES	FULL	GOOD
6589	40	0	2	23	23	20	8		YES	FULL	GOOD
6592	45	10	1	17	10	10	0		YES	FULL	GOOD
6594	47	0	1	18	7	12	3		YES	FULL	GOOD
6596	45	6	1	16	7	10	8	II	YES	FULL	SUSPECT
6693	47	20	0	23	23	4	2		YES	FULL	GOOD
6696	42	8	0	24	22	3	0		YES	FULL	GOOD
6697	43	4	2	28	28	3	3	II	YES	FULL	SUSPECT
6698	45	8	3	30	27	10	3		YES	FULL	GOOD
6699	43	3	4	29	28	7	5	I,II	YES	FULL	BIASED
6700	41	10	0	23	22	5	0		YES	FULL	GOOD
6701	40	5	2	26	23	10	10	II	YES	FULL	SUSPECT
6702	44	1	0	31	29	5	3	II	YES	FULL	SUSPECT
6703	29	2	0	15	11	11	2		YES	FULL	GOOD

Table 1, continued

Catno	Number of samples in catalog	Number of unreplicated samples in catalog	Number of Type I deviants in catalog	Number of groups in catalog	Number of groups replicated outside catalog	Number of control samples in catalog	Number of Type II deviants in catalog	How catalog is listed	Are there 5% controls?	Level of evaluatability	QCERROR code
6703	29	2	0	15	11	11	2		YES	FULL	GOOD
NMES_082	32	1	0	16	9	16	0		YES	FULL	GOOD
NMES_083	26	3	0	12	8	13	0		YES	FULL	GOOD
NMES_125	21	0	0	12	10	2	0		YES	FULL	GOOD
NMES_127	15	0	0	8	8	2	0		YES	FULL	GOOD
NMES_128	17	0	0	8	5	6	0		YES	FULL	GOOD
6231	43	0	1	15	1	12	0		YES	PARTIAL	GOOD
6211	39	0	0	15	4	8	0		YES	PARTIAL	GOOD
6170	35	31	0	3	2	8	8	II	YES	PARTIAL	BIASED
6545	48	48	0	0	0	5	0		YES	PARTIAL	GOOD
6547	48	48	0	0	0	8	0		YES	PARTIAL	GOOD
6550	34	31	0	3	3	7	4	II	YES	PARTIAL	SUSPECT
6580	46	32	0	6	3	16	2		YES	PARTIAL	GOOD
6585	42	0	0	16	3	18	0		YES	PARTIAL	GOOD
NMES_129	17	0	0	7	2	6	0		YES	PARTIAL	GOOD
NMES_183	15	13	0	2	2	1	0		YES	PARTIAL	GOOD
NMES_184	30	30	0	0	0	2	0		YES	PARTIAL	GOOD
6166	43	23	0	13	11	1	0		NO	PARTIAL	GOOD
6167	85	40	0	35	30	0	0		NO	PARTIAL	GOOD
6471	44	4	19	40	40	2	2	I,II	NO	PARTIAL	BIASED
6474	44	2	22	40	40	0	0	I	NO	PARTIAL	BIASED
6476	43	10	10	33	33	1	1	I,II	NO	PARTIAL	BIASED

Table 1, continued.

Catno	Number of samples in catalog	Number of unreplicated samples in catalog	Number of Type I deviants in catalog	Number of groups in catalog	Number of groups replicated outside catalog	Number of control samples in catalog	Number of Type II deviants in catalog	How catalog is listed	Are there 5% controls?	Level of evaluatability	QCERROR code
6578	43	5	0	21	18	0	0		NO	PARTIAL	GOOD
6579	32	5	0	12	8	4	0		NO	PARTIAL	GOOD
6581	47	7	1	22	19	2	0		NO	PARTIAL	GOOD
6583	48	3	0	22	17	0	0		NO	PARTIAL	GOOD
6586	46	1	1	23	16	0	0		NO	PARTIAL	GOOD
6587	46	0	1	24	20	1	0		NO	PARTIAL	GOOD
6590	41	0	1	25	25	0	0		NO	PARTIAL	GOOD
6591	44	0	1	31	31	0	0		NO	PARTIAL	GOOD
6595	42	1	3	19	9	0	0	I	NO	PARTIAL	SUSPECT
NMFS_078	13	0	0	6	5	0	0		NO	PARTIAL	GOOD
NMFS_137	36	0	0	18	16	1	0		NO	PARTIAL	GOOD
NMFS_141	12	0	1	8	7	0	0		NO	PARTIAL	GOOD
NMFS_174	44	8	0	15	5	9	0		NO	PARTIAL	GOOD
NMFS_175	21	6	5	9	8	0	0	I	NO	PARTIAL	SUSPECT
6104	10	10	0	0	0	0	0		NO	MARGINAL	GOOD
6162	15	6	1	3	0	0	0		NO	MARGINAL	GOOD
6165	9	0	1	3	0	0	0		NO	MARGINAL	GOOD
6230	44	0	1	13	4	0	0		NO	MARGINAL	GOOD
6234	43	0	3	15	2	0	0		NO	MARGINAL	GOOD
6240	43	0	2	13	4	1	1	II	NO	MARGINAL	SUSPECT
6546	46	45	0	1	1	1	1	II	NO	MARGINAL	SUSPECT
6593	48	9	0	16	1	0	0		NO	MARGINAL	GOOD

Table 1. continued

Catno	Number of samples in catalog	Number of unreplicated samples in catalog	Number of Type I deviants in catalog	Number of groups in catalog	Number of groups replicated outside catalog	Number of control samples in catalog	Number of Type II deviants in catalog	How catalog is listed	Are there 5% controls?	Level of evaluatability	QCERROR code
6593	48	9	0	16	1	0	0		NO	MARGINAL	GOOD
6658	17	17	0	0	0	0	0		NO	MARGINAL	GOOD
6694	49	42	1	4	4	2	2	II	NO	MARGINAL	SUSPECT
6695	45	45	0	0	0	1	1		NO	MARGINAL	GOOD
6713	37	37	0	0	0	0	0		NO	MARGINAL	GOOD
6714	20	20	0	0	0	0	0		NO	MARGINAL	GOOD
NMFS 075	12	0	0	5	3	0	0		NO	MARGINAL	GOOD
NMFS 081	1	0	0	1	1	0	0		NO	MARGINAL	GOOD
NMFS 126	8	0	0	5	4	0	0		NO	MARGINAL	GOOD
NMFS 191	9	1	0	4	4	0	0		NO	MARGINAL	GOOD

Table 2. Number of samples in each catalog and number of Type I and II deviants, level of evaluability and final QCERROR CODE for catalogs containing mussel tissue samples

Catno	Number of samples in catalog	Number of unreplicated samples in catalog	Number of Type I deviants in catalog	Number of groups in catalog	No. of groups replicated outside catalog	Number of control samples in catalog	Number of Type II deviants in catalog	How catalog is listed	Are there 5%s controls?	Level of evaluatability	QCERROR code
6473	27	11	0	13	11	3	0		YES	FULL	GOOD
6475	30	19	0	11	11	3	0		YES	FULL	GOOD
NMFS_084	40	0	0	19	11	12	0		YES	FULL	GOOD
NMFS_085	8	0	0	7	7	2	0		YES	FULL	GOOD
NMFS_125	21	0	0	11	10	2	0		YES	FULL	GOOD
NMFS_127	19	0	0	10	10	2	0		YES	FULL	GOOD
NMFS_159	26	0	0	14	9	11	0		YES	FULL	GOOD
6243	35	35	0	0	0	20	1		YES	PARTIAL	GOOD
6244	10	10	0	2	0	5	0		YES	PARTIAL	GOOD
NMFS_027	6	4	0	1	0	1	0		YES	PARTIAL	GOOD
NMFS_030	2	2	0	0	0	1	0		YES	PARTIAL	GOOD
NMFS_031	8	8	0	0	0	1	0		YES	PARTIAL	GOOD
NMFS_077	4	4	0	0	0	3	0		YES	PARTIAL	GOOD
NMFS_099	24	24	0	0	0	12	0		YES	PARTIAL	GOOD
NMFS_124	7	7	0	0	0	1	0		YES	PARTIAL	GOOD
NMFS_126	24	0	0	10	4	6	0		YES	PARTIAL	GOOD
NMFS_128	14	1	0	6	4	4	0		YES	PARTIAL	GOOD
NMFS_129	12	2	0	5	1	3	0		YES	PARTIAL	GOOD
NMFS_136	35	2	0	11	4	2	0		YES	PARTIAL	GOOD
NMFS_147	29	1	0	10	0	9	0		YES	PARTIAL	GOOD
NMFS_185	1	0	0	1	1	1	0		YES	PARTIAL	GOOD
6659	37	6	1	24	17	0	0		NO	PARTIAL	GOOD
6692	72	36	0	18	17	2	0		NO	PARTIAL	GOOD

Table 2 continued

Catno	Number of samples in catalog	Number of unreplicated samples in catalog	Number of Type I deviants in catalog	Number of groups in catatalog	Number of groups replicated outside catalog	Number of control samples in catalog	Number of Type II deviants in catalog	How catalog is listed	Are there 5% controls?	Level of evaluatability	QUERROR code
6104	13	13	0	0	0	0	0		NO	MARGINAL	GOOD
6116	6	0	0	2	0	0	0	H	NO	MARGINAL	SUSPECT
6122	3	3	0	0	0	0	0		NO	MARGINAL	GOOD
6157	9	0	0	3	0	0	0		NO	MARGINAL	GOOD
6159	6	4	0	1	0	0	0		NO	MARGINAL	GOOD
6160	55	53	0	2	2	0	0		NO	MARGINAL	GOOD
6161	57	55	0	2	2	0	0		NO	MARGINAL	GOOD
6162	4	2	0	1	0	0	0		NO	MARGINAL	GOOD
6165	11	2	0	3	0	0	0		NO	MARGINAL	GOOD
6166	9	3	0	2	0	0	0		NO	MARGINAL	GOOD
6167	3	1	0	1	0	0	0		NO	MARGINAL	GOOD
6542	35	35	0	0	0	0	0		NO	MARGINAL	GOOD
6543	47	47	0	0	0	0	0		NO	MARGINAL	GOOD
6544	46	44	0	1	0	0	0		NO	MARGINAL	GOOD
6642	32	32	0	0	0	0	0		NO	MARGINAL	GOOD
6653	1	1	0	0	0	0	0		NO	MARGINAL	GOOD
6691	32	32	0	0	0	0	0		NO	MARGINAL	GOOD
NMFS_028	1	1	0	0	0	0	0		NO	MARGINAL	GOOD
NMFS_032	4	4	0	0	0	0	0		NO	MARGINAL	GOOD
NMFS_033	5	3	0	1	0	0	0		NO	MARGINAL	GOOD
NMFS_089	2	0	0	1	1	0	0		NO	MARGINAL	GOOD
NMFS_141	12	3	0	5	4	0	0		NO	MARGINAL	GOOD

Table 2 continued.

Catno	Number of samples in catalog	Number of unreplicated samples in catalog	Number of Type I deviants in catalog	Number of groups in catalog	Number of groups replicated outside catalog	Number of control samples in catalog	Number of Type II deviants in catalog	How catalog is listed	Are there 5% controls?	Level of evaluatability	QCI ERROR code
NMFS_089	2	0	0	1	1	0	0		NO	MARGINAL	GOOD
NMFS_141	12	3	0	5	4	0	0		NO	MARGINAL	GOOD
NMFS_176	28	1	0	13	4	0	0		NO	MARGINAL	GOOD